

[Ex/66]

UNIVERSITY OF ROORKEE,
ROORKEE (U.P.)

Certified that the attached Thesis/Dissertation on.....
.....
.....
was submitted by
.....
and accepted for the award of Degree of Doctor of Philosophy/Master of Engineering in
.....
.....
vide Notification No. Ex/1007/7-65 (Exam.)
dated..... 17.12.1977.

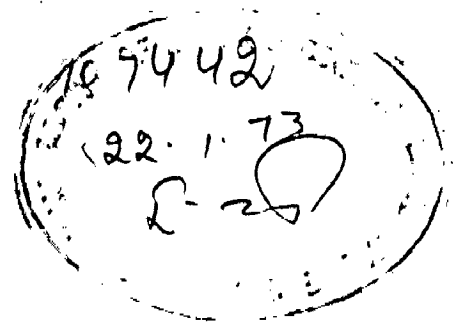
Dated.....

Assistant Registrar (Exam.)

**KINETIC STUDIES OF OXIDATION
OF
COPPER SULPHIDE**

A Dissertation
submitted in partial fulfilment
of the requirements for the degree
of
MASTER OF ENGINEERING
in
METALLURGICAL ENGINEERING
(EXTRACTIVE METALLURGY)

By
SURINDERA DEWAN



084

DEPARTMENT OF METALLURGICAL ENGINEERING
UNIVERSITY OF ROORKEE
ROORKEE, U. P.

1972

A large, stylized handwritten signature or mark in the bottom left corner.

C O N T E N T S

Chapter	Page	
CERTIFICATE	i	
SYNOPSIS	ii	
ACKNOWLEDGEMENTS	iv	
LIST OF TABLES	v	
LIST OF SYMBOLS USED	vi	
I	KINETIC STUDIES OF OXIDATION OF COPPER SULPHIDE	
1.1	Introduction	1
1.2	Products of Oxidation of Copper Sulphide	4
1.3	Cu-S Phase Diagram	9
1.4	Cu-S-O Phase Diagram	9
II	MECHANISM & RATE CONTROLLING STEP IN THE OXIDATION OF CUPROUS SULPHIDE	
2.1	Mechanism	10
2.2	Rate of Reaction	12
2.3	Rate Controlling Step in the Oxidation of Cuprous sulphide	15
2.3.1	Role of heat & Mass Transfer	16
2.3.2	Effect of Diffusion & Mass Transfer	18
2.3.3	Effect of heat Transfer	20
2.3.4	Mechanism during Isothermal Period	22
2.4	Factors affecting the rate of oxidation	23-26
2.5	Methods of Studying oxidation kinetics	26
III	EXPERIMENTAL WORK	
3.1	Introduction	28
3.2	Materials used	29
3.3	Preparation of Pellets	30
3.4	Porosity measurement of pellets	31
3.5	Experimental Set up	31
3.6	Oxidation Procedure	35
IV	CALCULATIONS	
4.1	Calculations for non-isothermal period	37
4.2	Calculations for Isothermal period	44

Contents ...(Contd..)

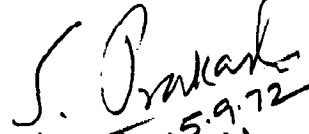
V	RESULTS AND DISCUSSIONS	
	5.1 Results	46
	5.2 Discussion of the Results	48
VI	CONCLUSIONS	56
	SUGGESTIONS FOR FURTHER WORK	58
	BIBLIOGRAPHY	59-62
	APPENDIX	i - xviii

C E R T I F I C A T E

Certified that the dissertation entitled " KINETICS STUDIES OF OXIDATION OF COPPER SULPHIDE" which is being submitted by Shri SURENDRA DEWAN in partial fulfilment of the award of the Degree of Master of Engineering in Extractive Metallurgical Engineering of University of Roorkee ,Roorkee is a record of student's own work carried out by him under my supervision and guidance. The matter embodied in this dissertation has not been submitted for the award of any other Degree or Diploma.

This is further to certify that he has worked for a period of six months from March, 1972 to August 1972 for the preparation of this thesis at this University.

September , 1972.


(Satya Prakash)
5.9.72
Lecturer,

Extractive Metallurgical Engg.,
University of Roorkee,
Roorkee.

S Y N O P S I S

Reactions between gases and solids play an important part in many metallurgical processes and the need for understanding the mechanisms involved in these reactions cannot be overemphasized. In the present work, kinetics of oxidation of compacted spheres of synthetic cuprous sulphide in air was studied in the temperature range of 750-950°C. The reaction was followed by measuring SO₂ titrimetrically. The reaction is highly exothermic and the heat generated at the reaction front can influence the kinetics and this aspect has been taken into consideration in the present work. The temperature of the sample was measured by using fine Pt-Pt/13% Rh thermocouple wires embedded in the centre of the pellet.

The process was found to be topochemical and the heat released at the reacting interphase of the compact manifested itself in rise in temperature of the sample than its surroundings. These temperature differences subsequently levelled off after 20 minutes and remained constant during rest of the experiment. The previous investigators¹⁻⁵ unfortunately failed to recognize the significant contribution of the exothermic nature of the reaction towards deciding the true controlling mechanism, therefore, led to conclude that the reaction is chemically controlled.

The results obtained are analysed on the basis of heat and mass transfer phenomenon. Systematic study was made by analysing separately the experimental results in well defined two regions. The one is referred as 'Transition Period' or 'non-isothermal' period where temperature of the sample initially overshoots the temperature of surrounding. The second is referred as isothermal period where the temperature differences cease and practically no 'offset' was observed during this period. Attempt was also made to study the effect of certain variables, viz., a flow rate, porosity, pellet dia., etc., etc. on the oxidation kinetics of copper sulphide pellets.

Transport steps are found to be the rate controlling and in the later case, i.e., the effect of variables is in fair agreement with the work reported earlier ¹⁻⁵.

A C K N O W L E D G E M E N T S

The author feels intense pleasure and scarcity of adequate words to record his heart-felt gratitude to Shri Satya Prakash, Lecturer, Metallurgical Engineering for imparting his expert guidance, fullest cooperation, prudent advices, useful discussions and high hearted encouragement throughout the course of his work.

Dr. M.N.Saxena, Professor and Head, Metallurgical Engineering Department deserves author's sincerest thanks for providing various facilities in the department in connection with this work.

The author is profoundly indebted to all staff Members particularly Lecturers, Extractive Metallurgical Engineering for taking keen interest and extending cooperation of every sort whenever he needed them.

Finally he would like to thank every body, whosoever, has directly or indirectly contributed towards this work.

LIST OF TABLES

- Tables 1- 5 Percentage oxidation versus time in the temperature range of 750 - 950°C.
- Table 6 - 10 Calculated values of $[1-(1-f)^{1/3}]^2$ and $[1-(1-f)^{1/3}]$ at different time intervals at 750 - 950°C .
- Table - 11 Calculated values of $\log k$ and $1/T$ in non-isothermal and isothermal period respectively and thereby calculation of apparent activation energies.
- Table 12- 15 Experimental data showing the effect of porosity on the rate of oxidation of Cu_2S
- Table 16 - 17 Experimental data showing the affect of increasing flow rate of air from 500 cc min^{-1} to 1.50 min^{-1} on the oxidation rate of Cu_2S
- Table 18 Showing the comparison of theoretical rates based on mass transfer and diffusion and theoretical rates based on heat transfer with those of experimental rates in the non-isothermal period.
- Table -19 Showing the calculated value of $(1/r^{*1} - 1)$ and $(P_{\text{O}_2} / \dot{q})$ (in the isothermal period)
- Table -20 Comparison of experimental and calculated values in the isothermal period. (D_{eff} and α)
- Table -21 Calculation of Parabolic rate constants at different partial pressures of SO_2 in the Atmosphere.

LIST OF SYMBOLS USED

d	dia. of the cylindrical compact, cm.
D	Diffusion coefficient, $\text{cm}^2 \text{sec}^{-1}$
D_{eff}	Effective Diffusion coefficient in the product layer, $\text{cm}^2 \text{sec}^{-1}$
h	Heat transfer coefficient, $\text{Cals} \cdot \text{cm}^{-2} \text{sec}^{-1} \text{ } ^\circ\text{K}$
H	Heat of reaction $\text{Cal} \cdot \text{g.mole}^{-1}$
k_{CuO}	Thermal conductivity of product solid (CuO), $\text{Cal} \cdot \text{cm}^{-1} \text{sec}^{-1} \text{ } ^\circ\text{K}$
K_C	Chemical rate constant, $\text{cm} \text{sec}^{-1}$
K_G	Thermal conductivity of gas $\text{Cal} \cdot \text{cm}^{-1} \text{sec}^{-1} \text{ } ^\circ\text{K}$
$\dot{\eta}$	rate of reaction, g mole sec^{-1}
p	Partial pressure, atm.
q	Heat transfer rate, Cal sec^{-1}
r_0	Initial radius of reacting compact, cm.
r'_0	Radius of reaction front at the beginning of isothermal period, cm.
r	Radius of reaction front, cm.
R, R'	Gas constant in Mechanical Units, $\text{cm}^3 \text{atm} \cdot \text{g-mole}^{-1} \text{ } ^\circ\text{K}$ in heat units $\text{Cals g-mole}^{-1} \text{ } ^\circ\text{K}$.
t	time, see (unless otherwise stated).

V_G Linear Velocity of gas past a reacting compact,
cm sec⁻¹

GREEK SYMBOLS

α Mass Transfer Coefficient, cm sec⁻¹

δ Boundary layer thickness, cm.

θ Temperature, deg. C

μ Viscosity of gas, g sec⁻¹ . cm.

ν Kinematic viscosity of gas, cm² sec⁻¹

ρ Molar density of compact, g-mole cm⁻³

σ Stefan-Boltzman constant, Cal cm⁻² sec⁻¹ °K⁴

[ζ_M] Mass transfer resistance, Sec. cm⁻³

DIMENSIONLESS VARIABLES

K_{eq} Equilibrium constant

N_a Nussett Number, hd / k_G

P_r Prandtl number $\frac{\nu C_p}{K_G}$

S_c Schmidt Number, $\frac{\nu}{D}$

Sh Sherwood Number $\frac{\alpha d}{D_G}$

Re Reynolds Number, $\frac{V_G d}{\nu}$

r^* , $r^{*'}$ Dimensionless radius of reaction front

$$r^* = r / r_0 , \quad \& \quad r^{*'} = r / r'_0$$

- V** Porosity factor in the porous solid
G Emissivity
T Tortuosity factor in porous solid

SUFFIXES

- G** Value in gas flow through the reaction tube
R Value at Reaction front
I Value for reactant gas
II Value for product gas
O Value at beginning of reaction.

CHAPTER - I

KINETIC STUDIES OF OXIDATION OF COPPER SULPHIDE

1.1 INTRODUCTION

In the extraction of several of the important non-ferrous metals, like copper, Lead, Zinc, Cobalt, Nickel, Mercury, etc. Sulphide minerals constitute an important source. Roasting is practised as an intermediate operation which is defined as heating a material without fusion for the purpose of adding to it some desired element, or elements, usually oxygen. Roasting is usually undertaken in order to affect the complete or partial removal of sulphur at some similar elements, such as Arsenic or Tellurium as a volatile oxide.

Rapid and complete oxidation would require fine particle size, constant stirring of the bed to expose the lower layers of ore and a rapid flow of air for the removal of gaseous products of combustion. Practical considerations, however, limit these conditions, for fine grinding is expensive and all three would result in heavy dusting loss and so add to the cost of operation. It follows thus that complete elimination of the undesired element is impracticable⁶.

Cuprous sulphide, above all, is an important mineral source of copper. It also finds use in the preparation of

CuSO_4 and has been used as a component of electrodes for thermoelements. Cuprous sulphide has catalytic activity and has been described as a catalyst in the cracking of dicylopentadiene⁷. Cuprous sulphide melts at 1130°C , shows transition points at 103° and 350°C and has ZnS structure with N-interstitial⁸.

Recent innovations like flash smelting⁹ electric smelting¹⁰, WORCRA continuous process¹¹, all converter process¹² etc. has revolutionised the sphere of copper production technology. These innovations are, undoubtedly, based upon the complete physico-chemical explanation of the fundamental processes taking place in the production of copper. Oxidation of cuprous sulphide, no need to say, is the most fundamental process in copper pyrometallurgy and physico-chemical nature of this process must need be understood thoroughly well which requires the knowledge of the structural, thermo-dynamic and kinetic factors involved¹³.

Regarding thermodynamics, standard free energy of a reaction at a given temperature is a measure of its tendency to occur under those conditions when all the participating substances are at unit activity. In a closed system the consumption of reactants and formation of products of variable activity (substances in gaseous state or in unsaturated solutions) leads to a progressive decrease in the free energy, which would become zero at equilibrium. Although at the temperatures used in

pyrometallurgical practice a positive tendency for a reaction to occur generally means that it does, in fact, takes place at an appreciable rate, the magnitude of the free energy for the reaction as a whole at any stage affords no indication of the rate of occurrence under those conditions though the velocity must, of course, tend towards zero as equilibrium is approached. Reaction velocities must, therefore, be subjected to independent study, and any calculation of their magnitude requires a knowledge of the mechanism of the reactions concerned.

The study of kinetics helps to determine the rate controlling step in the overall reaction and the evaluation of the rate controlling step may help in increasing the overall rate of a reaction by hastening the rate controlling step.

Oxidation kinetics of cuprous sulphide or the mineral chalcite (Cu_2S) has been a subject of many investigations¹⁻⁵. There has always been a controversy regarding the rate determining step in the oxidation of cuprous sulphide. According to Peretti¹, a diffusion step involving the diffusion of reacting gas is rate controlling whereas Henderson² says that chemical reaction at the inter-phase, viz., formation of Cu_2O is rate controlling process. McCabe and Morgan³ who carried out the oxidation in an atmosphere of oxygen, are in favour of a mechanism involving transport of gases through the porous oxide layer.

Recent investigators^{14,15,16,17,18,19} have emphasized the role of heat and mass transfer in M-S-O System. They say that heat liberated during oxidation greatly affects the kinetics and must be paid due consideration towards deciding the true nature of the rate controlling step.

The present work, therefore, has been undertaken mainly with view point to visualise the effect of heat generation at the reacting interphase on the oxidation kinetics of cuprous sulphide and on the basis of this study, the previous concept that chemical reaction at the interphase is rate controlling is ruled out.

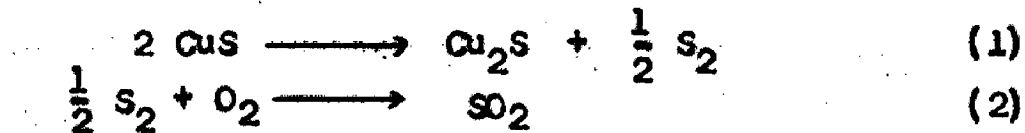
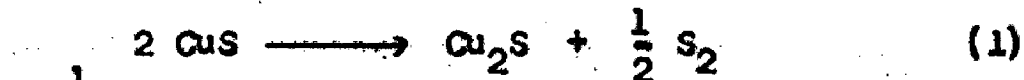
1.2 PRODUCTS OF OXIDATION OF CUPROUS SULPHIDE

Diev et.al^{20a}, investigated the roasting of chalcocite (Cu_2S) in air and oxygen enriched air. Lewis et.al²¹ also studied the oxidation of natural and synthetic chalcocite in air and oxygen atmosphere. Their studies have indicated that the maximum formation of water soluble sulphates occurred at 450°C .

Aschcroft²² reported that oxide production during the roasting of chalcocite resulted only from secondary decomposition of sulphates which were formed as primary products.

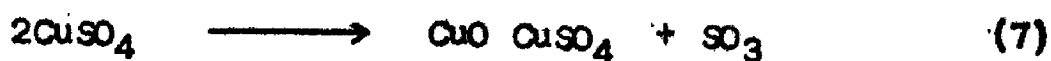
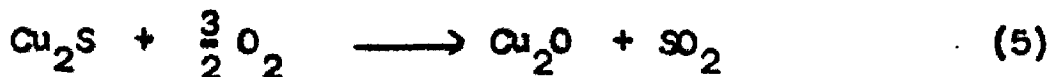
Peretti¹ refuted this claim by showing that a layer of Cu_2O appeared directly adjacent to the Cu_2S during roasting of cylindrical briquettes of cupric sulphide,

CuS. The linear advance of the $\text{Cu}_2\text{S}/\text{Cu}_2\text{O}$ interphase was used as a measure of the kinetics of the roasting reaction. The reactions proposed were -



At temperature 663°C only CuO has been reported to be the final product in solid phase. Below 663°C increasing amounts of sulphates were found mixed with the CuO. These products were analysed by X-ray diffraction, photograms are shown in Figure 1.

McCabe and Morgan²³ have investigated the roasting of discs of Synthetic chalcocite and reported the following sequence of products beginning at the sulphide surface, Cu_2O , a mixture of Cu_2O and CuSO_4 , CuSO_4 , $\text{CuO} \cdot \text{CuSO}_4$ and CuO. The principal reactions were reported to be -



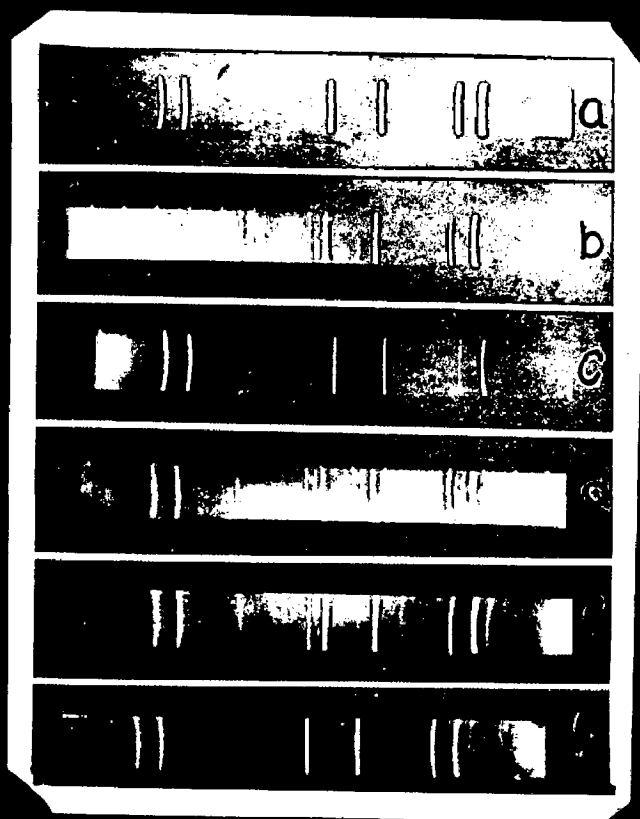
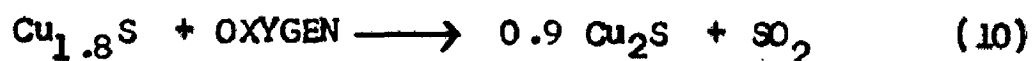
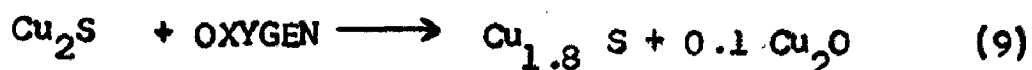


Fig 1 X-ray photographs of C.P. Cu_2O and Primary Solid phase formed during the roasting of Cu_2S at various temperatures -
A - C.P. Cu_2O , B- 965°C , C - 787°C , D - 663°C
E - 572°C , F - 525°C .

Equation (5) supports the claim of Peretti while Equation (3) supports the finding of Ashcroft that Cu_2O is formed directly from Cu_2S rather than as a secondary product from a sulphate. On the other hand CuO was found to form as a secondary product from the decomposition of copper sulphate and basic copper sulphate as given by Equation (7) and (8). The formation of sulphates was explained by McCabe and Morgan to be a direct reaction of Cu_2O with O_2 and SO_2 or SO_3 at distinct regions in which the partial pressures of each were such as to form sulphates.

Thornhill and Pidgeon²⁴ roasted both natural and synthetic chalcocite grains in air at temperatures between 450° to 550°C . They found a dense primary oxide layer in contact with the sulphide. A secondary layer of porous oxidation products was found to expand with increase in roasting time. The oxide products were leached away and the remaining core was studied by X-Ray diffraction. The X-ray patterns showed an increased conversion of chalcocite to digenite. Digenite²⁵ has a defect structure of cuprous sulphide and occurs naturally as Cu_{2-x}S where $x = 0.12-0.45$. with an average analysis of $\text{Cu}_{1.8}\text{S}$. The mechanism of the Digenite formation was proposed as -



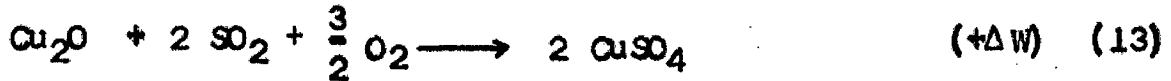
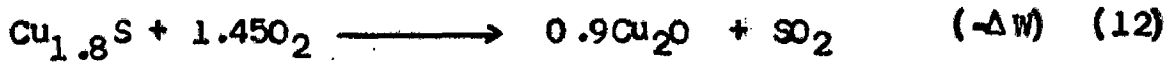
It is apparent from the above studies that the oxidation of Cu_2S ultimately ends in the formation of CuO and thus can be divided into 3 general stages (all of which may occur simultaneously).

- (i) Primary oxidation to Cu_2O
- (ii) Secondary sulphate formation
- (iii) Sulphate decomposition

Smyth and Roberts²⁶ concluded that there is no miscibility of CuO and Cu_2O . This was later confirmed by Reuter and Schröder²⁷. Heats of formation of the oxides of copper were determined by Balesdent²⁸ and dissociation pressures at several temperatures were measured by Hastings et.al²⁸ and Becker²⁹.

Garner et.al³⁰ made adsorption studies of O_2 and SO_2 on Cu_2O which has been reviewed by Trapnell³¹. SO_2 chemisorption was observed at room temperatures on Cu_2O . Garner proposed that there are two distinct mechanisms. One is the primary adsorption followed by chemisorption. Chemisorption is characterised by slow increase in the heat of adsorption and irreversibility, for upon desorption only SO_3 is removed.

Wadsworth et.al³² gave out the following sequence of reactions which was later confirmed by X-Ray Diffraction technique -



Overall reaction is



On the basis of the X-ray diffraction analysis the following list of oxidation products at different temperatures has been compiled by Wadsworth et.al.

Temperature	Products formed
650°C	CuO, CuSO ₄ (Some had spots of CuO.CuSO ₄)
700°C	CuO, CuSO ₄ , CuO, CuSO ₄
750°C	CuO, CuO.CuSO ₄ , CuSO ₄
785°C	CuO, CuO.CuSO ₄ , CuSO ₄
800°C	CuO, CuO.CuSO ₄
850°C	CuO
900°C	CuO
950°C	CuO

CuO has monoclinic structure⁸ with lattice constants as 4.65, 3.41, 5.11 and 99°29', is a covalent compound and is more acidic than Cu₂O⁷.

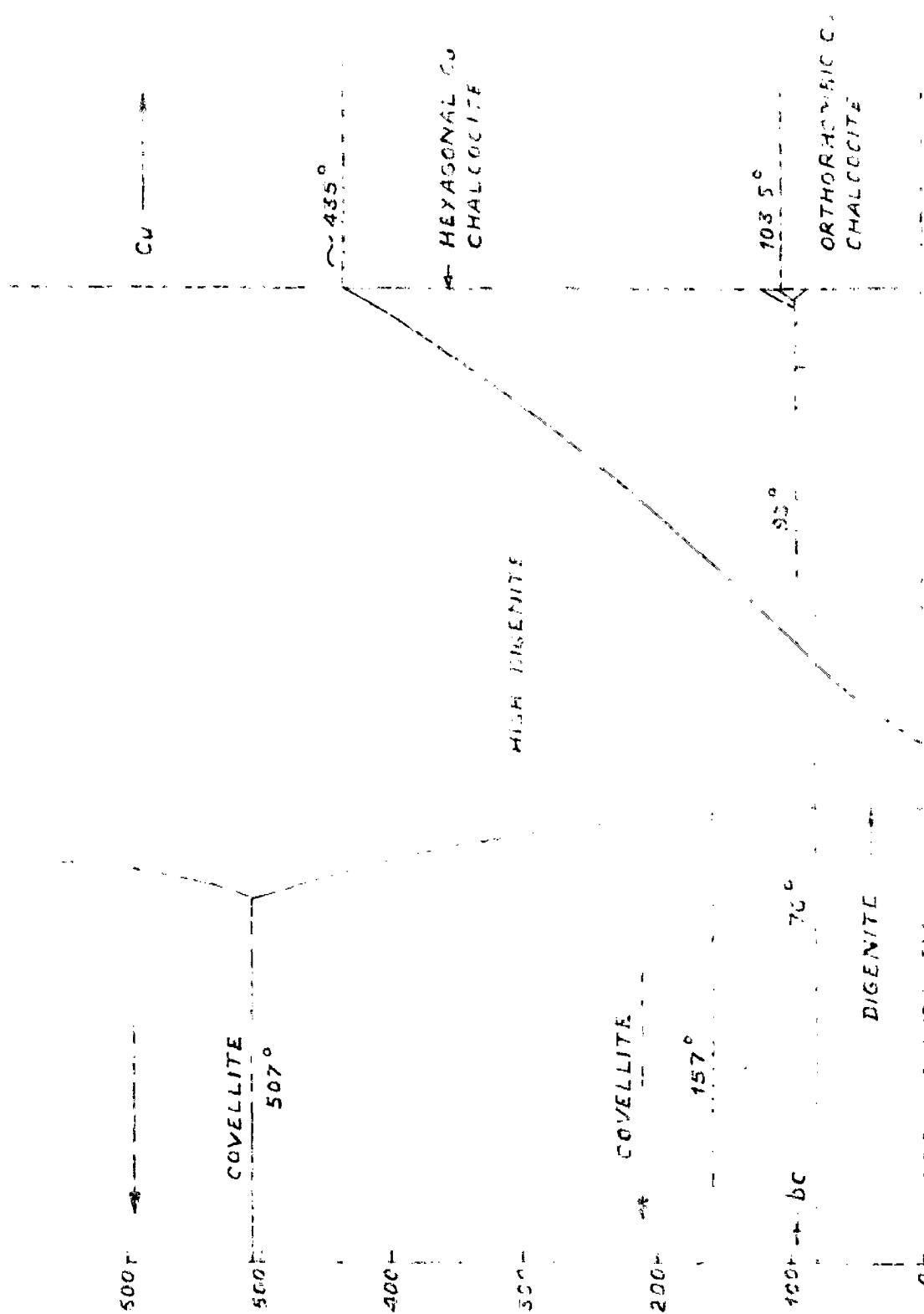
1.3 Cu-S PHASE DIAGRAM

Figure (2) shows the expanded portion of Cu-S phase diagram at low temperatures based upon the work of Roseboom³³. According to Rau³⁴, Digenite is known to be a p-type semi-conductor. S-atoms are fixed at their lattice sites while Cu-atoms are mobile through the interstices of this structure.

1.4 Cu-S-O PHASE DIAGRAM

From the Figure 3, it is quite evident that Cu_2O must initially form as an intermediate product during the conversion of Cu_2S to CuO . At higher partial pressures of O_2 in air, Cu_2O is then converted to CuO . This pattern of behaviour has also been reported by Peretti¹ and Henderson².

Wodsworth³² while studying the oxidation of chalcocite, has cited one very important phenomenon, i.e., the formation of repeated 'Puff-Balls' or hollow gas filled pockets which formed during roasting. "Puff-Balls" as large as 3/4" diameter were formed on several occasions. The presence of SO_2 and O_2 within the porous sulphate layer stabilised CuSO_4 above its melting point thus providing a viscous fluid phase which expanded as the internal pressure increased. He observed in many instances, an internal kernel completely surrounded by a trapped gas phase, within a large sulphate CuO shell. Figures 4 and 5 amply illustrate this phenomenon.



S.Wt. % = 23

Cu S, wt % = 7

FIG. 4N APPROVED PHASE DIAGRAM FOR Cu-S (1975)

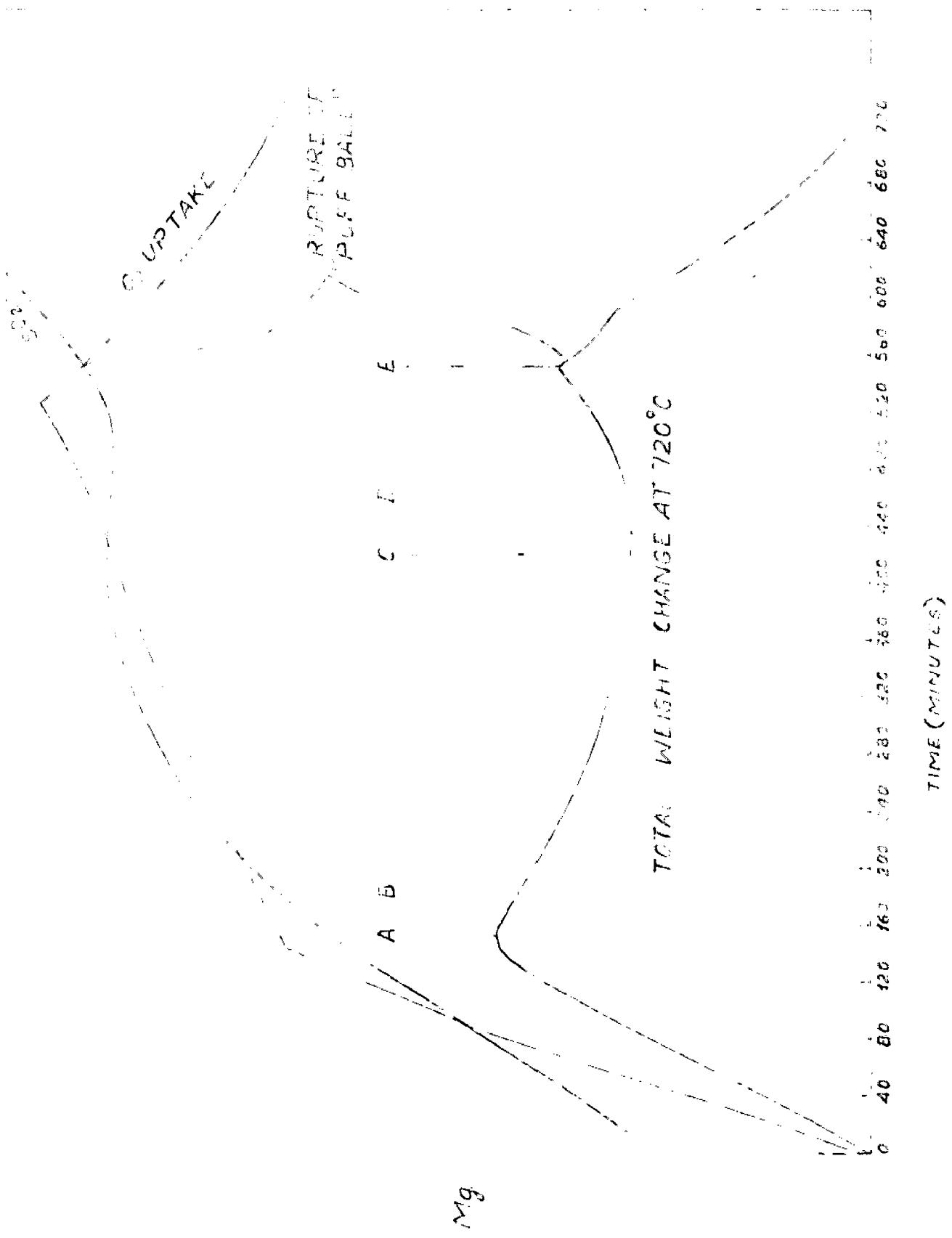


FIG. 4 GRAPHICAL REPRESENTATION OF THERMOGRAVIMETRIC CHANGE AND SO₂ & O₂ VALUES AT 720°C WITH STAGES A, B, C, D & E SHOWS THE STAGES OF FORMATION, EXPANSION AND RUPTURE OF PUFF BALLS (Mg = MILLIGRAMS)

CHAPTER - II

MECHANISM AND RATE CONTROLLING STEP IN THE
OXIDATION OF CUPROUS SULPHIDE

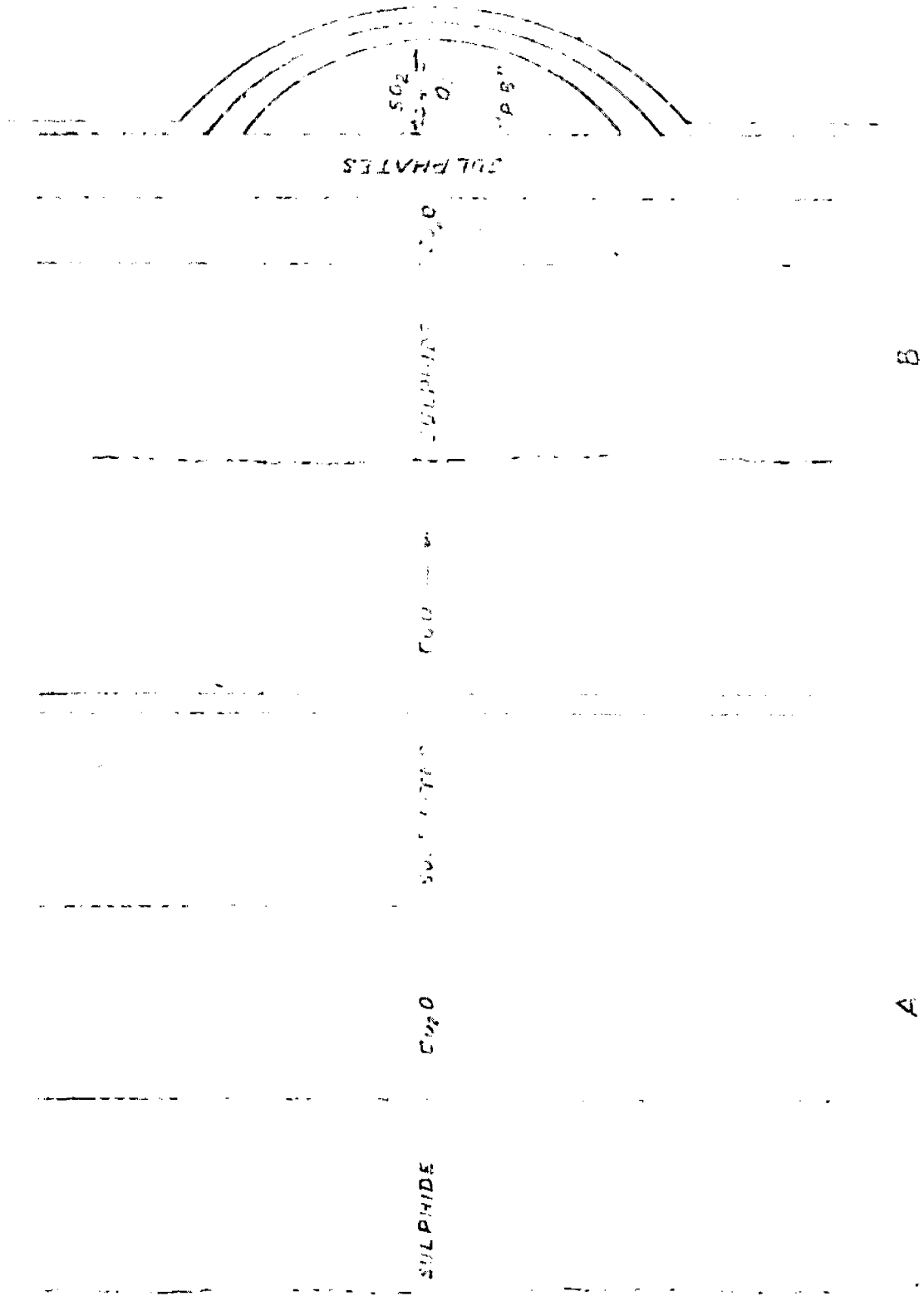


FIG. 1 "DUFF BALL" FORMATION SHOWING TRAPPED GASES WHICH STABILISE INTERNAL OXIDES.
 (WADSWORTH ET AL. 1950)

C H A P T E R - I I

MECHANISM AND RATE CONTROLLING STEP IN THE
OXIDATION OF CUPROUS SULPHIDE

MECHANISM AND RATE CONTROLLING STEP IN THE
OXIDATION OF CUPROUS SULPHIDE2.1 MECHANISM

Oxidation of cuprous sulphide has been found to proceed in a topochemical manner (Figure 6¹⁶). Progressively increasing layer of cupric oxide is formed at the expense of cuprous sulphide on the exterior surface and the reaction front marches onwards to the interior as the time lapses.

The generalised model for gaseous oxidation of copper sulphide is illustrated in Figure 7. This shows a partially oxidised sphere of copper sulphide in a gas stream surrounded by a stagnant boundary layer of gas.

Anderson³⁵ discussed the detailed mechanism of the reactions of the type :



These gas/solid reactions e.g. the oxidation of cuprous sulphide involve gaseous product (SO₂) as well as a gaseous reactant (O₂). The continuous removal of former (SO₂) from the sphere of action in a gas stream may have an important effect on the velocity of the whole process, for the P_{SO₂} may be kept down to an extremely low value. By these means, reactions that would be thermodynamically impossible may be caused to proceed rapidly³³.



Fig 6 Partially roasted section of Cu_2S pellet¹⁶

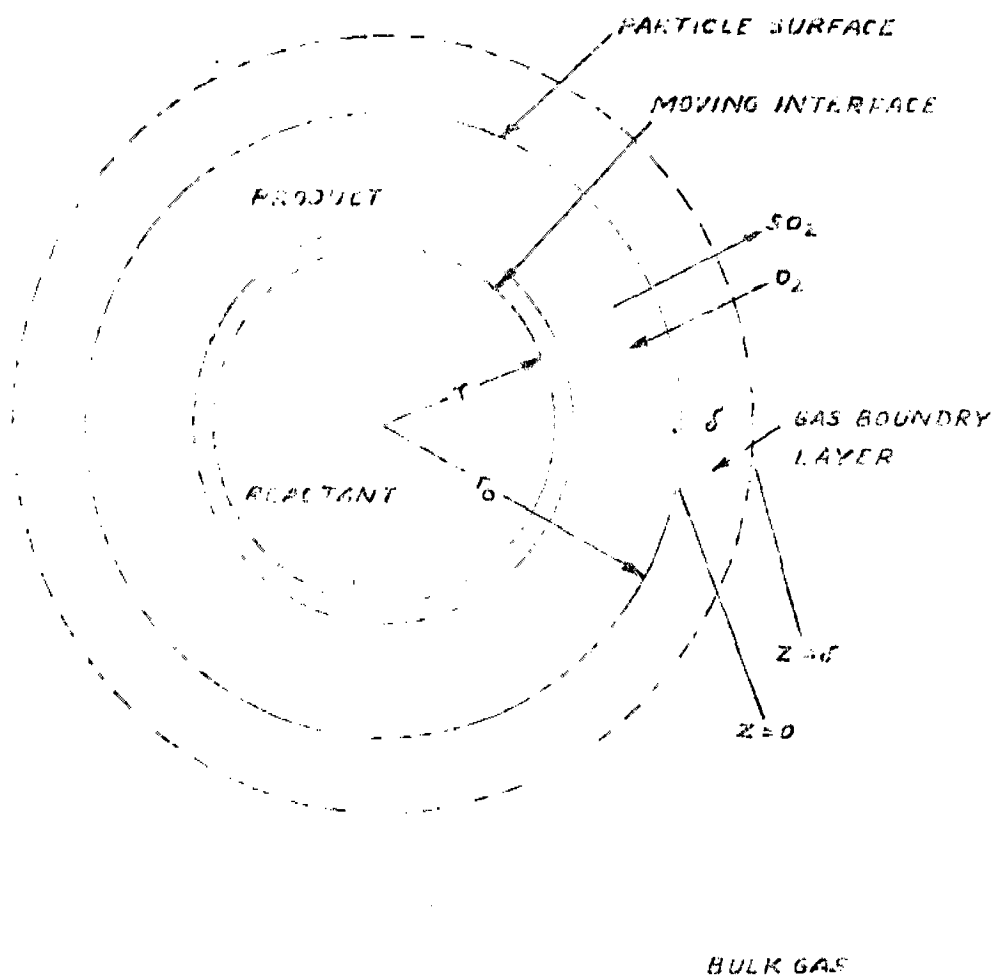


FIG. 1. SCHEMATIC DIAGRAM REPRESENTING THE OXIDATION OF A CUPROUS SULPHIDE PELLET.

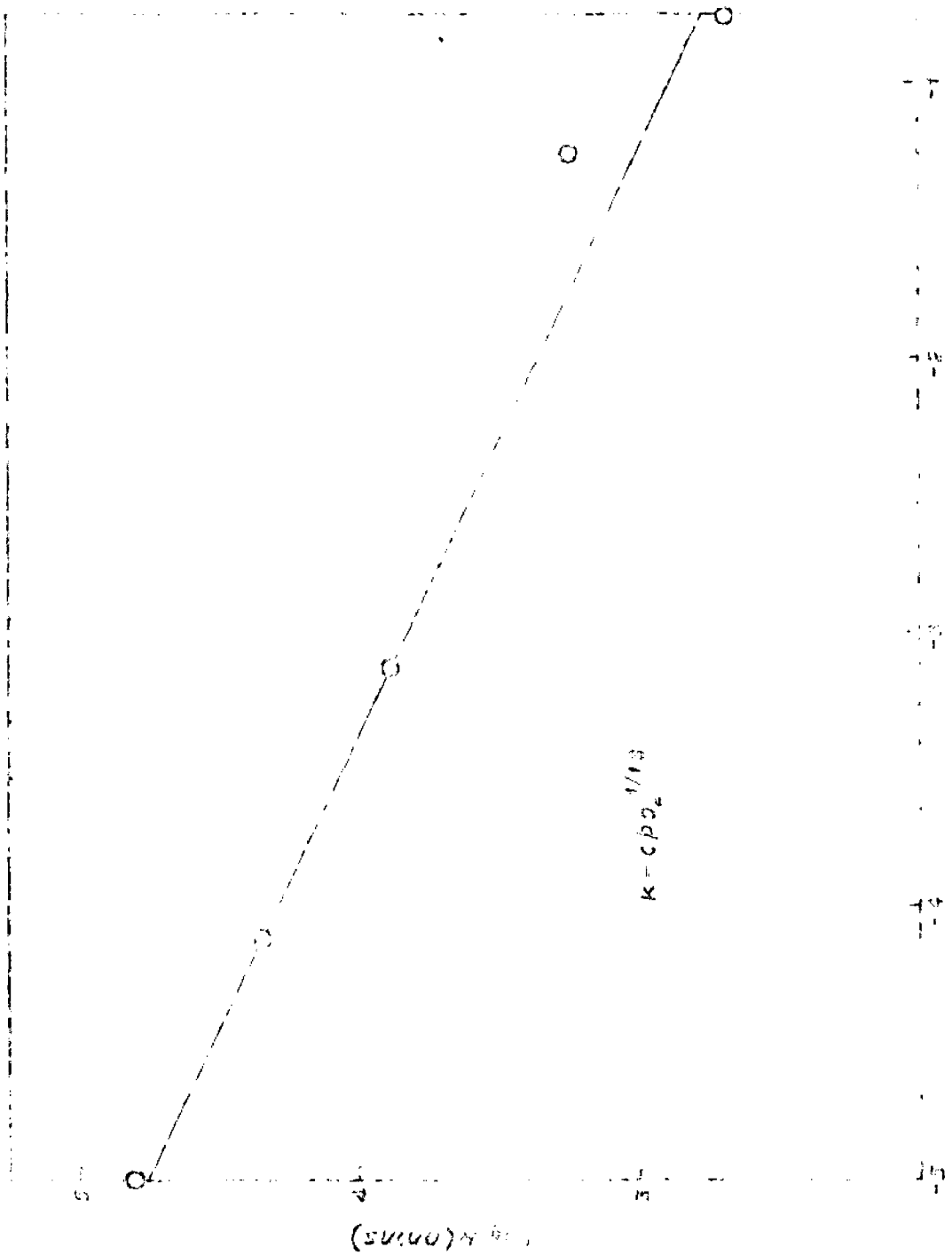


Fig. 2. Conductivity changes that follow with increase of P_{O_2} in case of S_{O_2} (standard P_{O_2} is 0.21 atm, S_{O_2} is 0.001 M, $T = 25^\circ C$, $V = 100$ ml, $P = 1$ atm).

Fig. 2. Conductivity changes that follow with increase of P_{O_2} in case of S_{O_2}

Anderson described the mechanism in relation to the lattice defects as follows :

The reactions involved in roasting and reduction processes are largely heterogeneous, occurring at solid/liquid, liquid/liquid, solid/gas or liquid/gas interphases. The sulphides of transition metals like copper sulphide, possesses wide range of composition and are thus coupled with moderate or high electronic conductivity. The conductivity varies with composition, but is intrinsically too great to be markedly effected by surface reactions. Buerger³⁶ has attributed the part of uncertainty attached to the polymorphism of chalcocite to be due to the readiness with which oxygen is built on to the crystal structure to give an oxy-sulphide with the symmetry of the digenite phase, $Cu_2S_{1.11}$.

Anderson³⁵ proposed an electronic model upon the data plotted by him in Figure 8 by taking SnS as per example. It has been proposed that similar expression can be obtained in case of copper sulphide to fit the Log R versus Log p_{O_2} plot. For SnS , the expression is,

$$k = C_{p_{O_2}}^{1/1.8}$$

and explained it as follows :

*Approximately 2 positive holes are created per molecule of oxygen, Chemisorbed. If this interpretation be correct, oxygen is built on to the crystal lattice either as

20^- ions per molecule of O_2 added or as molecular O_2^{2-} ions. The chemisorption process is very rapid at room temperature, so that the former process which would presumably involve higher activation energy, appears to be less likely Figure 9(B). This then provides a mechanism for the first stage in the roast reaction. Stage 2, which does involve an activation energy and so proceeds with measurable speed at moderately high temperatures, would then be represented by Figure 9(C), in which the positive hole is destroyed and some oxide of sulphur formed.

2.2 RATE OF REACTION

Rate Equation for an irreversible heterogeneous reaction of a gas with a solid has been derived³⁷ by considering contributions of chemical reaction at interphase boundaries and diffusion through solid product layer simultaneously. The equation is given as:-

$$\left(\frac{C_{10}}{\ell} \right) t = \frac{x}{k_1} + \frac{1}{2 D_{\text{eff}}} x^2 \quad (17)$$

where,

- C_{10} = Concentration of gaseous reactant at the outside surface of solid.
- ℓ = Density of solid reactant
- t = Time in seconds
- x = Thickness of solid product layer
- k_1 = Chemical reaction rate constant per unit area of reacting interphase for forward reaction.

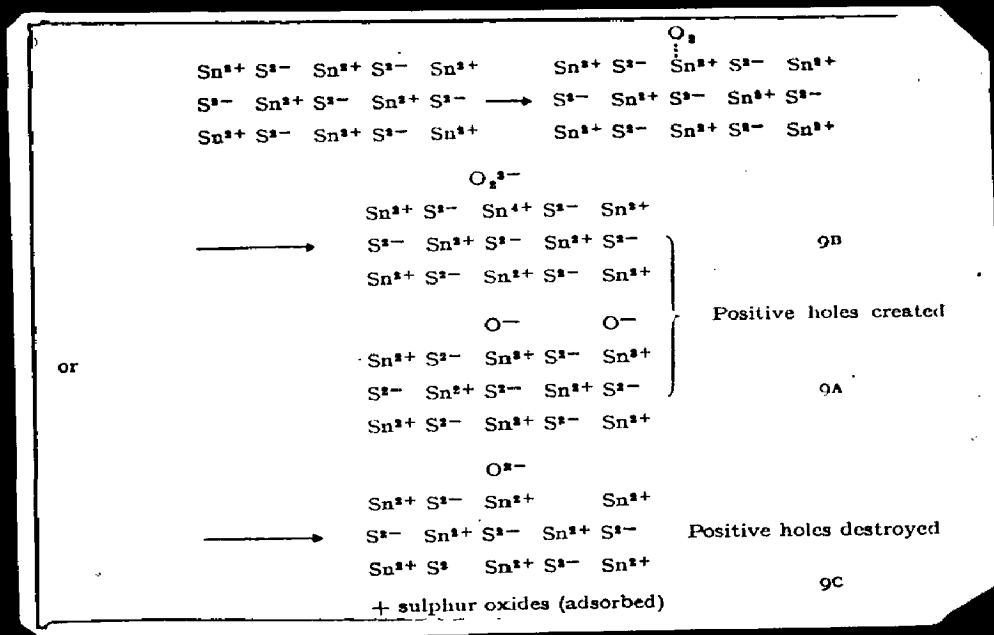


Fig. 9 Oxidation Model³⁵

D_{eff} = Effective diffusivity of gaseous reactant

In deriving Equation (17), diffusion rate of gaseous product was not considered³⁸.

The first term on the R.H.S. of Equation (17) represents the contribution of interfacial chemical reaction and the second term that of gaseous diffusion.

Wei-Kao Lu³⁸ has derived general rate equation for gas/solid reactions in Metallurgical processes by considering the contributions of chemical reaction at interphase boundaries and diffusion through the solid product layer simultaneously. This equation takes care of the whole range of reaction continuously from diffusion control to purely chemical reaction control.

If R_1 denotes the overall reaction rate at the solid/solid interphase, then,

$$R_1 = J_g(r_1, C_{g1}) = 4\pi r_1^2 k_1 G_{g1} \quad (18)$$

and at gas/solid interphase,

$$R_0 = J_s(r_1, C_{s0}) = 4\pi r_0^2 C_{s0} C_{g0} \quad (19)$$

Where C_{g1} (C_{s1}) = The activity of gaseous (solid) reactant at the interphase boundary of solid product and solid reactant as $r = r_1$.

C_g (C_s) = The activity of gaseous (solid) reactant.

In these derivations, exothermic nature of the reactions has not been taken into consideration, for the reactions¹⁶ are

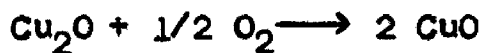


followed by



and as such temperature differences are bound to set up between sample and surroundings. According to Hill¹⁴ the previous workers neglected the significant contribution of the heat generation and so were misled to believe that the reaction is chemically controlled.

Wadsworth et.al³² has noticed another interesting result plotted in Figure 10 at 850^o C. At this temperature, the only product formed is CuO, yet the rate of reaction,



was greatly influenced by an overpressure of SO₂ with a maximum at 2 parts SO₂ to 1 part O₂. According to him, since the rate is diffusion controlled, it is very surprising that if SO₂ could have any effect and also since no sulphates were present because rapid weight loss occurred when SO₂ supply was cut off.

The same effect has also been reported by Hauffe and Engell³⁹ for the oxidation of zinc metal where the parabolic rate constant was found to vary with p_{O₂}, according to the relation

$$k = a \ln p_{\text{O}_2} + b \quad (22)$$

This equation was developed considering development of an electrical potential at the solid/gas interphase.

On this model, Wadsworth et.al³² has derived the following equation for copper sulphide oxidation.

$$k = a \log (x) (1-x)^{1/2} + b \quad (23)$$

Where a and b were evaluated to be 13.9 and 7.61 respectively

and x is the fraction of SO₂ in the atmosphere, on the assumption that SO₃ adsorbs on the CuO surface forming SO₃²⁻ or

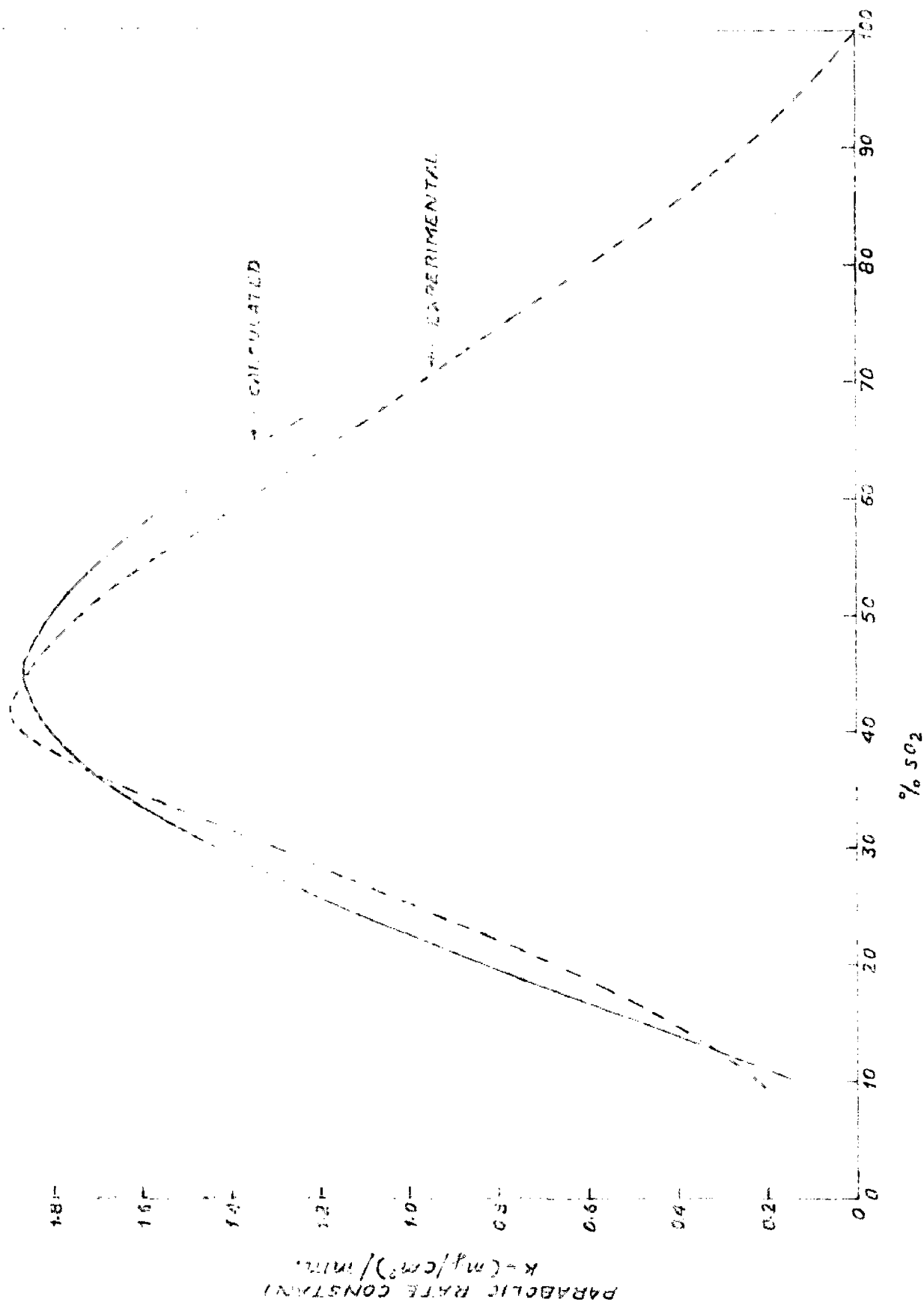


FIG. 10 DEPENDANCE OF PARABOLIC RATE CONSTANTS ON OVERPRESSURES OF SO_2
 (WADSWORTH et. al.²²)

even SO_4^{2-} .

2.3 RATE CONTROLLING STEP IN THE OXIDATION OF CUPROUS SULPHIDE

The possible rate controlling steps in the oxidation of cuprous sulphide pellets in a stream of dry air may be grouped as follows :-

(1) Diffusion of the reactant and the product gases through the gas film surrounding the sample.

(2) Diffusion of these gases through the porous oxide layer (also interparticle diffusion, if any), and

(3) Chemical reaction at the interphase is not considered⁴, for reaction 21 is as fast as, if not faster than, reaction 20. According to Rajouk⁴ if reaction 20 is slow, the stoichiometry demands a Cu_2O build-up which should result in a gradual continuous decrease in the weight of the sample, throughout the course of oxidation. According to the thermograms obtained by Wadsworth³² et.al and Abraham¹⁶, there does occur small loss in weight initially which indicates the formation of thin layer of Cu_2O , afterwards there is no weight change observed, confirming to the fact that there is absence of major Cu_2O build up.

Examination of the literature has shown that some doubt still persists as to the nature of rate controlling step involved in the oxidation of cuprous sulphide. One hand the reaction rate is assumed to be controlled by a chemical step at an interphase whereas on the other hand it is assumed that transport processes between the reaction front and the gas phase are rate controlling.

It would appear that in the initial period when the product layer is not sufficiently thick, the reaction at the interphase is rate controlling to be followed by the diffusion controlled process as the oxide layer is build up but in this consideration the effect of heat release at the reacting interphase cannot be overlooked¹⁴⁻¹⁹ and so the result must be analysed on the basis of heat and mass transfer phenomenon.

2.3.1 Role of Heat and Mass Transfer

There can be three possible control mechanisms,

(1) Complete chemical control

(2) Complete transport control

and (3) Heat and mass Transfer control.

If the reaction is not heat and mass transfer controlled, one can easily distinguish between the nature of chemically controlled reaction and transport controlled reaction because they possess absolutely different characteristics. Confronting situation arises when we distinguish between mechanism (1) and (3) controlled reactions because they possess many of the characteristics in common¹⁴, viz.,

(a) Constant reaction rate per unit area of the reaction front.

(b) Rate of reaction is virtually independent of gas flow rate once a certain critical flow rate is reached.

(c) Very high activation energy.

(d) Linear or nearly linear, relation between reaction rate and product gas partial pressure.

For a chemically controlled reaction, the following equation applies,

$$r_o d_o \left[1 - (1-f)^{1/3} \right] = \frac{k_c}{R\theta_G} P_{O_2} G \cdot t \quad (24)$$

Which shows that plot between $\left[1 - (1-f)^{1/3} \right]$ versus t should be linear. Rao and Abraham¹⁶ carried out the oxidation of cuprous sulphide in the temperature range of 750-950°C, in a stream of dry air and observed that during initial half an hour period (Non-isothermal period), the plot between $\left[1 - (1-f)^{1/3} \right]$ versus t is a straight line, higher value of the activation energy during this period and also found that, rate is independent of gas-flow rate after 500 cc per minute and still maintained that the reaction is heat and mass transfer controlled in this period. According to him, reaction can not be chemically controlled because:-

(1) Since the particle temperature is significantly higher than its surroundings and high activation energy has also been obtained, the rate of advance of the reaction front should vary rapidly with time during this period if it were to be an exclusively chemically controlled process but it is seen that the reaction front velocity does not substantially deviate from linearity.

(ii) With the release of exothermic heat at the reaction front resulting in higher temperatures, the reaction rate should continuously increase for a chemically controlled process. Instead a tendency for the reaction rate to decrease after few minutes from the start of reaction has been observed.

He, thus, concluded that chemical reaction is not rate controlling but that the reaction is likely to be controlled by a transport mechanism.

Even if the diffusive steps are likely to be the rate controlling the diffusivities are no doubt increased by the higher sample temperature generated by exothermic heat, however, higher diffusivities do not cause higher reaction rates because of the increase in the diffusional resistance as a result of the progressive increase in the thickness of the product layer¹⁶.

2.3.2 Effect of Diffusion and Mass Transfer^{14,16,}

Even though a moving interphase is involved in the present topochemical oxidation process, the analysis assumes a quasi-steady state process. This assumption is justified in view of the fact that only an infinitesimal small fraction of the total flux diffusing is likely to be accumulating, if at all within the pores of the product layer.

Assuming a chemical equilibrium at the reaction front, a rate equation for the non-isothermal period has been given by

Hills¹⁴. Considering mass transfer of both product and reactant gases :

$$\dot{\eta} = \frac{[P_{O_2}]_G - [P_{SO_2}]_G / k_{eq}}{R \theta_G \left\{ \frac{[\tilde{r}_M]_{II}}{k_{eq}} + \frac{3}{2} [\tilde{r}_M]_I \right\}} \quad (25)$$

Where $[\tilde{r}_M]_I$ and $[\tilde{r}_M]_{II}$ are mass transfer resistances due to both boundary layer and porous product layer relevant to the reactant and product gases respectively.

Since k_{eq} at $850^\circ C \gg \gg [\tilde{r}_M]_{II}$, therefore Equation (25) becomes,

$$\dot{\eta} = \frac{[P_{O_2}]_G}{R \theta_G^{3/2} [\tilde{r}_M]_I} \quad (26)$$

Expanding $[\tilde{r}_M]_I$ and $[\tilde{r}_M]_{II}$, Equation 26 becomes,

$$\dot{\eta} = \frac{[P_{O_2}]_G}{\frac{R \theta_G}{4 \pi [D_{eff}] r_0} \left[\left(\frac{1}{r^*} - 1 \right) + \frac{[D_{eff}]_I}{\alpha r_0} \right]} \quad (27)$$

where

$$\frac{\alpha d}{[D]_G} = Sh = 2 + 0.69 (Re)^{1/2} (Sc)^{1/3} \quad (28)$$

(From the work of Rowe, Claxton, and Lewis⁴⁰)

$$\text{and } D_{\text{eff}} = \frac{[D_G] r^2}{\tau} \quad (29)$$

(Wakao and Smith⁴¹ relation)

$$\text{and } [D_G] = 0.0043 \frac{\tau^{3/2}}{F (v_1^{1/3} + v_2^{1/3})} \sqrt{\frac{1}{M_1} + \frac{1}{M_2}} \quad (30)$$

(Gilliland, Hirshfelder and Coworkers⁴²)

The equation (29) is used in view of the bidisperse structure of pores in the product layer of reacting compact as revealed by the microscopic examination.

For many of the reactions¹⁴ $\gamma = 0.4 - 0.6$
and $\tau = 1.1$ to 4.0

Thus theoretical reaction rates based on diffusion and mass transfer can be calculated at different time intervals from equation (27) and can be compared with experimental rates. For mass transfer to be the rate controlling, theoretical rates should never be greater than their corresponding experimental rates.

2.3.3 Effect of Heat Transfer

Since the high temperature rise of the reacting compact during the initial period of oxidation, heat transfer effects may play an important role in the rate controlling step. Consequently the experimental data has to be correlated with an

equation based on the heat transfer process . Heat is generated at the reaction front as a result of the exothermic nature of the oxidation process. Therefore,

$$\dot{q} = \dot{\eta} H \quad (31)$$

Considering the heat transfer by conduction , convection, and radiation through the porous product layer and the outer boundary layer on quasi-steady state terms, a simplified eq. can be derived^{14,16} as :

$$\dot{\eta} = \frac{\Theta_R - \Theta_G}{\frac{H}{6 \pi k r_0} \left[\left(\frac{1}{r^*} - 1 \right) + \frac{k}{hr_0} \right]} \quad (32)$$

Various values can be computed as follows

$h = h, \text{ convection} + h, \text{ radiation}$

$$h, \text{ convection} = \frac{k_G}{d} \left[2 + 0.6 (Re)^{1/2} (Pr)^{1/3} \right] \quad (33)$$

(Ranz and Marshall correlation⁴³)

$$h, \text{ radiation} = 4 \epsilon \sigma \Theta_G^3 \quad (\text{A.W.D.Hills}^{14}) \quad (34)$$

This relation is obtained by approximating the furnace to an enclosure completely surrounding the sample, and at more or less the same temperature as the gas.

Substituting the relevant values in Equation 32, the rate of reaction, $\dot{\eta}$, can be obtained at various time intervals and can be compared with the experimental results and ,

$\dot{\eta}$ values for diffusion and transfer to decide the true nature of the rate controlling step involved in the oxidation of copper sulphide.

2.3.4 Mechanism During the Isothermal Period

According to Rao and Abraham¹⁶, the non-linearity of the plot in the isothermal region together with small value of activation energy could be taken as positive indication of transport controlled mechanism in this period. Equation 26 is still valid in this region where $[\sum M]_I$ stands for the total mass transfer resistance offered to the diffusion of the reactant gas from the bulk gas phase to the reaction front. With this view point, Equation $[\sum M]_I$ takes the form,

$$\frac{[PO_2]_G}{\dot{\eta}} = \frac{R \Theta_G}{4 \pi [D_{eff}] r'_0} \left(\frac{1}{r^{*'}} - 1 \right) + \frac{R \Theta_G}{4 \pi r_0^2 \alpha_1} + \frac{r_0 - r'_0}{4 \pi r_0 r' [D_e]} \quad \dots(35)$$

where resistance,

$$[\sum M]_I = R_1 + R_2 + R_3$$

$$= \frac{1}{6 \pi r_0^2 [\alpha_1]} + \frac{r_0 - r'_0}{6 \pi r'_0 r [D_{eff}]_I} + \frac{r'_0 - r_0}{[D_{eff}]_I 6 \pi r'_0 r_0}$$

R_1 = Resistance offered by the outer boundary layer.

R_2 = constant resistance offered by the product layer of thickness $(r'_0 - r)$ at time t , from the beginning of the isothermal period.

R_3 = The resistance offered by the product layer of thickness $(r'_0 - r)$ at time t , from the beginning of the isothermal period.

According to Equation (35), plot of $\frac{[p_{O_2}]_G}{\dot{\eta}}$

versus $(\frac{1}{r^{*'}} - 1)$ should be straight line whose slope should yield the value of D_{eff} and the intercept should give the value of mass transfer coefficient, α .

2.4 FACTORS AFFECTING THE RATE OF OXIDATION

2.4.1. Effect of Temperature^{16,32}

Oxidation of copper sulphide is a thermally activated process, therefore, the rate of oxidation increases with increase in temperature as it leads to increase the chemical reaction rate as well as Diffusion. Figure 11.

2.4.2 Effect of Gas Flow Rate¹⁴

When the flow rate is low the reaction rate is found to be strongly dependent upon on gas-velocity increasing the flow rate has less and less effect on the reaction rate until a 'plateau' is reached when the reaction rate is virtually independent of the gas velocity. Figure 12.

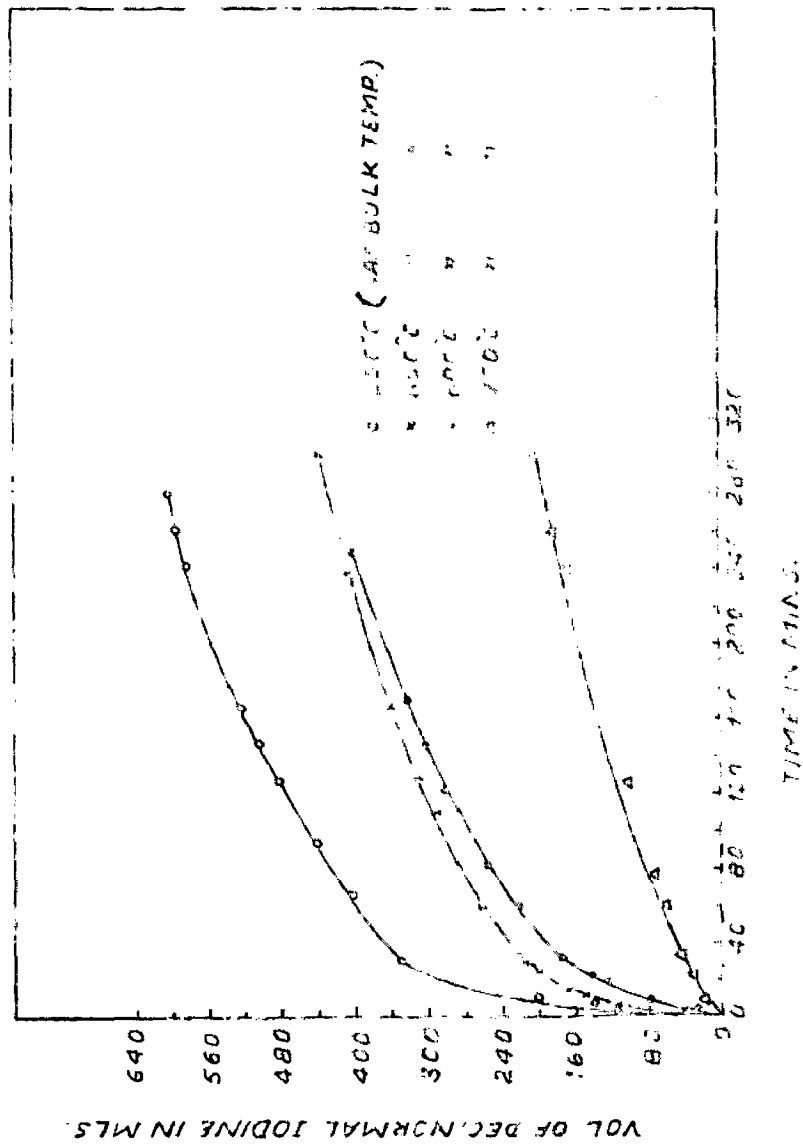


FIG. 14 PLOT SHOWING THE PROGRESS OF THE COUS PELLET IN TERMS OF THE IODINE SOLUTION CONSUMED (REF. 16)

When the molar flow rate of gas through the furnace is low, the following equation governs the rate,

$$\frac{\dot{\eta}}{[P_{II}]_{eq.} - [P_{II}]_G} = \frac{2 \dot{N}}{p_T} \quad (36)$$

where,

\dot{N} = Total molar flow rate of gas through reaction tube and

p_T = Total pressure, atm.

According to Equation (36), reaction rate is proportional to the flow rate of gas.

For higher gas velocities through the reaction chamber, the following equation is derived -

$$\frac{\dot{\eta}}{[P_{II}]_{eq.} - [P_{II}]_G} = \frac{1}{\frac{R \Theta}{4 r^2 d_{II}} + \frac{p_T}{2 \dot{N}}} \quad (37)$$

which is the usual mass transfer equation.

2.4.3. Porosity and Particle Size

Other factors remaining constant, oxidation rate increases with increase in porosity.⁴⁴ (Figure 13⁴⁵) Increased porosity facilitates higher diffusion rates while smaller particle size affords more surface area for the reaction. The following equation gives the effect of porosity on reaction rate -

$$\left(\frac{dn}{dt} \right)_{Cu_2S} = DA \epsilon_0 \beta \cdot \frac{\Delta C}{x} \quad (38)$$

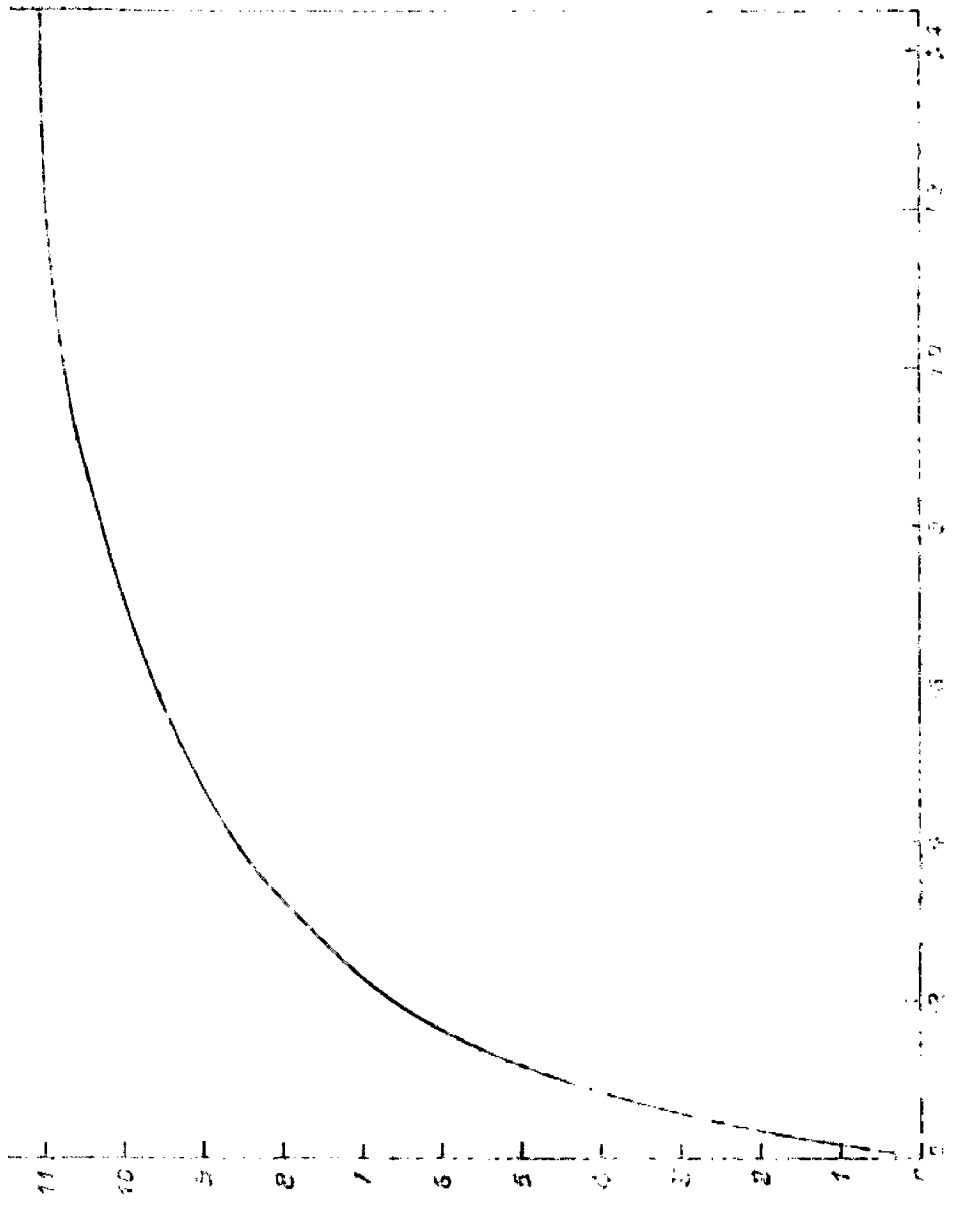


FIG. 14 THEORETICAL IMPROVEMENT OF REACTION RATE WITH GAS FLOW RATE FOR A SPHERICAL PARTICLE WHOSE REACTION IS CONTROLLED BY BOUNDARY LAYER MASS TRANSFER (COPPER AND MULL¹⁴)

SE 14

FIG. 14 THEORETICAL IMPROVEMENT OF REACTION RATE WITH GAS FLOW RATE FOR A SPHERICAL PARTICLE WHOSE REACTION IS CONTROLLED BY BOUNDARY LAYER MASS TRANSFER (COPPER AND MULL¹⁴)

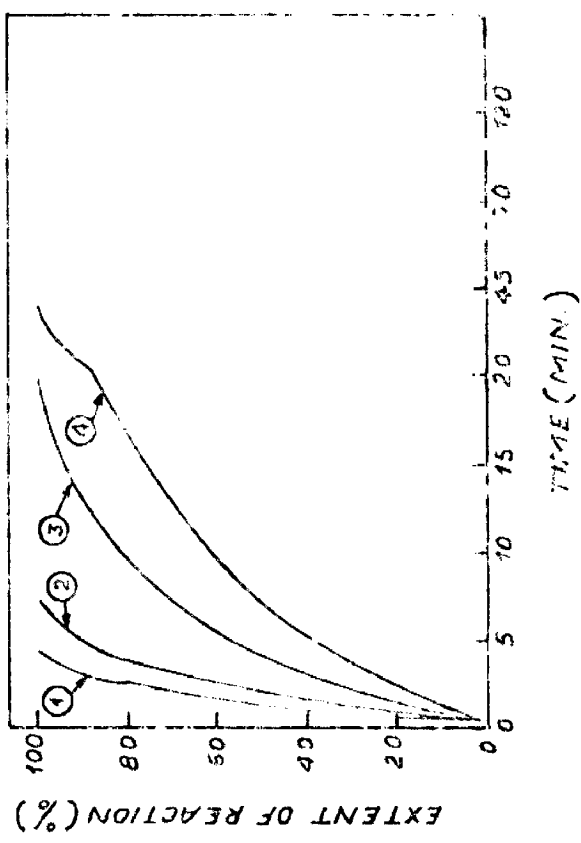


FIG. 13 PLOT OF THE EXTENT OF REACTION AGAINST TIME. THE EFFECT OF PELLET SIZE AND INITIAL FACILITY. (REF. 45)

NO.	TEMP °C	R_p (CM)	P_i INITIAL
1	229	0.711	0.723
2	301	1.179	0.734
3	303	0.800	0.334
4	253	1.110	0.384

where,

D	Diffusion coefficient
A	Surface area of sulphide pellet
ϵ_0	Porosity of the oxidised pellet
β	Labyrinth factor = Viscosity x Porosity of Sulphide pellet
ΔC	Difference in concentration of gaseous product.
SO_2	at reaction front and at the exposed surface.
x	length of diffusion

Thus the rate is directly proportional to porosity.

2.4.4 Pellet Diameter

It has been found that under same experimental conditions of temperature, gas composition etc.etc. smaller is the diameter of the reacting pellet⁴⁶, faster will be the oxidation rate as more surface area is exposed per unit volume Figure 13.

2.4.5 Effect of Oxygen Enrichment

Partial pressure of Oxygen in air influences the oxidation kinetics greatly⁴⁶. Upto certain limit, rate increases linearly with increase in oxygen partial pressure beyond which effect is very little and almost negligible at higher partial pressures because reaction leads to be zero order. This is shown in Figure 14.

2.4.6 Effect of Impurities⁴⁷

Main impurities associated with the mineral chalcocite are $As_2 S_3$, $Sb_2 S_3$, FeS , ZnS , MnS , SnS etc., etc. Hot SiO_2 and Fe_2O_3 which are almost always present in roasting operation act as catalysts and increase the rate of oxidation

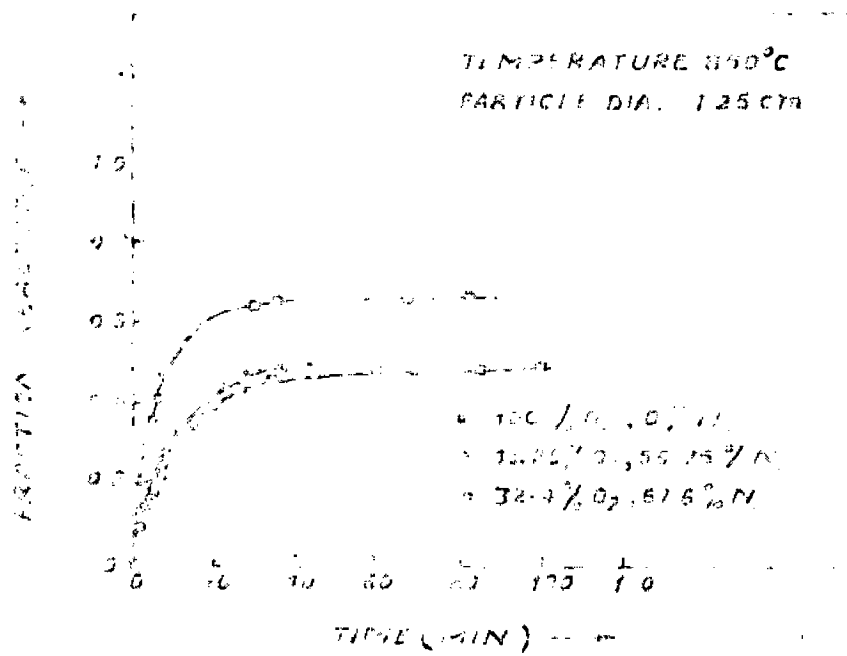


FIG. 1. FRACTION REACTED VS TIME PLOTS FOR PELLETS REACTED IN DIFFERENT O₂/N₂ MIXTURES (REFERENCE 4)

of copper sulphide.

2.5 METHODS OF STUDYING OXIDATION KINETICS

Various methods have been employed to study the oxidation kinetics. One of the earliest and probably most commonly used, is the gravimetric technique. Other methods are volumetric, Manometric, Electrolytic and electron diffraction.

2.5.1 Thermogravimetric Technique

By this method, change in weight due to oxidation of sulphide may be made with the help of special single pan balance⁴⁸. (Owa labor. type 707.04) which can record change in weight to a sensitivity of 0.1 mg Figure 15.

Gulbransen⁴⁹ has designed a vacuum microbalance which is more sensitive. Figure 16. Here the specimen is suspended from the beam of a very sensitive, all quartz micro-balance operating in all glass vacuum system. The tube is then sealed off. A scale micrometer microscope is used to observe the beam position relative to a fixed point on the supporting frame.

2.5.2 Volumetric and Manometric Methods

The consumption of oxygen during oxidation may also be followed by volumetric and manometric methods. The apparatus consists of a reaction chamber, connected

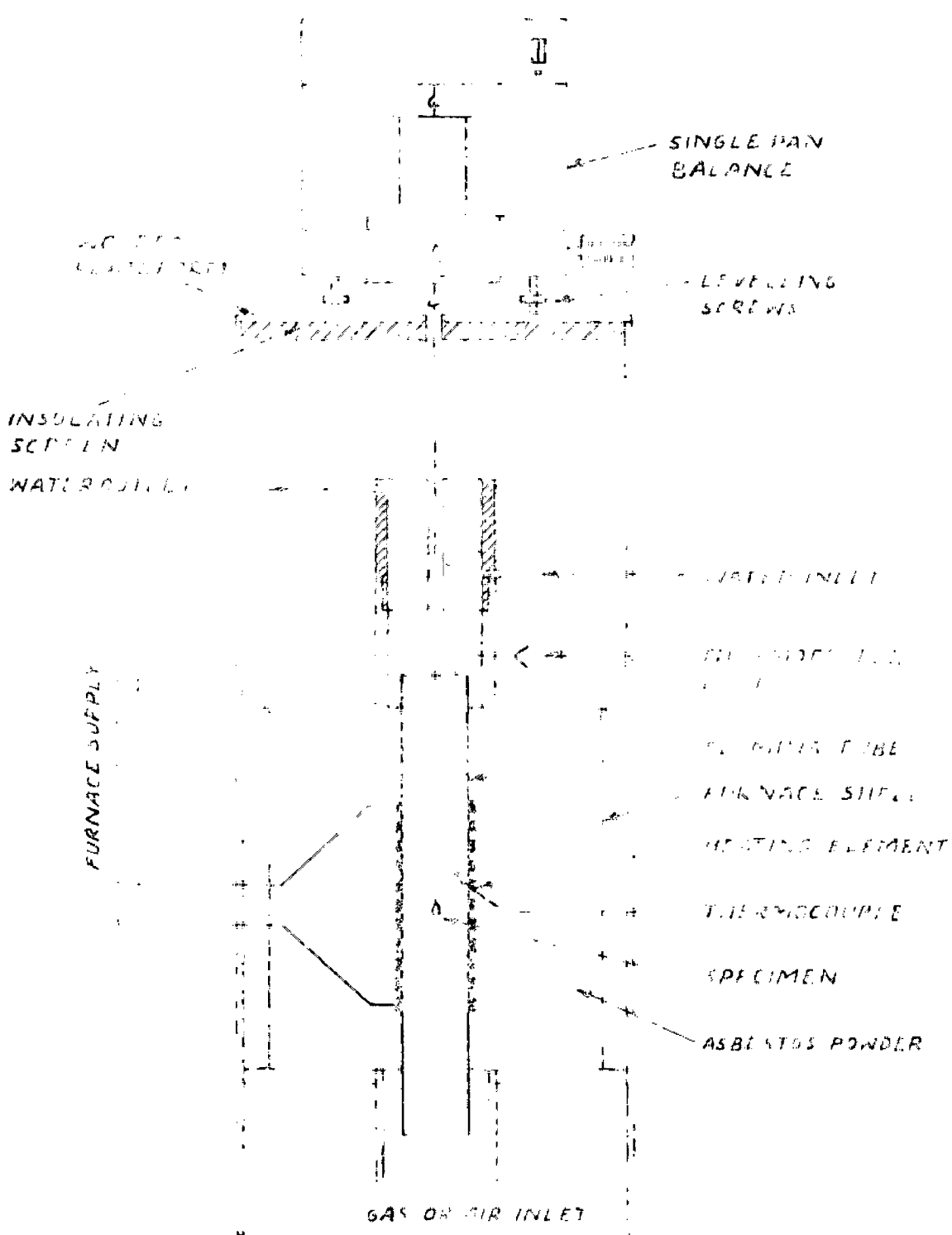


FIG 15 THERMOGRAVIMETRIC METHOD⁴⁶

to a reservoir of reactor gas. The reaction is followed by measuring the pressure drop or volume consumed. Apparatus used by Kubaschewski⁵⁰ and others is shown in Figure 17.

2.5.3 Electrometric Method

This method consists in determining the quantity of electricity needed to reduce the oxidation product either to metallic state or to a lower state of oxidation. Campbell and Thomas⁵¹ have designed an electrolysis cell as shown in Figure 18.

$$\begin{aligned} \text{The film thickness, } \bar{x}, \text{ in } \overset{\circ}{\text{A}} \text{ is given by} \\ \bar{x} = \frac{ItM \times 10^5}{2A \times 96500} \end{aligned} \quad (39)$$

where,

I Current in milliamperes

t time in seconds

M Weight in gms of oxidation product giving 1 g atom of oxygen or equivalent on reduction.

A Area in Cm^2 .

2.5.4 Electrical Resistance Method

According to Anderson³⁵, the sulphides of the transition metals possess moderate or high electronic conductivity and progressive changes in the semi-conductivity reflect the course of chemical reactions, following the initial step of chemisorption. See Figure 8. Thus change in electrical resistance of a pellet after heating for various time can be used to measure the oxidation velocities.

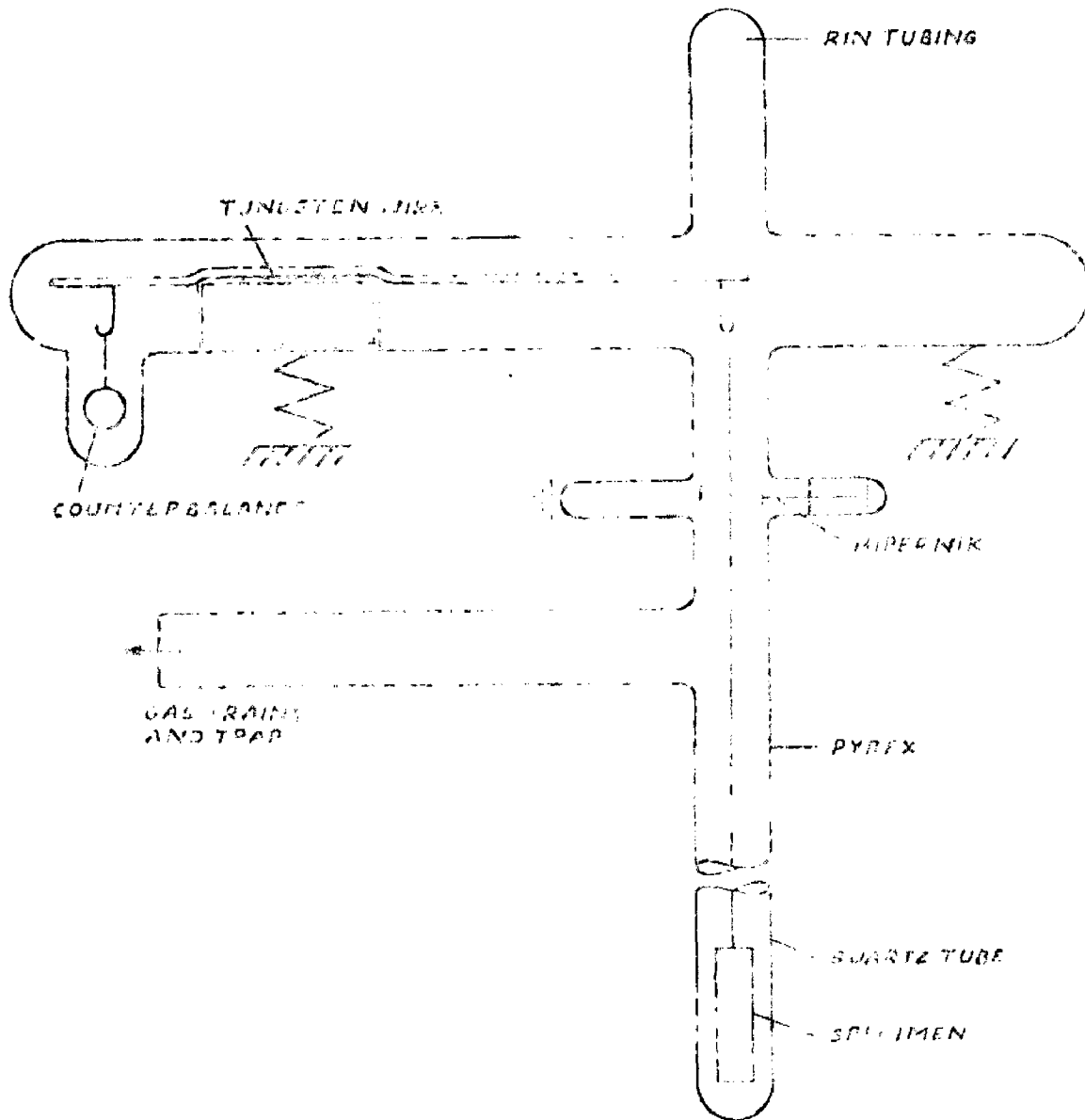


FIGURE 1. GRAVIMETRIC TECHNIQUE OF STUDYING OXIDATION KINETICS USING VACUUM MICROBALANCE (AFTER GULBRANSEN⁴⁹)

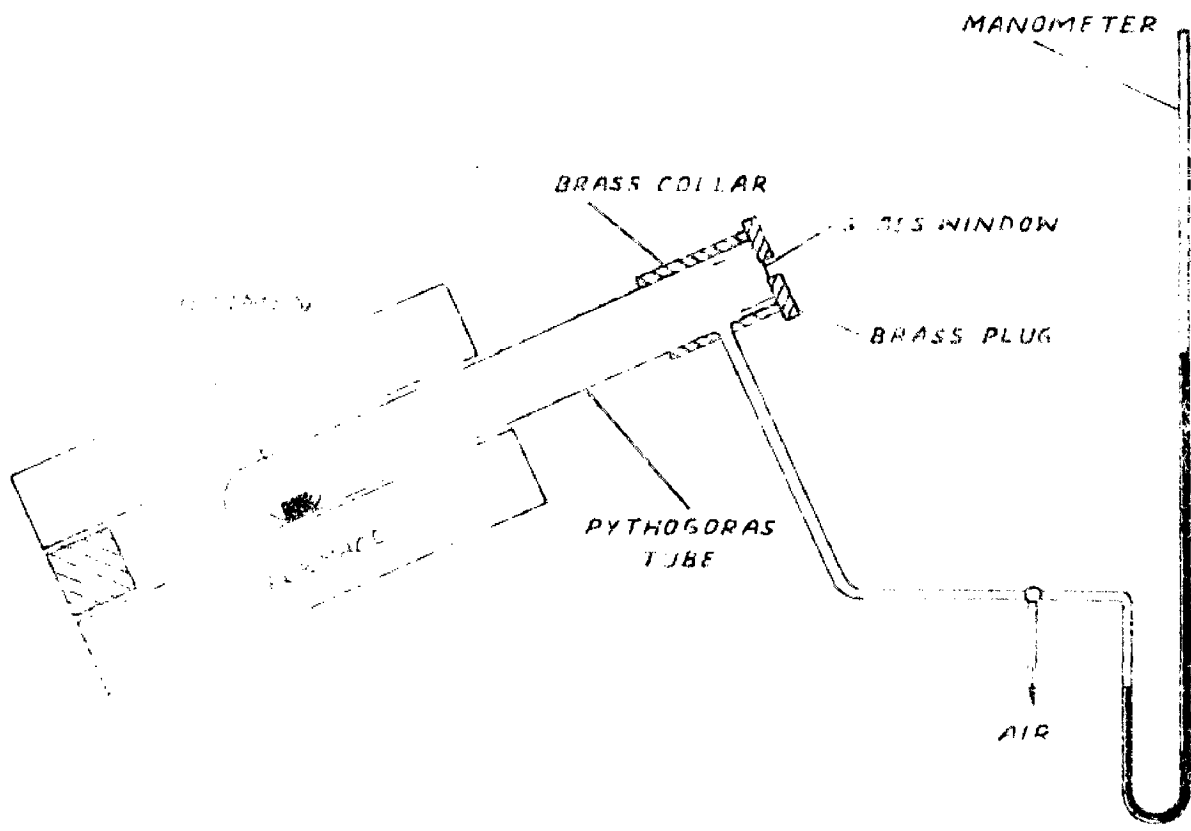


FIG 31 MANOMETRIC EQUIPMENT
 (KUBASCHEWSKI⁵⁰)

CHAPTER - III

EXPERIMENTAL WORK

3.1 INTRODUCTION

Out of the numerous methods employed to study the oxidation kinetics of sulphide minerals, thermogravimetric methods have been generally applied using a special balance which can record weight change to an accuracy of 0.1 mg. But in case of copper sulphide, thermogravimetric technique cannot be applied to study the reaction kinetics because overall reaction follows with no weight change, viz.,



Evidently $\Delta W = 0$

This is also manifested in the thermogram obtained at 850°C (Figure 19) by suspending a pellet of known weight into a vertical furnace by nichrome wire, the other end of which is attached to a very sensitive electronic single pan balance (Owa labor. type 707-04) placed vertically above the reaction chamber (Figure 15).

Thus the reaction rate was measured by estimating SO₂ quantitatively by absorption in iodine solution of known normality. The unreacted iodine solution was titrated against N/10 Sodium thiosulphate solution to determine the volume of iodine reacted with SO₂.

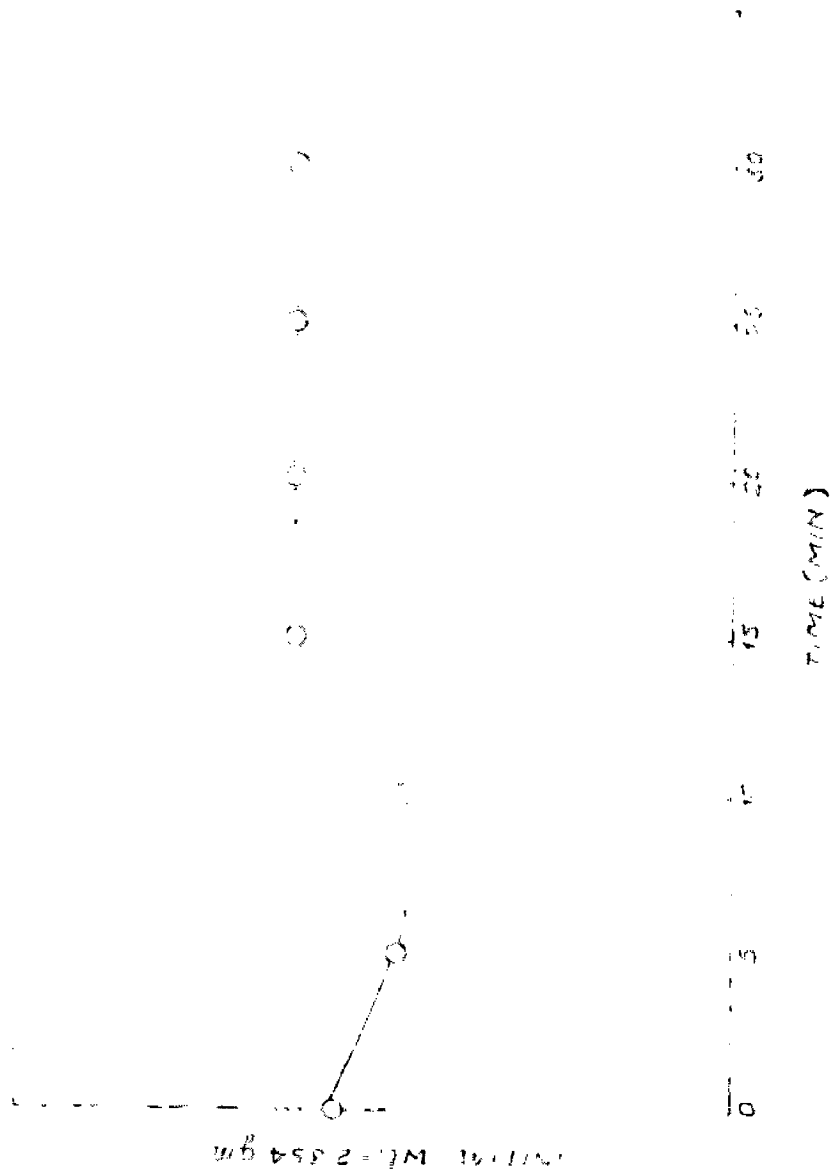


FIG. 19 THERMOGRAM SHOWING THE CHANGES IN HEIGHT THAT FOLLOW DURING OXIDATION OF CARBON MONOXIDE BLEND IN A STREAM OF AIR AT 15°C

If Z corresponds to the burette reading, V, the volume of iodine solution of normality N, then,

Volume of iodine consumed by N/10 sodium thiosulphate solution

$$= \frac{Z}{10N} \text{ cc}$$

Volume of iodine consumed by SO₂ = $\left(V - \frac{Z}{10N} \right)$ cc

We know that 1 cc of N-iodine solution = 0.03203 gm SO₂

Therefore Amount of SO₂ evolved = $0.03203 N \left(V - \frac{Z}{10N} \right)$ gm

(40)

3.2 MATERIALS USED

The details of the materials used in this investigation are as follows : -

Material	Purity	Make
Copper sulphide	Cu= 98.7% as Cu ₂ S Fe= 1.3% as FeS (By spectrographic analysis)	Vimu Chemicals, Bombay-2
Iodine crystals	99.9% Medicinal grade.	Janta Medical Hall, Roorke
Potassium Iodide	A.R.	Feeta Lab. Chemicals, Bombay-2.
Anhydrous Calcium Chloride	A.R.	Belami and Co, Bombay-4.
Sodium thiosulphate Crystals	A.R.	Apex Chemicals, Bombay-1

Concentrated H ₂ SO ₄	A.R.	Vimu Chemicals-Bombay-2.
Hydrochloric Acid	A.R.	-do-
Pyrogallol Solution	A.R.	-do-

Attempt was made to convert all FeS of copper sulphide to FeO by roasting the powder 450°C in a stream of air where oxidation of FeS is favoured but this resulted in the formation of copper sulphate which inevitably forms at lower temperatures of oxidation. Since the amount of FeS is very low so it was safely assumed that it does not greatly interfere with the reaction kinetics. This assumption appears justified in the sense that in a mixture of these two sulphides, FeS is always oxidised first just instantaneously but it does slightly increase the initial oxidation rate of cuprous sulphide by adding extra heat to that liberated alone by cuprous sulphide by increasing heat transfer which is the rate controlling step in the beginning¹⁶.

3.3 PREPARATION OF THE PELLETS

Copper sulphide powder was screened and -100 to +150 mesh size was selected for the present work. The powder was dried for about 3 hours at 110°C in a drier. About 4.5 gms of finely powdered copper sulphide was then compacted in a cylindrical die of diameter 1.55 cm to produce approximately unit height to diameter cylindrical pellets. Compacting was done, in each case, by applying a load of 1 T in a universal Testing machine (Model 2D 20 Tons, Make GDR) The pellets were having sufficient

strength to permit handling.

3.4 POROSITY MEASUREMENTS OF PELLETS

The bulk porosity of the pellet is readily measured by weighing, provided the volume of the sample is known and information is available on the true solid density⁴⁵. If w gms is the weight of the pellet, d is the dia of pellet and h the height of pellet, then,

$$V_p, \text{ Volume of the pellet} = \frac{\pi d^2 h}{4} \text{ c.c.}$$

$$\rho_p, \text{ Density of the pellet} = \frac{w}{\frac{\pi d^2 h}{4}} = \frac{4w}{\pi d^2 h} \text{ gm/cc}$$

$$\rho_s, \text{ True density of solid}^{42} = 5.8 \text{ gm cm}^{-3}$$

$$\text{Therefore \% age porosity} = \frac{\rho_s - \rho_p}{\rho_s} \times 100 \quad (41)$$

Porosity was varied by compacting the same amount of powder at different loads. Height and dia of the pellets were accurately measured by micrometer.

3.5 EXPERIMENTAL SET UP

The complete experimental set up is shown in the Figure 20, a, b, c. The line diagram is shown in Figure 21. It consists of the following units -

- a. Air Compressor
- b. Air purification train

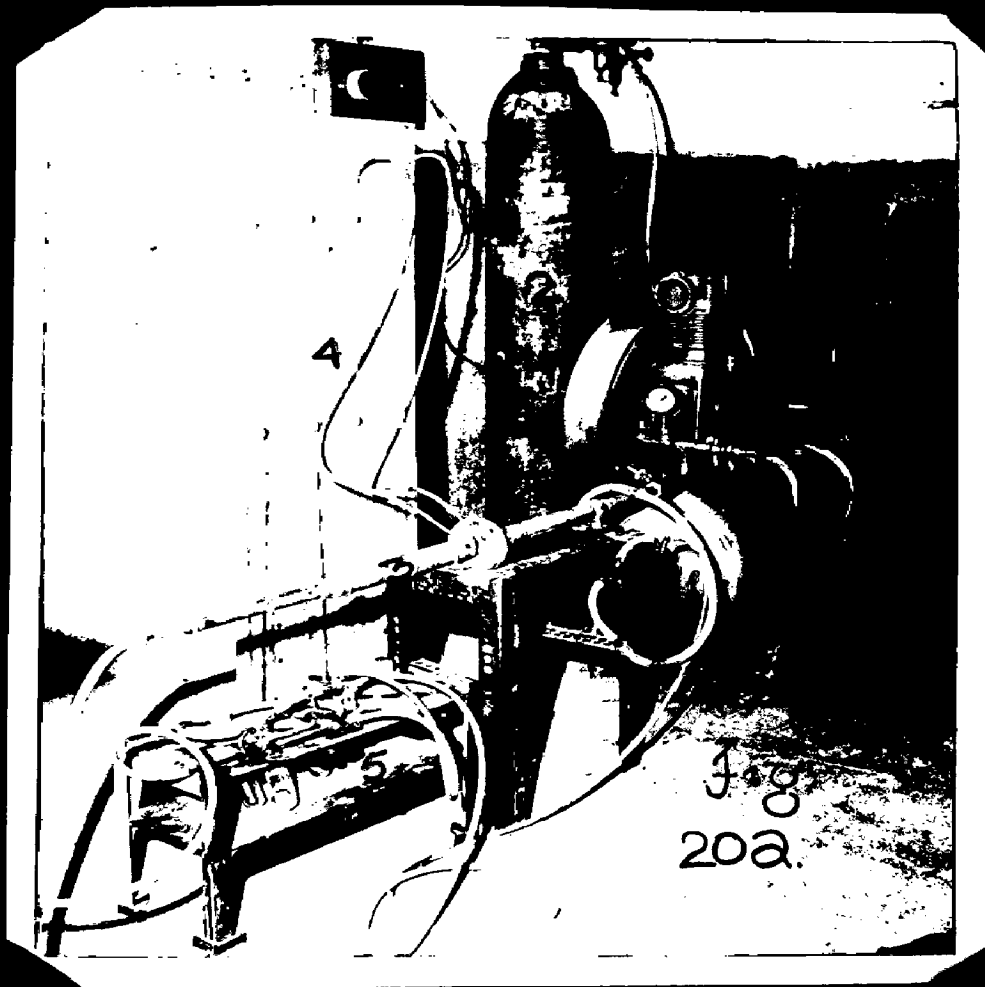
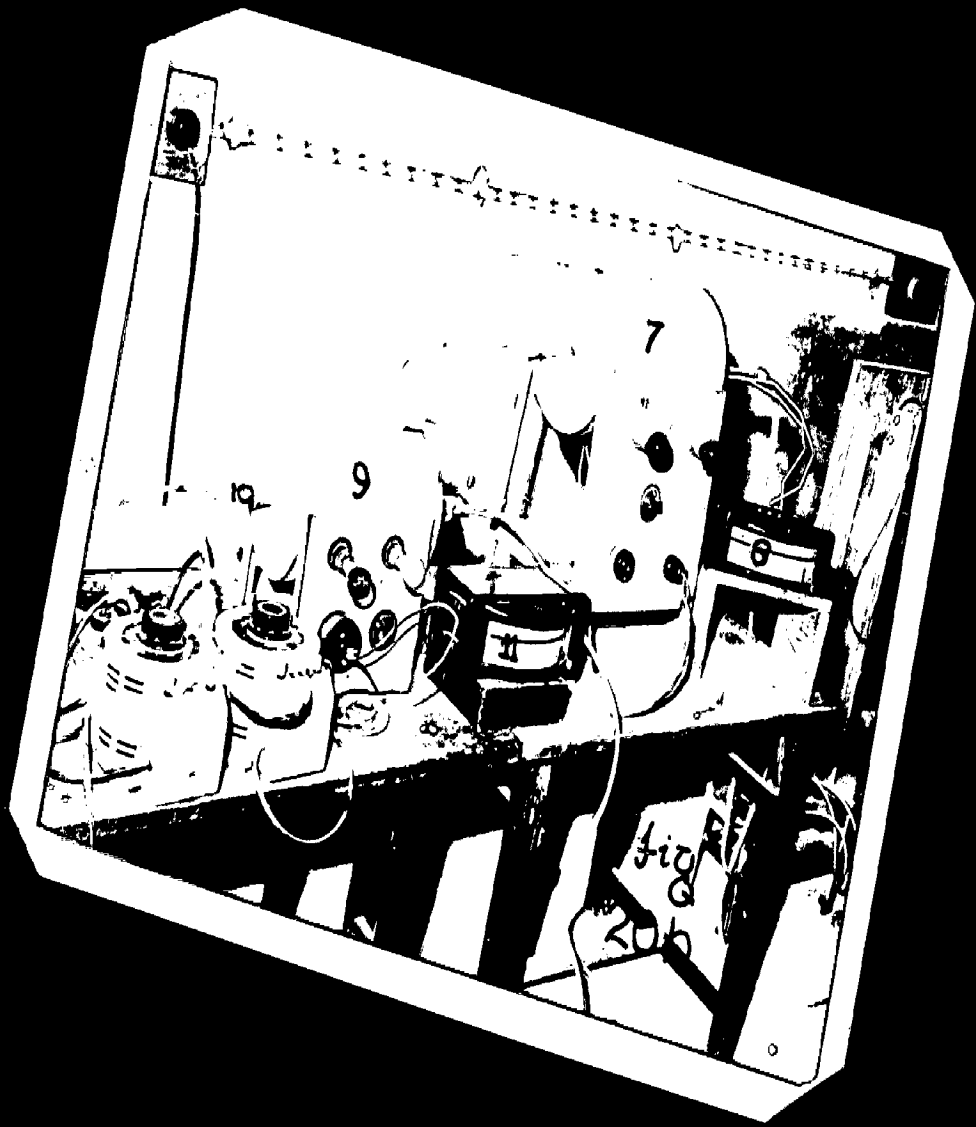
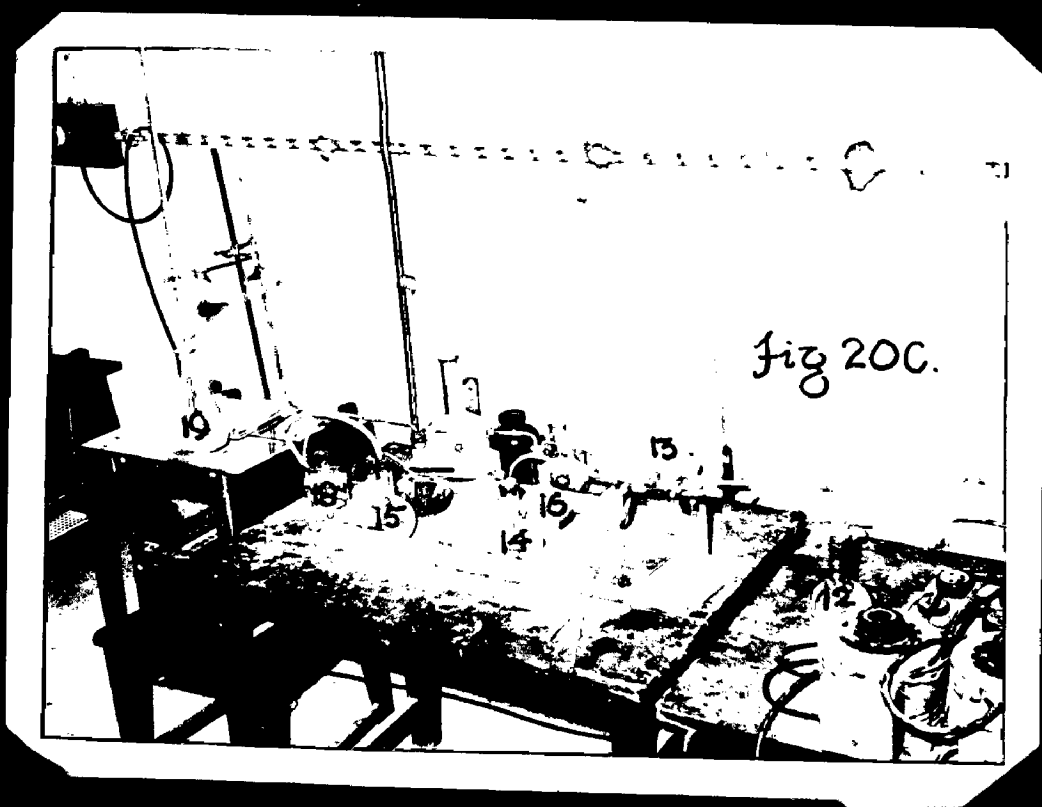


Fig
202.





- 20 , a,b,c - 1. Air Compressor , 2. N₂ Cylinder
 3. Orifice meter , 4. Manometer, 5. Air and N₂
 purification unit. , 6. Two way cock for Air
 and N₂ . , 7. Preheating furnace , 8. Chromel-
 Alumel Temperature recorder , 9. Reactor,
 10. Silica Tube, 11. Pt-Pt/13% Rh Temp.recorder
 12. Distilled Water bubbler to clean SO₂
 13. Two-fold distribution valve , 14-15, One set
 of Absorption unit, 16-17, 2 nd set of Absorption
 unit, 18. SO₂ Trap. 19. Titration Unit.

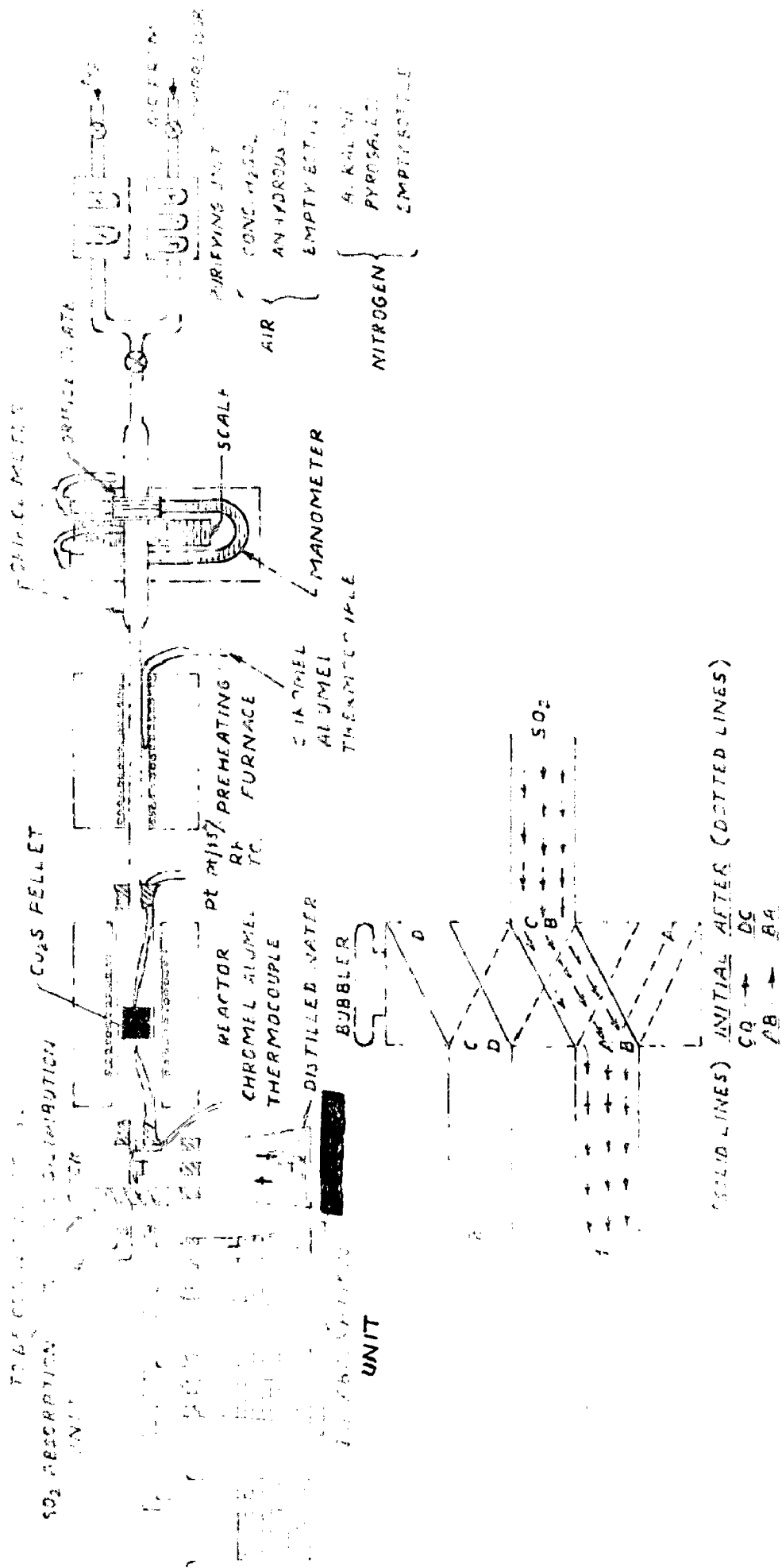


FIG. 21 SCHEMATIC DIAGRAM OF THE EXPERIMENTAL SETUP

- c. Flow meter with Manometer
- d. Preheating Furnace.
- e. Reactor
- f. Filtration Assembly.

3.5.1 Air Compressor

Oxidation of copper sulphide pellets was carried out in stream of air. This air was supplied by an air compressor. The rating of the compressor is

$$\text{H.P.} = 1$$

$$\text{R.P.M} = 75$$

$$\text{Max. Pressure} = 75 \text{ psi}$$

3.5.2 Air Purification Train

It consisted of concentrated sulphuric acid bubbler for removal of moisture in air and an anhydrous CaCl_2 tube to remove the traces of moisture left, if any. Empty bottles were connected on both sides of sulphuric acid bubbler to avoid flow of H_2SO_4 to the flowmeter and anhydrous CaCl_2 tube.

Nitrogen was purified by passing it through alkaline pyrogallol solution.

3.5.3 Flowmeter with Manometer

In order to measure the air flow rate, an orifice meter was designed and fabricated. The design is shown in the Figure 22. A U-tube manometer was attached to record

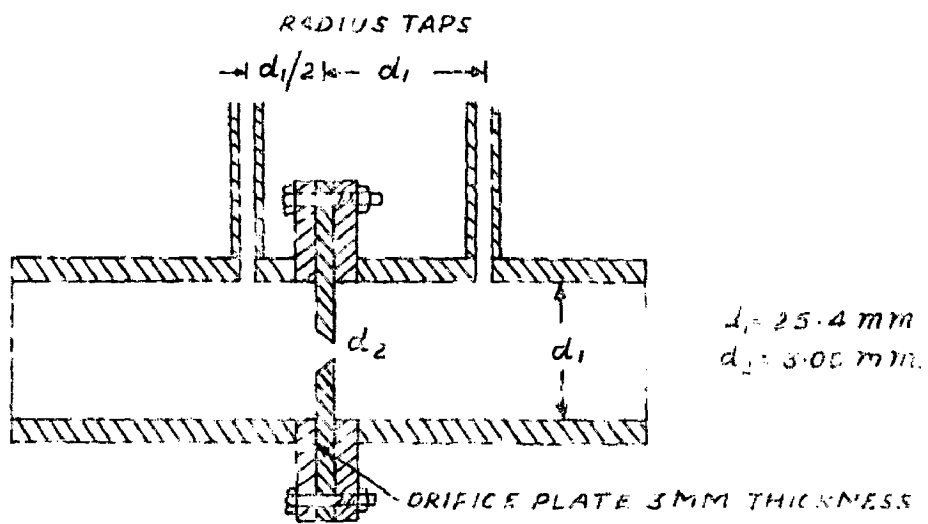


FIG. 22 DESIGN OF THE DRIFEMETER

drop in pressure on both sides of the orifice and this, in turn, was calibrated against Toshniwal wet gas flow meter (Type No. GG05.025, Capacity = 2.5 l/rev. Min. Dial Division = 0.02 Lit. and Accuracy = $\pm 5\%$). It could record minimum air flow rate of 250 cc per minute.

3.5.3 Pre-heating Furnace

It consisted of a mild steel tube of 1.25 cm diameter and overall length of 150 cm placed in a sillmenite tube furnace of 2.54 cm internal diameter. The temperature in the tube was recorded by chromel-alumel thermocouple and controlled by energy regulator within the limits of $\pm 5^{\circ}\text{C}$.

3.5.4 Reactor

It consisted of 25 mm diameter and 55 cm long silica tube placed in a 1.1 KW muffle furnace of 30 mm diameter and overall length of 30 cm. The furnace has resistance of 15 ohms. The muffle was externally wound by 18 SWG Kanthal wire. Pt-Pt/13% Rh thermocouple was introduced from the air admittance part, to minimise the leakage of SO_2 , if any, through thermocouple beads. The silica tube was fitted with referactory corks at its both ends. Stainless steel tubes of 6 mm dia were passed from centres of corks at both ends to entrain air and to make exit of the product gases. The all joints, tube connections and cork fittings were made perfectly gas tight by

affixing plaster of paris. Leakage of SO_2 was checked by wrapping potassium dichromate paper round the exit joint.

3.5.5 Titration Assembly

This assembly was designed with view point to record continuously the amount of SO_2 in various time intervals.

The reactor effluent gases first passed through distilled water bubbler to clean SO_2 then to a two fold distribution valve to a series of SO_2 absorbers as shown in Fig. 21.

3.5.6 Absorbers - Each fold was connected to a series of SO_2 absorbers. SO_2 absorber consisted of a 500 cc flat-bottomed flask containing a measured volume of iodine solution, normality of which is determined by titrating 25 cc of iodine solution against decinormal $\text{Na}_2\text{S}_2\text{O}_3$ solution, before the start of experiment.

To increase the absorption power, iodine solution was diluted several times with water and acidified with dilute HCl.

To ensure that SO_2 is not leaking to the atmosphere, a beaker containing 25 cc iodine solution was placed in series and the balance was titrated against N/10, $\text{Na}_2\text{S}_2\text{O}_3$ solution to estimate amount of SO_2 escaped to the atmosphere and to apply appropriate correction for the same.

It is found that in this titrimetric procedure adopted minimum SO_2 of the order of 1.6×10^{-4} gm can be estimated.

3.6 OXIDATION PROCEDURE

1. Pellet was weighed accurately on a single pan analytical electronic balance and its height and diameter determined accurately by micrometer.
2. 25 cc of iodine solution was pipetted out in a beaker and titrated against N/10 sodium thiosulphate solution taking starch solution as indicator. End point was indicated when dark blue colour of the solution becomes white. This determined the normality of iodine solution.
3. Each of the SO_2 absorber was filled up with 50 cc of iodine solution of known normality, diluted several times with distilled water, acidified with HCl and placed in series.
4. Preheating furnace and reactor furnace were switched on and air was flushed with nitrogen.
5. Pellet was transferred into the silica tube into the centre of the combustion zone, and titration assembly was attached to the exit tube via two fold distribution valve and distilled water bubbler.
6. Connections were made perfectly gas tight by applying plaster of paris, superheated wax and quick fix cement.

7. Temperature of the reactor was raised slowly to the desired one. When the temperature was stabilised, air flow rate was adjusted to 500 ml per minute.
8. At zero time, nitrogen was replaced by air and stop watch started, indicating the beginning of reaction.
9. After some fixed interval say 10 minutes, the cock was reversed and product gases redirected to the second set of SO_2 absorbers. Mean while the first absorption unit was detached and balance of the iodine unreacted by SO_2 was titrated against N/10, $\text{Na}_2\text{S}_2\text{O}_3$ solution to know the volume of iodine reacted by SO_2 and thus the amount of SO_2 liberated in 10 minutes. was estimated according to Equation 40. This absorption unit again filled in as in step 3 and replaced in original position . Agains the cock was reversed say after next 15 minutes and the product gases were channelised to the first absorption unit and likewise the 2nd absorption unit was detached and balance titrated against N/10 $\text{Na}_2\text{S}_2\text{O}_3$ solution.
10. The same process was continued for about 6 hours and at the end of experiment, the air flow was replaced back to the nitrogen flush in order to collect last traces of SO_2 , if any.

CHAPTER - IV

CALCULATIONS

CALCULATIONS4.1 CALCULATIONS FOR NON ISOTHERMAL PERIOD

In this section theoretical rates based on heat and mass transfer has been calculated from the physico-chemical data under experimental conditions and have been compared with experimental rates.

Diameter of the pellet	1.552 Cms.	
Weight of the pellet	4.1 gm.	
Height of the pellet	1.04 cm	From Gilliland's
Diffusivity of oxygen in air	0.83 cm ² sec ⁻¹	formulae ⁴²
Temperature under considerations	850°C	
Air flow rate through the reaction tube	0.5 l mt ⁻¹	
Diameter of the reaction tube	25 mm	
Viscosity of air at 850°C	$\mu_{850^\circ\text{C}}^{\text{air}}$.00044 poise

Kinematic viscosity	$\nu_{850^\circ\text{C}}^{\text{air}}$	0.388
---------------------	--	-------

Reynold's number, Re	$= \frac{V_G d}{\nu}$	$= \frac{500 \times 1.552}{\frac{\pi}{4} \times 2.5^2 \times 60 \times 0.388}$
		$= 06.825$

$$\text{Schmidt Number, } Sc = \frac{v_{850^{\circ}\text{C}}}{\left[D_{\text{O}_2 / \text{Air}} \right]_{850^{\circ}\text{C}}} = \frac{.388}{.83}$$

$$= 0.4675$$

$$\text{Sherwood Number, } Sh = 2 + 0.69 (Re)^{1/2} (Sc)^{1/3}$$

$$= 2 + 0.69 \times 2.62 \times .775$$

$$= 3.41$$

$$\text{Mass Transfer coefficient}^{14} = \frac{Sh \left[D_{\text{O}_2 / \text{Air}} \right]}{d}$$

$$\therefore \alpha = \frac{3.41 \times .83}{1.552} = 1.82$$

$$\left[D_{\text{eff}} \right]_I^{41} = \frac{\left[D_G \right] v^2}{\tau}$$

$$v = \text{Porosity factor} = 0.6$$

$$\tau = \text{Tortuosity factor} = 3$$

$$\therefore \left[D_{\text{eff}} \right]_I = \frac{6.83 \times (.6)^2}{3} = 0.0996 \text{ cm}^2 \text{ sec}^{-1}$$

DIFFUSION AND MASS TRANSFER CALCULATIONS

$$\dot{\eta} = \frac{\left[P_{\text{O}_2} \right]_G}{\frac{R_{\text{O}_2}}{4 \pi \left[D_{\text{eff}} \right]_I r_0 \left[\left(\frac{1}{r^*} - 1 \right) + \frac{\left[D_{\text{eff}} \right]_I}{\alpha_1 r_0} \right]}}$$

Now,

$$\begin{aligned}
 [P_{O_2}]_{Air} &= 0.21 \text{ atm.} \\
 R &= 82.03 \text{ cm}^3 \text{ atm. g-mole}^{-1} \text{ K}^{-1} \\
 \theta_G &= 850 + 273 = 1123^\circ\text{K} \\
 [D_{eff}]_I &= 0.996 \text{ cm}^2 \text{ sec}^{-1} \\
 \alpha_1 &= 1.82 \text{ cm sec}^{-1} \\
 r_o &= 1.552/2 = 0.776 \text{ cm.}
 \end{aligned}$$

Substituting these values, we get,

$$\begin{aligned}
 \dot{\eta} &= \frac{0.21}{\frac{82.03 \times 1123}{4 \pi \times 0.0996 \times 0.776} \left[Y + \frac{.0996}{1.82 \times .776} \right]} \\
 &= \frac{2.22 \times 10^{-6}}{Y + 0.07053}
 \end{aligned}$$

From experimental plot between $1 - (1-f)^{1/3}$ Vs. t ($r^* = (1-f)^{1/3}$)

At minutes	$1 - r^*$	r^*	$Y = \frac{1}{r^*} - 1$	$\dot{\eta}$ gm-mole sec ⁻¹
2.5	0.012	0.988	0.01214	2.55×10^{-5}
5	0.026	0.974	0.02672	2.28×10^{-5}
10	0.050	0.950	0.05263	1.8×10^{-5}
15	0.074	0.926	0.07981	1.41×10^{-5}

Mean theoretical rate at 850°C , $\dot{\eta}_{850^\circ\text{C}} = 2.01 \times 10^{-5}$ g.molesec

HEAT TRANSFER CALCULATIONS

Specific heat of air at 850°C . $C_{p850^{\circ}\text{C}} = 0.269 \text{ Cals. gm}^{-1} \text{ deg C}^{-1}$

$\mu_{850^{\circ}\text{C}} = 0.00044 \text{ poise}$

Thermal conductivity of air at 850°C $= 1.7 \times 10^{-4}$

$\text{Cals cm}^{-1} \text{ sec}^{-1} \text{ C}^{-1}$

$$Pr = \frac{C_p \mu}{k} = \frac{0.269 \times 0.00044}{1.7 \times 10^{-4}} = 0.695$$

$$Re = 6.825$$

We know that,

$$\frac{h_{\text{convection}} \cdot d}{k_G} = 2 + 0.6 (Re)^{1/2} (Pr)^{1/3}$$

$$= 2 + 0.6 \times 2.618 \times 0.88$$

$$= 3.38$$

$$h_{\text{convection}} = \frac{3.38 \times 1.7 \times 10^{-4}}{1.552} = 3.68 \times 10^{-4} \text{ Cals.}$$

$$\text{and } h_{\text{radiation}} = 4 \epsilon \sigma \theta_G^3$$

where

$$\epsilon = \text{Emmissivity of copper sulphide} = 0.2$$

$$\sigma = \text{Stefans Boltzman Constant} = 1.36 \times 10^{-12} \text{ Cals Cm}^{-2}$$

$$\theta_G = 850 + 273 = 1123^{\circ}\text{K} \quad \text{sec}^{-1} \text{ K}^{-4}$$

107442

Therefore,

$$h_{\text{radiation}} = 4 \times 0.2 \times 1.36 \times 10^{-12} \times (1123)^3$$

$$= 1.54 \times 10^{-3} \text{ Cals cm}^{-2} \text{ sec}^{-1} \text{ C}^{-1}$$

$$\text{also } h = h_{\text{convection}} + h_{\text{radiation}}$$

$$= 15.4 \times 10^{-4} + 3.68 \times 10^{-4}$$

$$= 1.908 \times 10^{-3} \text{ cal s cm}^{-2} \text{ sec}^{-1} \text{ C}^{-1}$$

Thermal conductivity of product solid (CuO)^{52,42}

$$= K_{\text{CuO}} \quad 850^{\circ} \text{C} = 102 \times 10^{-4} \text{ watts cm}^{-1} \text{ }^{\circ}\text{C}^{-1}$$

$$= \frac{102 \times 694 \times 10^{-4}}{2903} = \frac{\text{g-cal}}{\text{sec. cm}^2 \frac{\text{deg C}}{\text{cm}}}$$

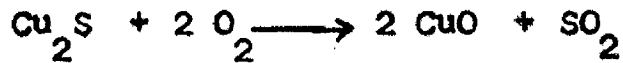
$$= 24.40 \times 10^{-4} \text{ g-cal sec}^{-1} \text{ cm}^{-1} \text{ deg}^{-1} \text{ C}^{-1}$$

(From International Critical Table⁵⁹)

Thermodynamic Data⁵³

	$-\Delta H_{298}^{\circ}$	S_{298}°	$C_p = a + bt - ct^{-2}$			Temperature Range $^{\circ}\text{C}$
			a	$b \times 10^3$	$c \times 10^{-5}$	
Cu	0	7.97	4	1.5	-	25 - 1084
Cu ₂ O	40,400	22.45	14.90	5.70	-	25 - 900
CuO	37,600	10.2	9.27	4.80	-	25 - 980
Cu ₂ S	19,600	28.5	20.3	-	-	350 - 1130

Overall reaction is,



$$\begin{aligned} \therefore -\Delta H_{298}^{\circ} &= 2 \times 37600 + 70950 - 19600 - 2(0) \\ &= 12,6550 \text{ Cals-g-mole}^{-1} \end{aligned}$$

(Assuming ΔH is independent of temperature)

Now reaction rate based on Heat Transfer is given by

$$\dot{\eta} = \frac{\Theta_R - \Theta_G}{\frac{H}{6 \pi k_{\text{CuO}} r_o} \left[\left(\frac{1}{r^*} - 1 \right) + \frac{k_{\text{CuO}}}{hr_o} \right]}$$

$$\Theta_R = \text{Temperature at the reaction front} = 980^{\circ}\text{C}$$

$$\begin{aligned} \therefore \dot{\eta} &= \frac{980 - 850}{\frac{126550}{6 \times 3.14 \times 24.4 \times 10^{-4} \times 0.776} \left[Y + \frac{24.4 \times 10^{-4}}{1.908 \times 10^{-3} \times 0.776} \right]} \\ &= \frac{0.3665 \times 10^{-4}}{Y + 1.65} \end{aligned}$$

Time (t) minutes	$r^* = (1-f)^{1/3}$	$Y = \frac{1}{r} - 1$	$\dot{\eta}_t$ (g-mole sec ⁻¹)
2.5	0.988	0.01214	2.20×10^{-5}
5.0	0.974	0.02672	2.18×10^{-5}
10.0	0.950	0.05263	2.50×10^{-5}
15.0	0.926	0.07981	2.11×10^{-5}

TABLE - 18

Time (t) Min.	Travel of reaction front $r_t = 1.552 r^*$ Cm	Volume of core reacted (V) cm ³	Experimental Rate $\dot{\eta} = \frac{V d_o}{\exp 60 t}$ g-mole sec ⁻¹	Theoretical rate (diffu- sion and Mass Trans- fer) $\dot{\eta}_{dmt}$ g-mole sec ⁻¹	Theoretical rate (Heat transfer) $\dot{\eta}_{ht}$, g-mole sec ⁻¹
2.5	1.533/2 = 0.7665	0.43603	8.25×10^{-5}	2.55×10^{-5}	2.20×10^{-5}
5.00	0.7508	0.771234	5.13×10^{-5}	2.28×10^{-5}	2.18×10^{-5}
10.00	0.7372	0.635376	2.75×10^{-5}	1.80×10^{-5}	2.50×10^{-5}
15.00	0.7185	0.85408	3.74×10^{-5}	1.41×10^{-5}	2.11×10^{-5}

MEAN			3.72×10^{-5}	2.01×10^{-5}	2.25×10^{-5}

4.2 CALCULATIONS FOR IOSTHERMAL PERIOD

TABLE - 19

(PLOT : $\left(\frac{1}{r^*} - 1\right)$ Vs $\frac{P_{O_2}}{\dot{\eta}}$)

$$r'_0 = r_{20} = r_{20}^* \times r_0 = 0.897 \times 1552/2 = 0.696984 \text{ Cm}$$

$$r^* = \frac{r_t}{r'_0}, \quad r_t = r_t^* \times r_0, \quad r_0 = 1.552 \text{ Cm}, \quad P_{O_2} = .21 \text{ Atm}$$

$$d_0 = \text{molar density} = 0.01315 \text{ g-mole cm}^{-3}$$

r_t^*	r_t Cm	$\frac{1}{r^*} - 1$ $= \frac{r'_0 - r_t}{r_t}$	$\dot{\eta} = \frac{w(r_{20}^2 - r_t^2) h \cdot d_0}{(t-20) \times 60}$ gm.mole sec ⁻¹	$\frac{P_{O_2}}{\dot{\eta}}$ atm.g-mole ⁻¹ sec.
0.880	0.682	0.01922	3.75×10^{-6}	55.92×10^3
0.858	0.665	0.04506	3.62×10^{-6}	58.0×10^3
0.838	0.650	0.07072	3.552×10^{-6}	59.1×10^3
0.794	0.616	0.1246	3.29×10^{-6}	63.8×10^3
0.782	0.607	0.1466	2.85×10^{-6}	73.6×10^3
0.778	0.605	0.1504	3.20×10^{-6}	65.6×10^3

Calculations (contd..) (Isothermal Period)

Slope of the plot between $\left(\frac{1}{r^*} - 1\right)$ and $\frac{P_{O_2}}{\dot{\eta}}$ i.e., slope of the straight line as calculated is $= 0.1012 \times 10^6$

$$\text{This slope} = \frac{R\theta_G}{4\pi [D_{\text{eff}}]_I r'_0}$$

$$\therefore D_{\text{eff}} \text{ (calculated)} = \frac{82.03 \times 1123}{4 \times 3.14 \times 0.1012 \times 10^6 \times 0.696}$$

$$= 0.0907 \text{ cm}^2 \text{ sec}^{-1}$$

$$\text{Also intercept} = 54 \times 10^3 = \frac{R\theta_G}{4\pi r_0^2 \alpha_1} + \frac{r_0 - r'_0}{4\pi r_0 r'_0 [D_{\text{eff}}]_I}$$

$$\text{or } 54 \times 10^3 = \frac{82.03 \times 1123}{4\pi \times (0.776)^2 \alpha_1} + \frac{0.776 - 0.696}{4\pi \times 0.776 \times 0.696 \times 0.0907}$$

$$\alpha_1 = 2.26 \text{ cm sec}^{-1}$$

TABLE - 20

	Experimental	Calculated
D_{eff}	$0.0907 \text{ cm}^2 \text{ sec}^{-1}$	$0.0996 \text{ cm}^2 \text{ sec}^{-1}$
α	2.26 cm sec^{-1}	1.82 cm sec^{-1}

As is conspicuous, a fair agreement is obtained between experimental and calculated values of D_{eff} and α values.

CHAPTER V

RESULTS AND DISCUSSIONS

In this Chapter the results of the present work are summarised in the first part followed by a brief discussion.

5.1 RESULTS

Figure 23 is the thermogram showing the changes in weight of the cuprous sulphide pellet that followed with time during oxidation in stream of dry air maintained at a flow rate of 500 cc/min. at 850°C.

Figure 24 is the percentage oxidation versus time plot at temperatures 750°C, 800°C, 850°C, 900°C and 950°C. The oxidation data, for this plot is presented in Tables 1-5.

Figure 25 represents the effect of air flow rate on the oxidation kinetics of cuprous sulphide in the range of 0.5 l mt⁻¹ to 1.5 l mt⁻¹. This plot is on the basis of the experimental data given in tables 13, 16 and 17, calculated values of $[1 - (1-f)^{1/3}]$ and $[1 - (1-f)^{1/3}]^2$ are given in Tables 6-10 and plots $[1 - (1-f)^{1/3}]$ versus t (min) and $[1 - (1-f)^{1/3}]^2$ versus t(min.) are represented by Figures 26 and 27 respectively.

Figure 28 gives the rise in temperature of the sample in each case when the temperature of the surroundings was maintained at 750°C, 800°, 850°, 900° and 950°C.

Figure 29 defines the boundaries of transition or non-isothermal period and isothermal period and nature of the $[1-(1-f)^{1/3}]$ versus t curve in the both periods.

This is in fact the superimposition of the plot 28 on plot 26 at 850°C . This helps to analyse the experimental results obtained in these two periods separately. Figure 30 is the $\log k$ versus $1/T$ plot for non-isothermal and isothermal periods respectively based upon the data given in Table 11

Figure 31 is the analysis of non-isothermal period and in this experimental rates in first 20 minutes are compared with heat and mass transfer rates obtained theoretically from equations (32) and (27) respectively. The calculated values are summarised in Table 18 and given in Chapter four .

Figure 32 is the $P_{\text{O}_2} / \dot{\eta}$ Versus $(\frac{1}{r^*}, -1)$ plot in the isothermal region. Calculated values from the experimental data for this plot are given in Table 19. Effective diffusion coefficient and mass transfer coefficient are calculated from the slope and intercept of this straight line plot are given and compared in Table 20.

Figure 33 gives the dependence of parabolic rate constants at 850°C on partial pressure of SO_2 in the product gases and Figures 34 and 35 represents the effect of variables viz., porosity and pellet dia on the oxidation kinetics of cuprous sulphide at 850°C . Experimental data for Figures 33, 34, & 35 are summarised in Tables 21, Tables 12-15 and Tables 3 and 15 respectively.

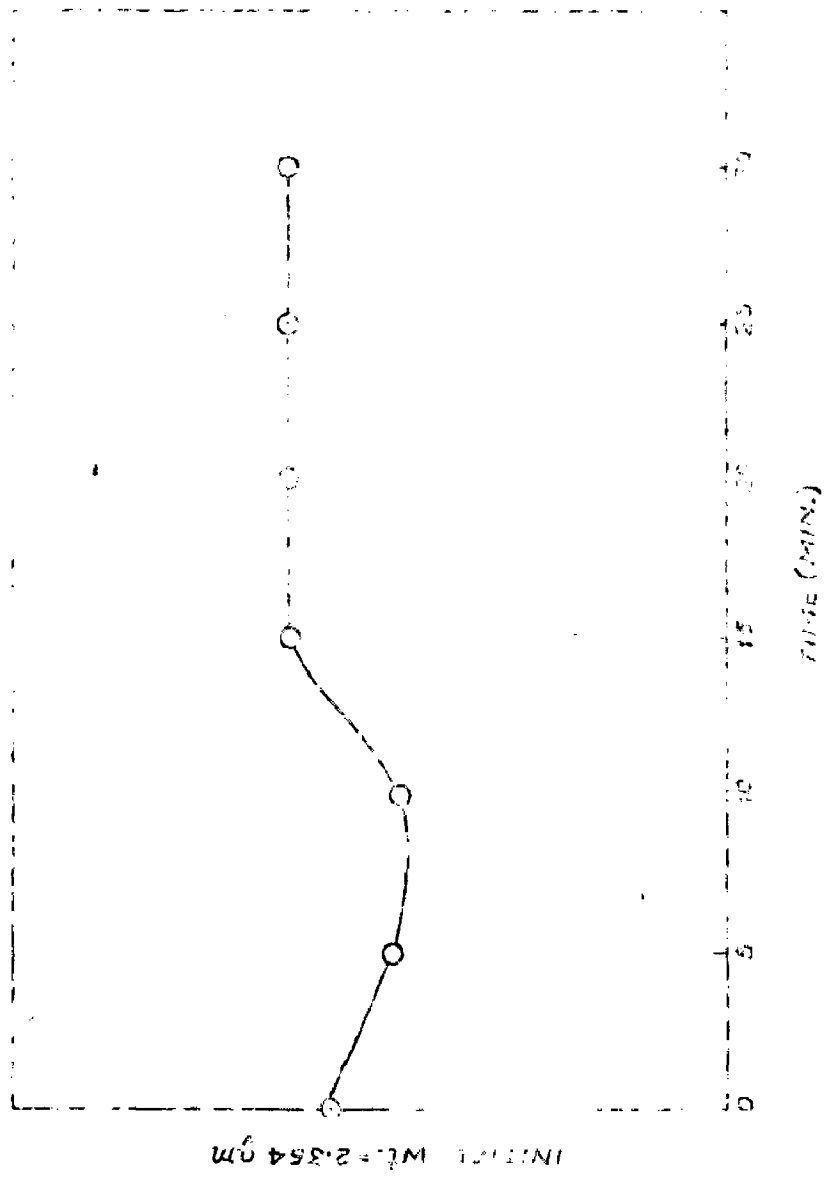


FIG. 23 THERMOGRAM SHOWING THE CHANGES IN WEIGHT THAT FOLLOW DURING OXIDATION OF COPEROUS SULPHIDE BEING SET IN A STREAM OF AIR AT 450°C.

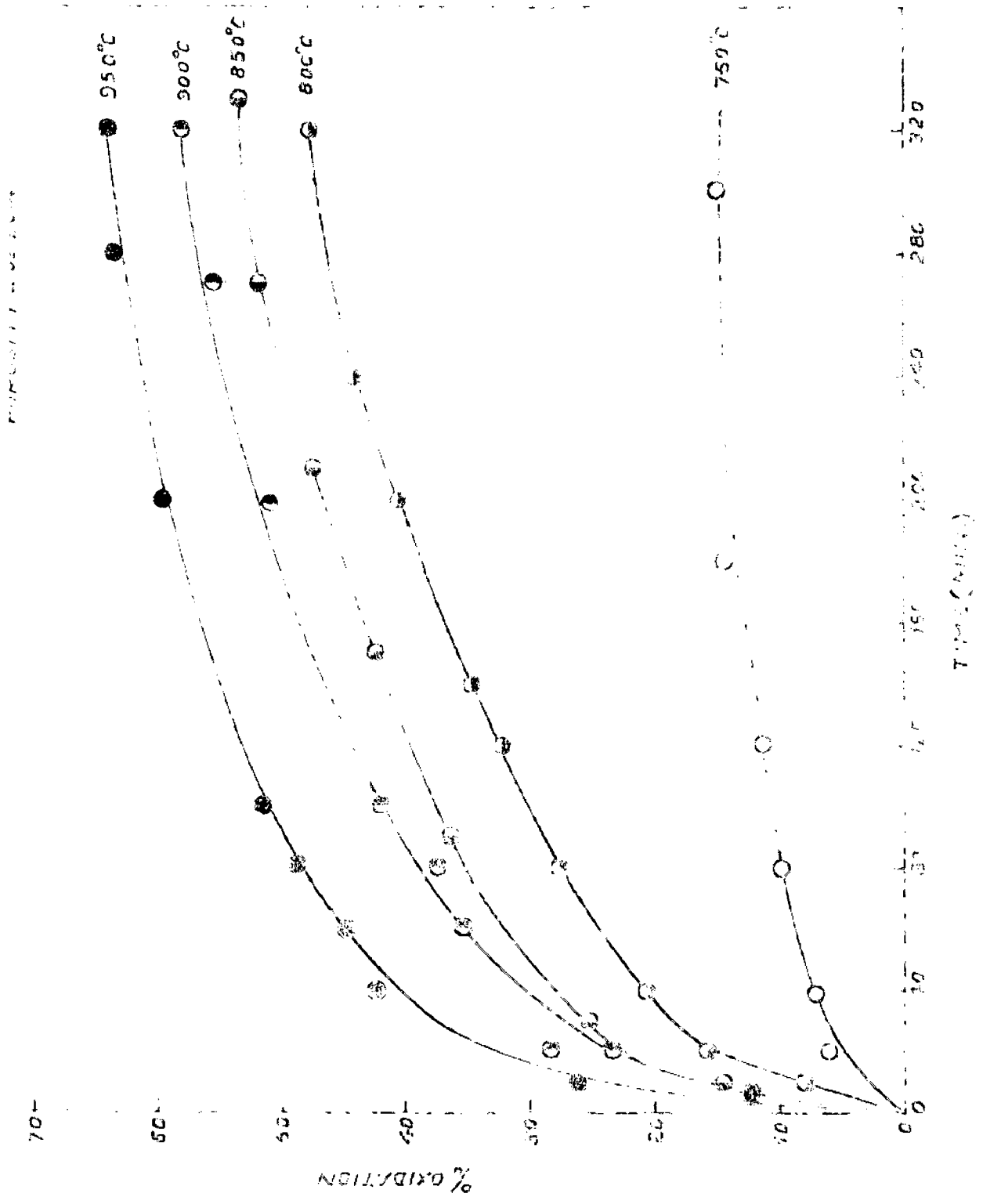


FIGURE EXPERIMENTAL RATE OF IRON OXIDATION VS TIME SHOWING THE EFFECT OF TEMPERATURE.

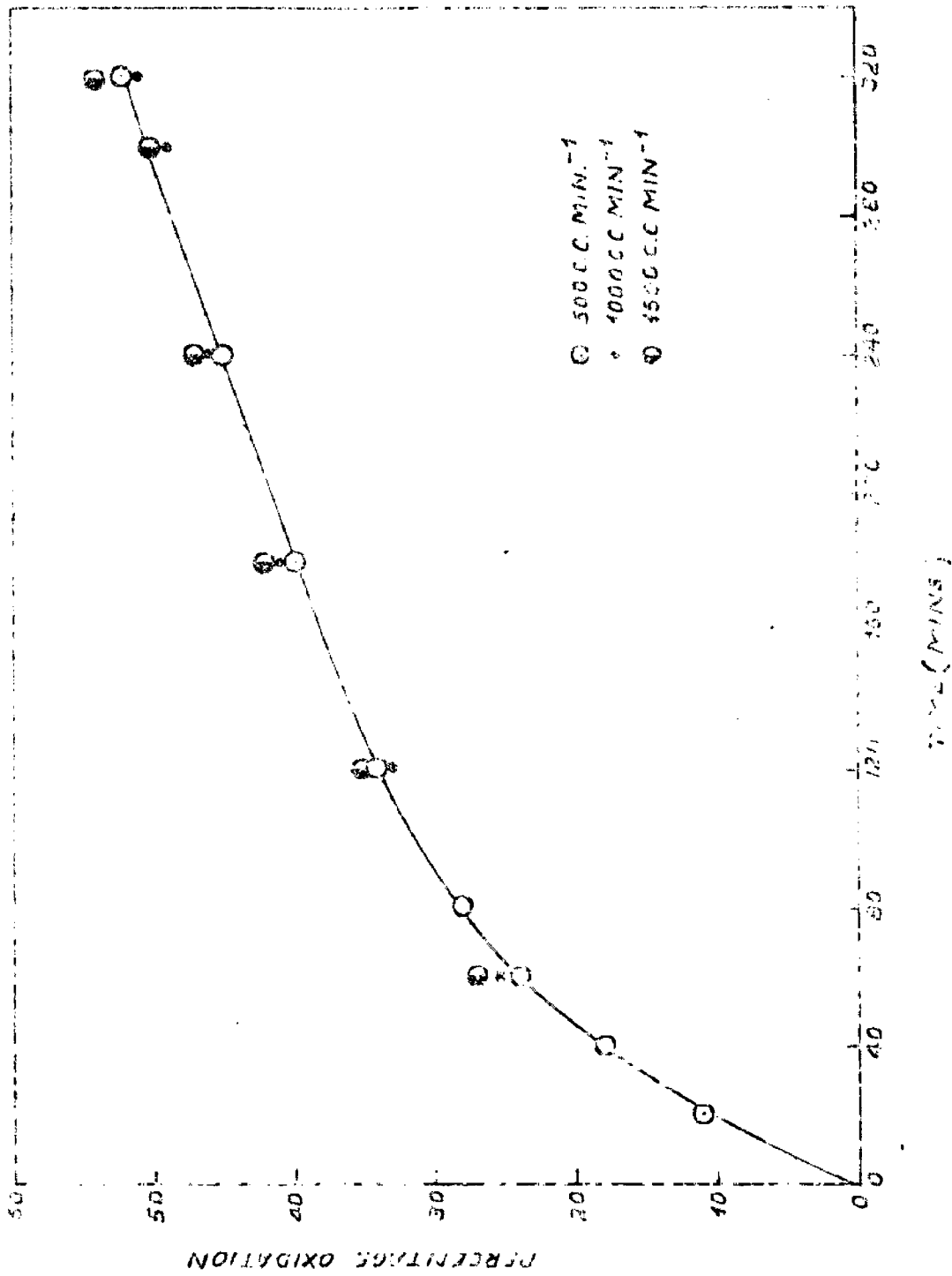


FIG. 25 EXPERIMENTAL PLOT OF TRACE OXIDATION VS T SHOWING THE
 EFFECT OF INCREASING THE FLOW RATE OF AIR FROM 1/2 LITRE TO 1 1/2
 LITRE PER MINUTE.

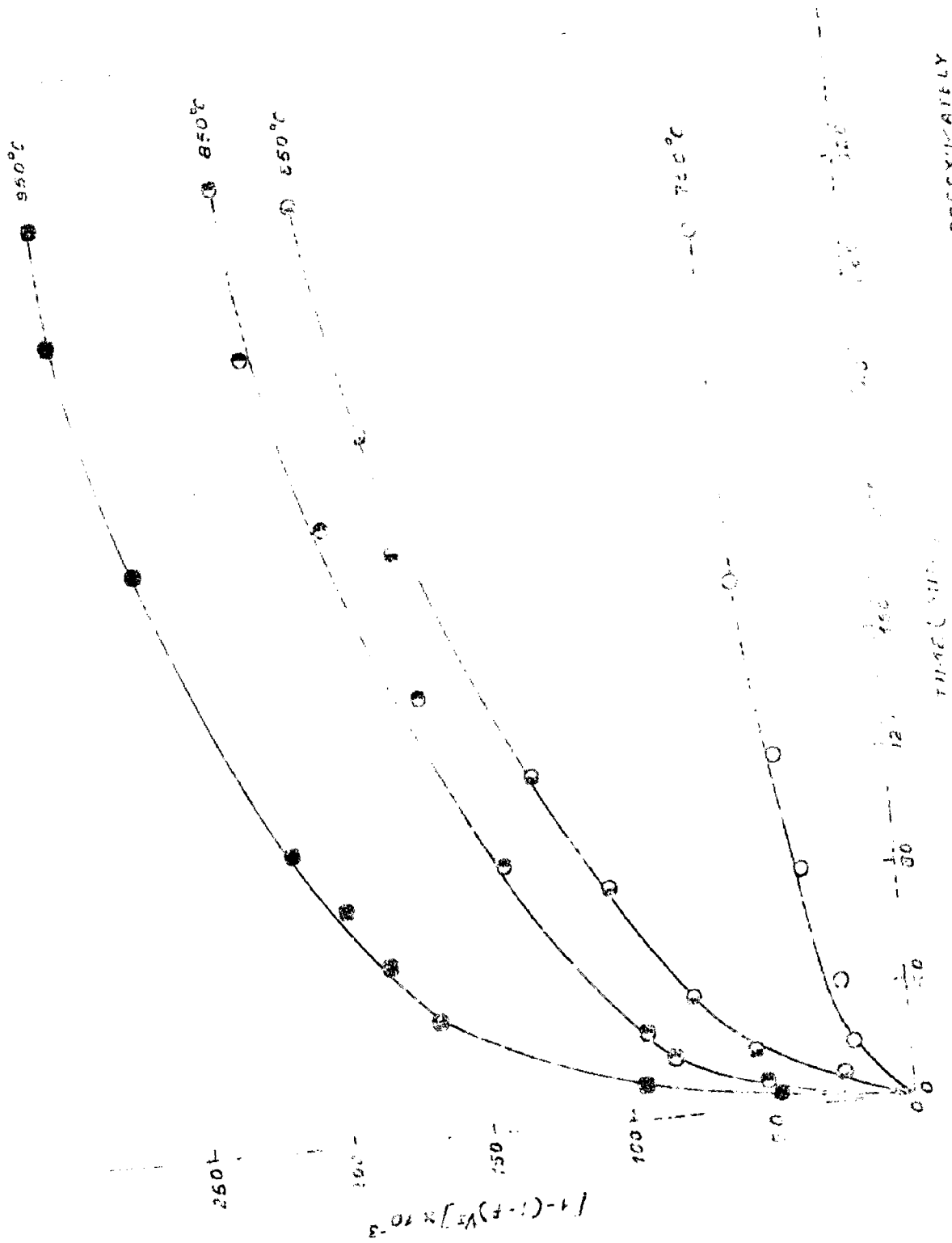


FIG. 25 EXPERIMENTAL PLOT OF $[1-(1-F)^{1/2}]$ VS T WHICH IS APPROXIMATELY LINEAR FOR INITIAL ABOUT 20 MINUTES.

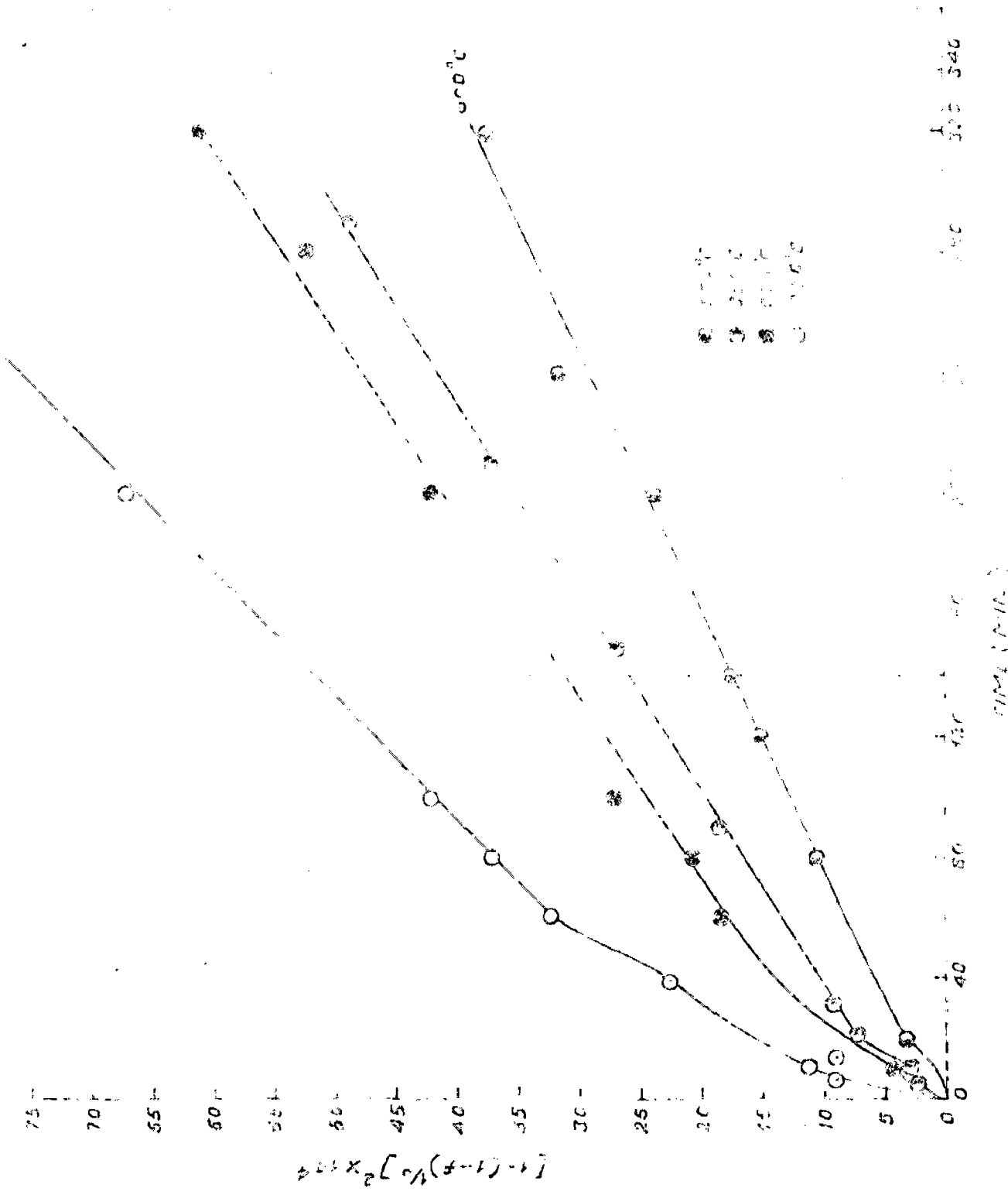


FIG. 7. AN EXPERIMENTAL PLOT OF $[1 - (1 - X)^2]$ VS. TIME FOR DIFFERENT TEMPERATURES IN THE ISOTHERMAL DEGRADATION OF PVC.

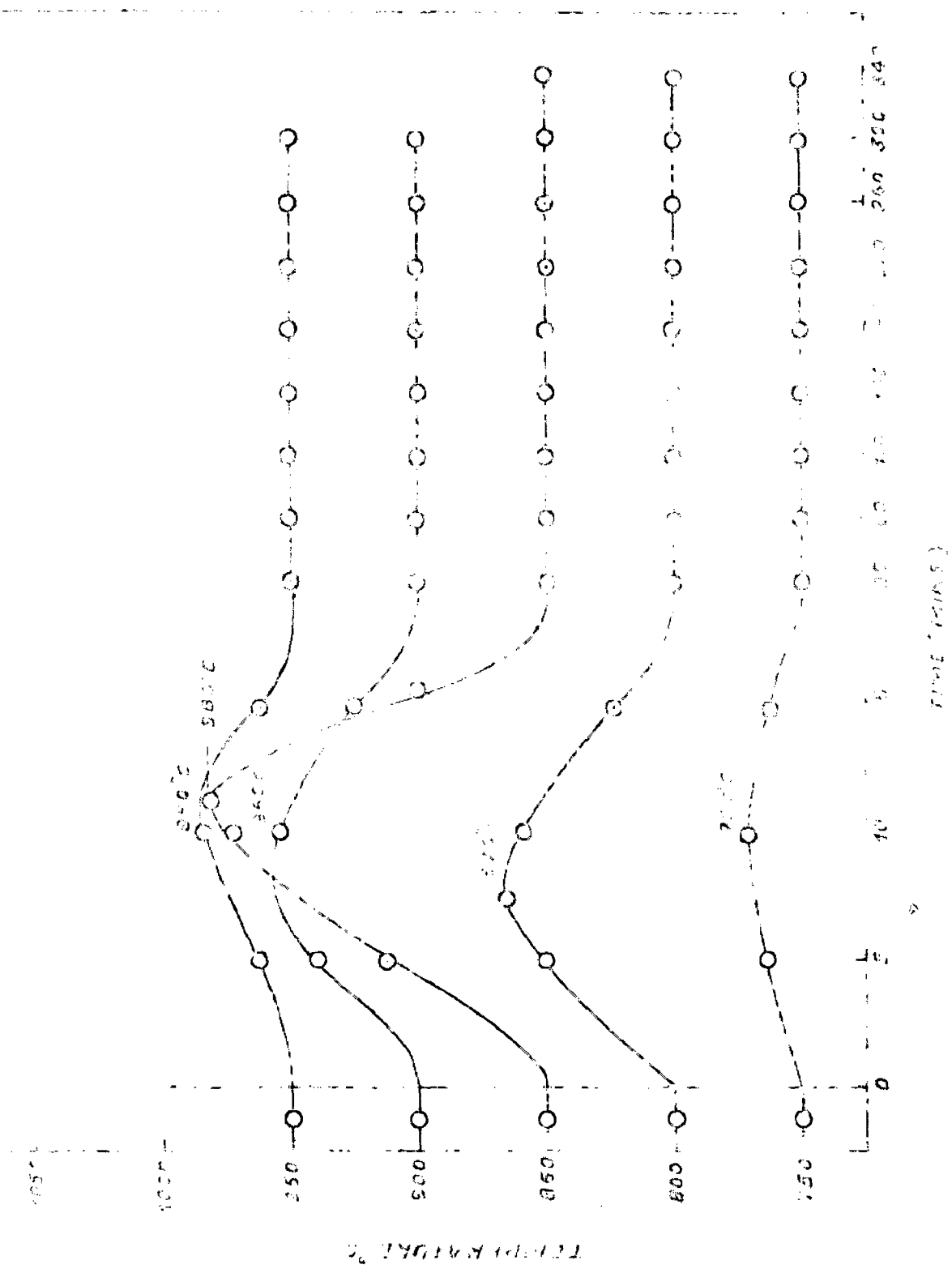


FIG. 28 RISE IN TEMPERATURE OF THE SURFACE OF THE SAMPLE UNDER DIFFERENT CONDITIONS DUE TO RELEASE OF CADMIUM FROM THE REACTION FRONT.

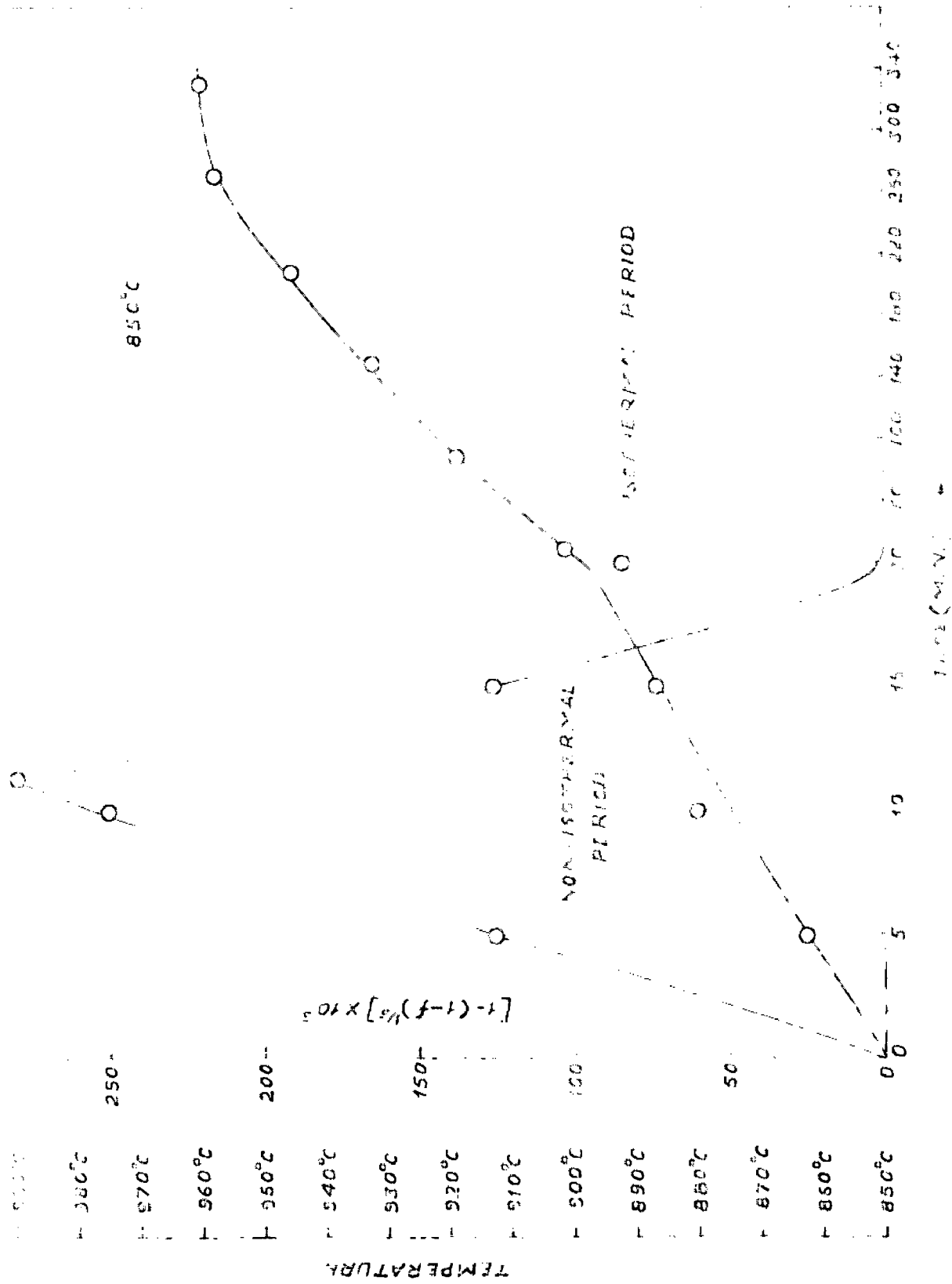


FIG. 29. DEFINES THE BOUNDARIES OF NON-ISOTHERMAL PERIOD & ISOTHERMAL PERIOD.



11- O NON-ISOTHERMAL PERIOD

SLOPE = 0.65×10^{-4}

10- O ISOTHERMAL PERIOD

SLOPE = $5/22 \times 10^{-4}$

$\theta = 19.57 \text{ kcal/mol}$

9- O ISOTHERMAL PERIOD

SLOPE = $5/22 \times 10^{-4}$

$\theta = 19.57 \text{ kcal/mol}$

DATA POINTS

Point	T	ln(A/T ²)
11	24	17.5
10	28	16.5
9	32	15.5
8	36	14.5
7	40	13.5
6	44	12.5
5	48	11.5
4	52	10.5
3	56	9.5
2	60	8.5
1	64	7.5

FIG. 10. EXPERIMENTAL DATA ON 50% VS 1 TO OBTAIN VALUES OF APPARENT ACTIVATION ENERGY IN NON-ISOTHERMAL AND ISOTHERMAL PERIODS RESPECTIVELY.

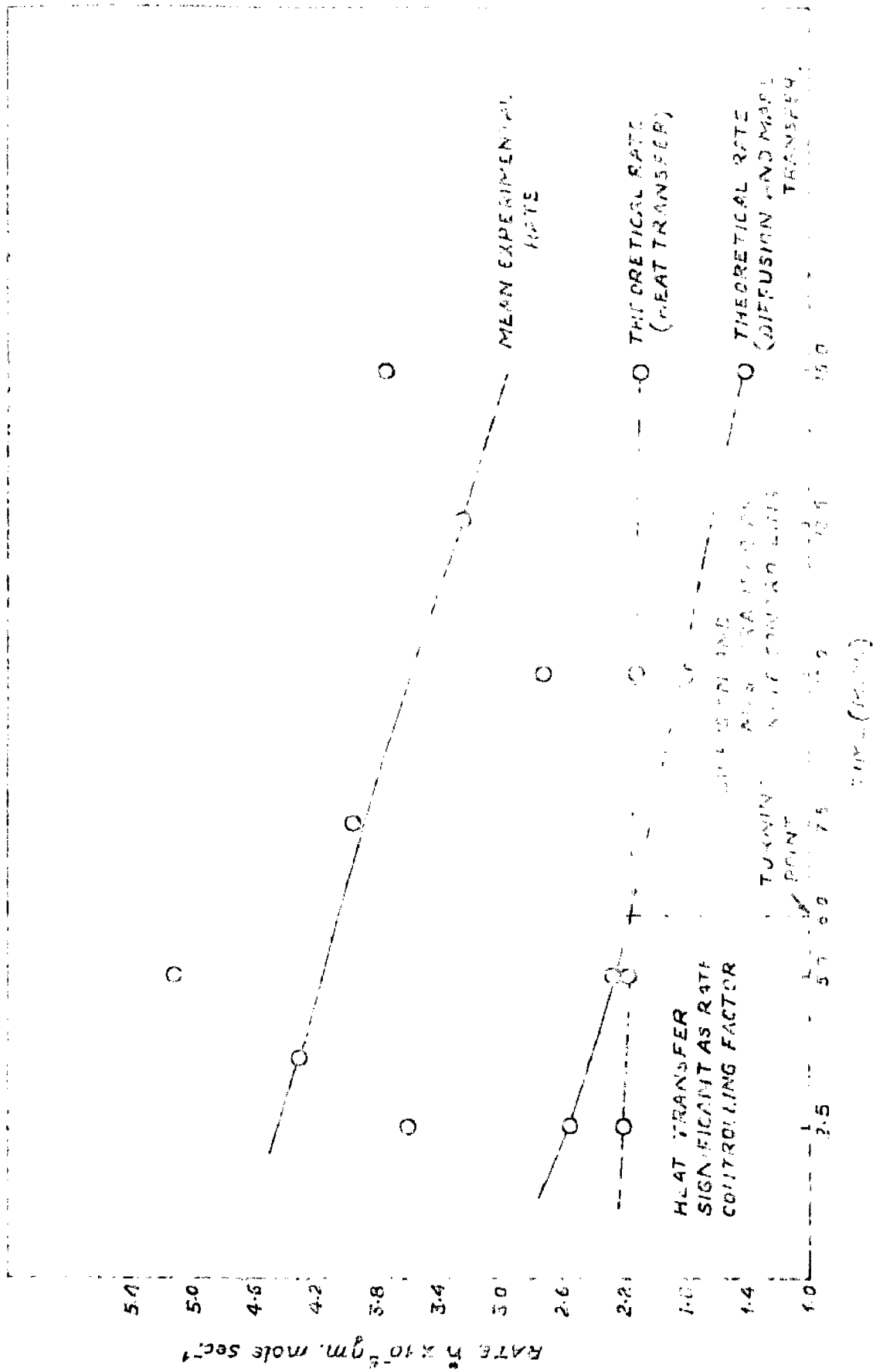


FIG. 31 GRAPHICAL ANALYSIS OF NON-ISOTHERMAL DATA.

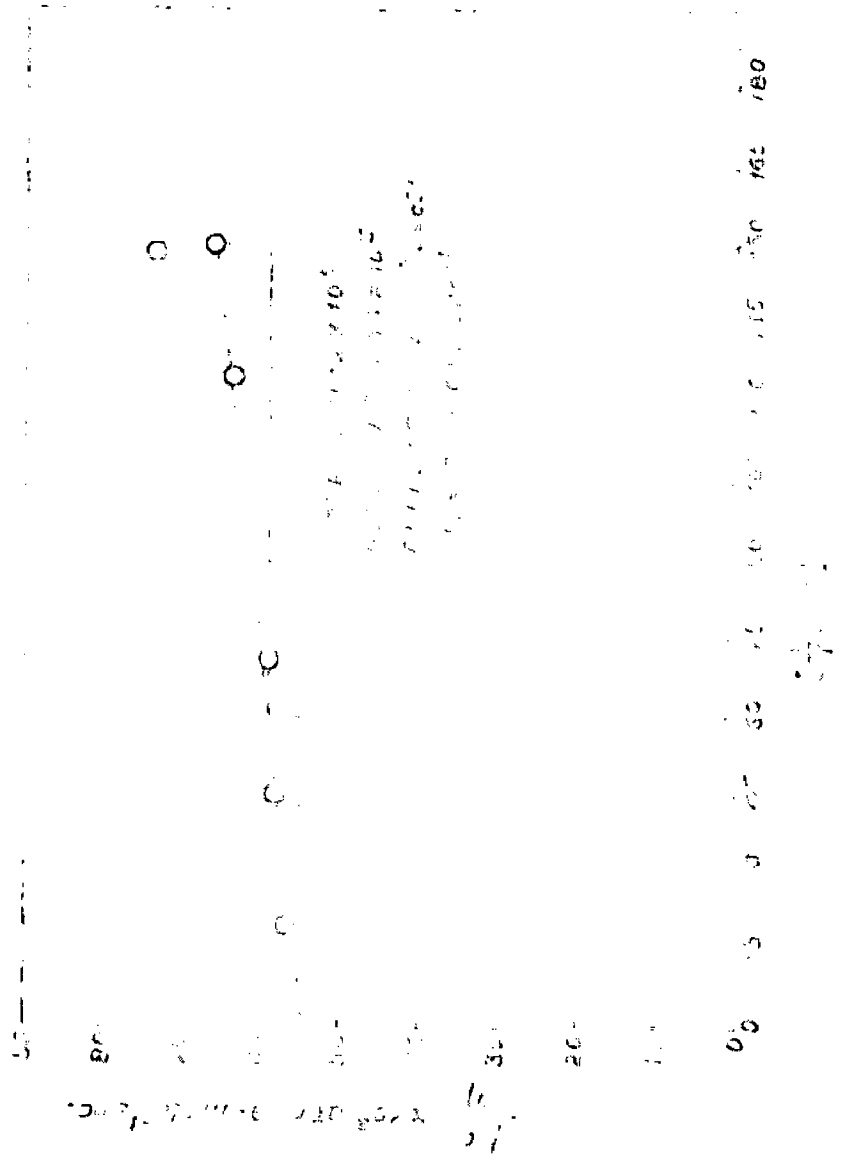


FIG. 32. SEM EXPERIMENTAL PLOT OF DTR/T VS $(\frac{1}{T} - \frac{1}{T_0})$, WHICH IS STRAIGHT LINE IN THE ISOTHERMAL PERIOD.

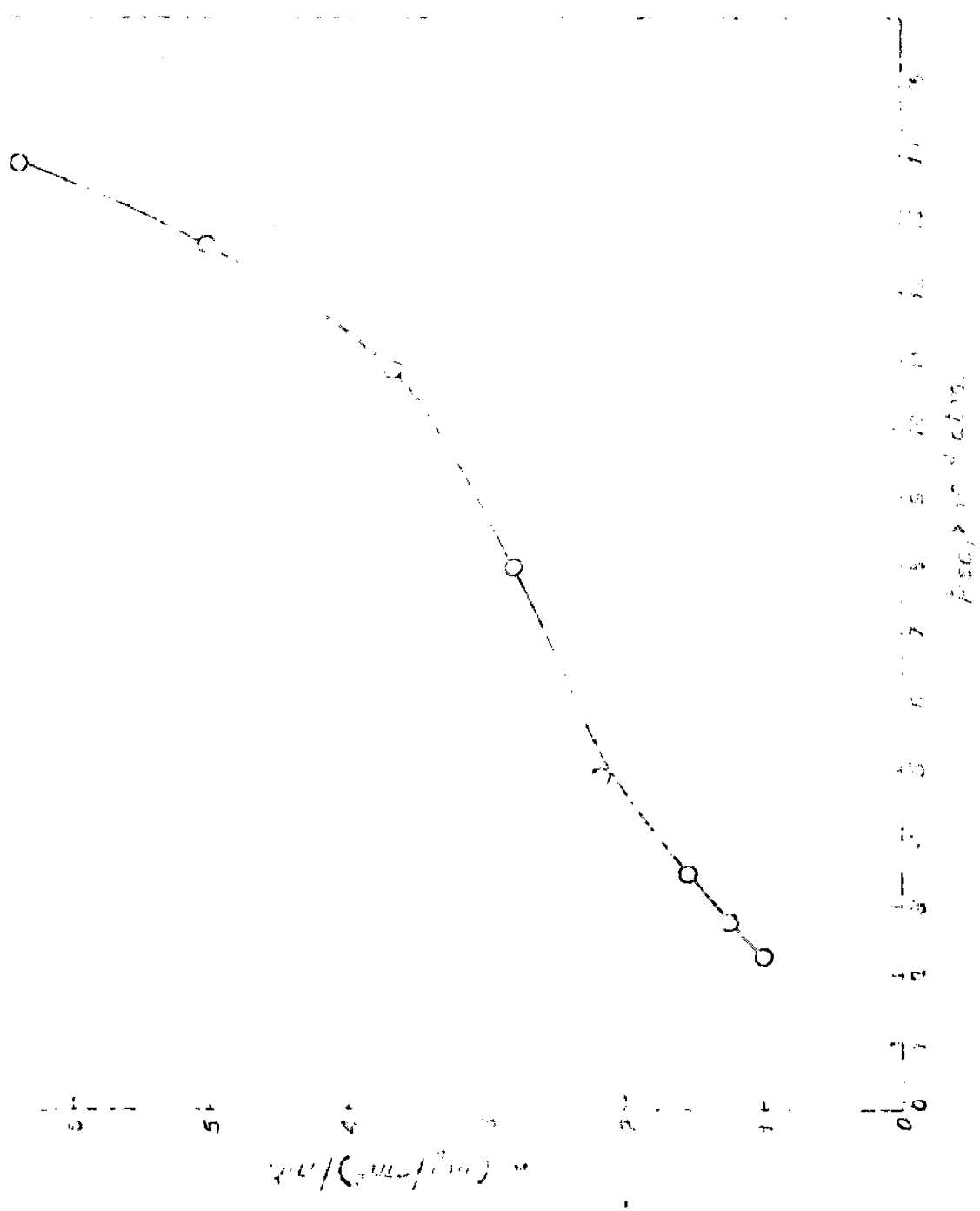


FIG. 30. DETERMINATION OF PRODUCT WEIGHT IN mg. vs. PERCENTAGE IN mg.

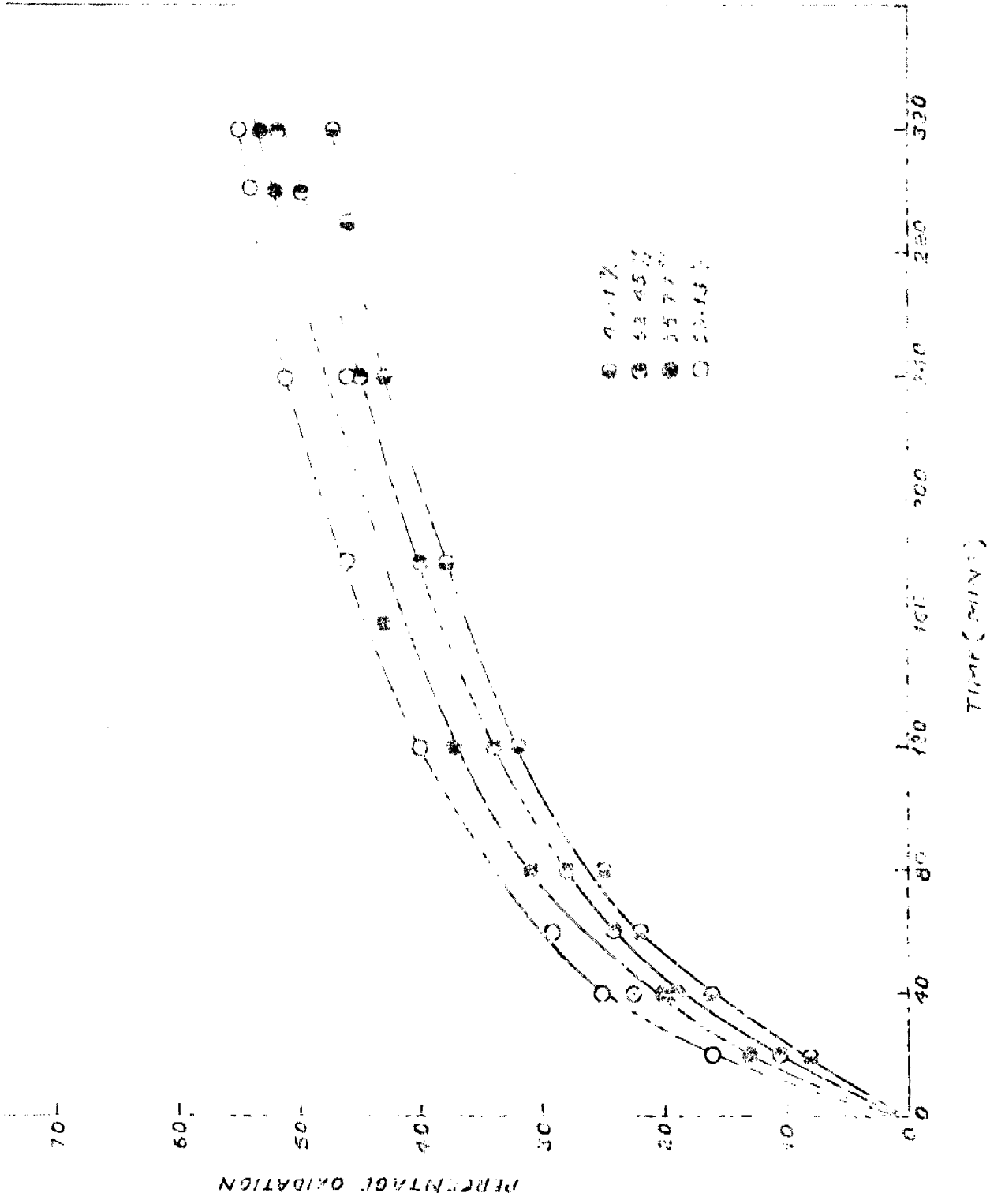


FIG. 34 EFFECT OF CONCENTRATION ON THE OXIDATION RATE OF CUPROUS SULPHIDE PELLETS AT 650°C.

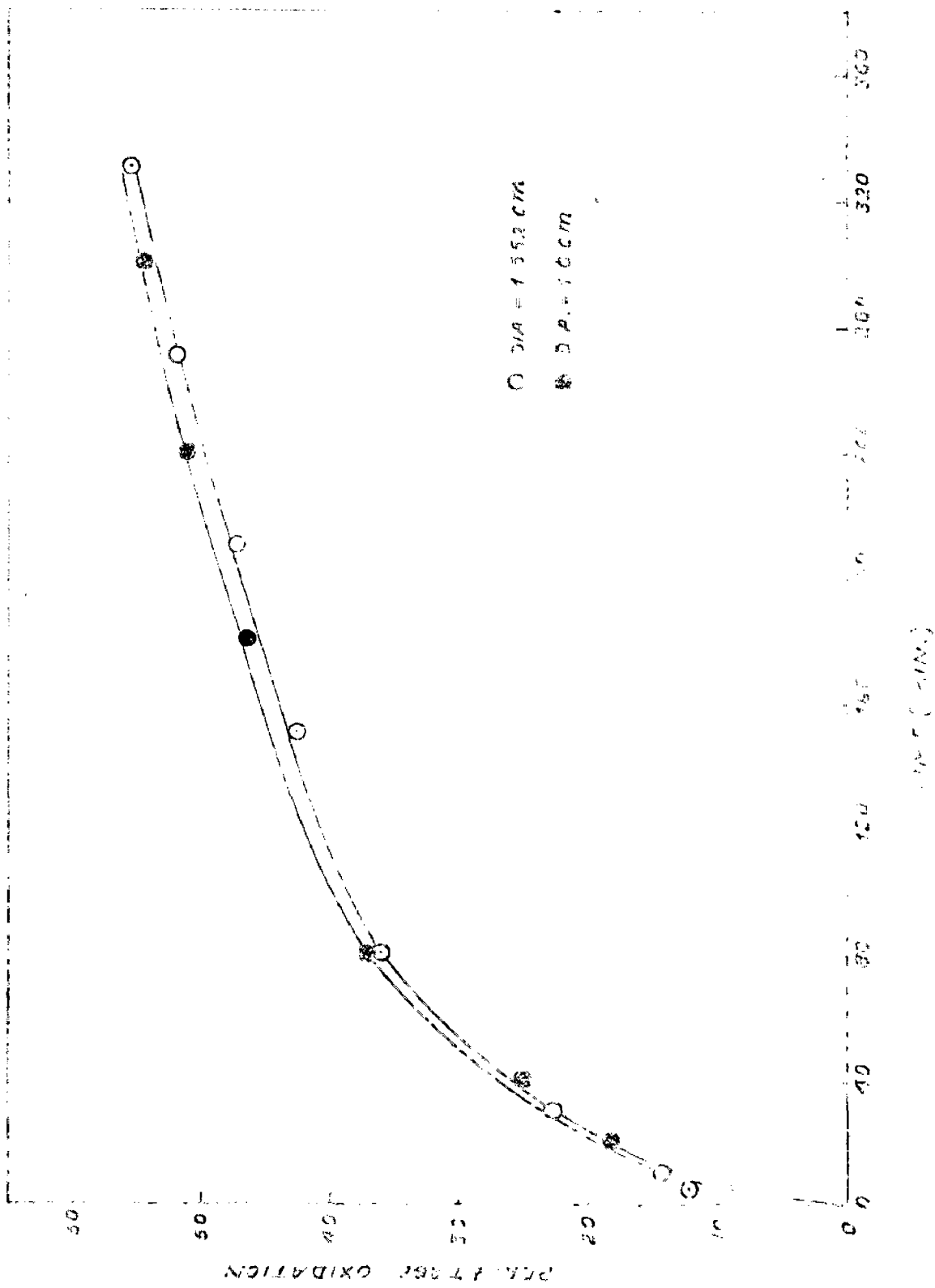


FIG. 34 EXPERIMENTAL PLOT OF PERCENT OXIDATION VS. TIME (MIN.) SHOWING THE EFFECT OF DIAMETER

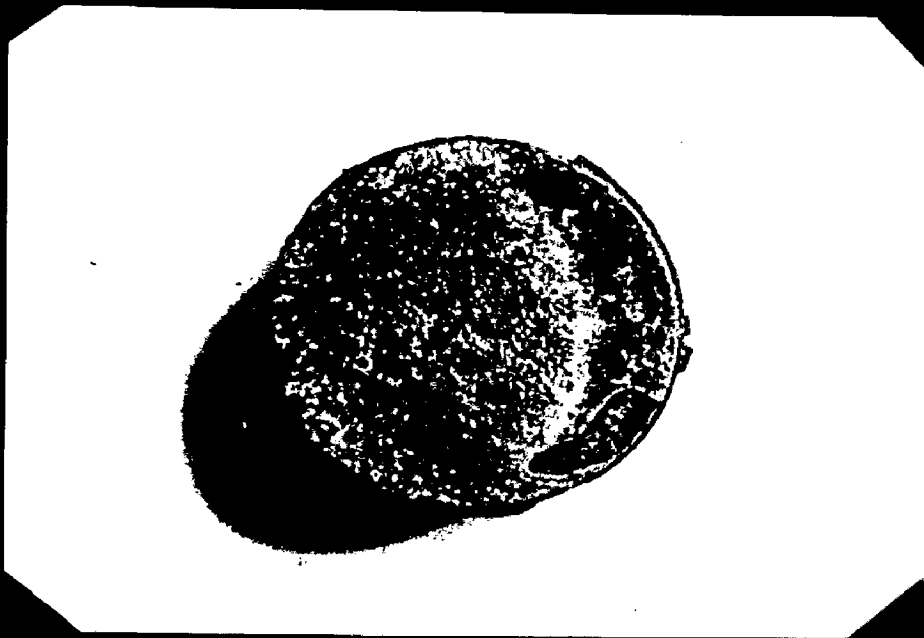


Fig. 36. Cross section of partly oxidised pellet of Cu_2S . Turning & roughening of corners indicate the exothermic heat generated at the reaction interphase. Hollow pockets indicate the rupture of 'puff-ball' with subsequent release of product gases.

5.2 DISCUSSION OF THE RESULTS

Figure 23 shows that there is small decrease in the weight of the copper sulphide pellet being oxidised at 850°C in a stream of air, for initial 10 minutes, increases in the next 5 minutes and remains practically constant during rest of the period. This can be attributed to the formation of thin layer of Cu_2O just adjacent to Cu_2S surface which is subsequently oxidised to CuO in higher partial pressures of oxygen. This confirms to the fact that copper sulphide shows polymorphism and at higher temperature exists as Cu_2S and is oxidised according to the reactions (20 and 21). Thus reactions (20 and 21) are in accordance with the thermogram and that the final product is always CuO . This finding is in agreement with the results of previous investigators^{1,5,16,23,30,32}

From Figure 25, critical air flow rate is 500 cc per minute. Increasing the air flow rate beyond this, does not affect the kinetics. This ensures the absence of gas starvation. According to Hill¹⁴, this is one of the characteristics displayed by Gas-solid reactions controlled either by chemical reaction or heat and mass transfer.

Figure (24) elucidates the effect of temperature on the roasting of cuprous sulphide pellet. It is evident from the plot that about 15%, 48%, 53%, 58% and 65% oxidation is complete in 6 hours at 750, 800, 850, 900 and 950°C respectively

Oxidation rate is very fast in the beginning and gradually slows down later on. From this it would appear that initially the interfacial chemical reaction is rate controlling followed by diffusion as sufficiently thick layer of CuO is build up. This claim is supported by Henderson², Wodsworth⁵, Lu, W.K.^{37,38}. But all these investigators failed to realise the significant contribution of heat release at the reacting interphase, which is manifested by the turning of the corners of copper sulphide pellet, showing that the reaction (20) is highly exothermic and as calculated huge amount of heat i.e., 126.55 K.cals is released per g-mole of cuprous sulphide reacted. This manifests itself in the higher temperature of the sample than its surroundings as shown in Fig. 28. These temperature differences later on subside. Recently several papers have got published¹⁴⁻¹⁹ who have greatly stressed the role of heat and mass transfer in M-S-O system. The overall treatment of the oxidation kinetics of cuprous sulphide will now be followed considering four rate controlling steps :

1. Boundary layer control
2. Chemical reaction control
3. Diffusion control
4. Heat and mass transfer control.

The diffusion of oxygen through stagnant gas boundary layer to the surface of Cu₂S pellet is ruled out as a rate controlling step because of high flow rate (Re=6.825) of air maintained during the oxidation of cuprous sulphide.

According to Hill¹⁴, the resistance offered by the stagnant gas boundary layer is negligible as compared to the solid product layer to the diffusion of reacting species, therefore, under this condition the rate of oxidation of cuprous sulphide pellet is controlled by any one of the rest of the three.

Experimental results are analysed separately in each period as discussed earlier at 850°C. At 850°C, heat effect is most pronounced (Fig. 28) and is, therefore, selected to enlighten the role of heat and mass transfer in the oxidation kinetics of cuprous sulphide.

5.2.1 Analysis of Transition Period

Fig. 29 shows that transition period exists upto 20 minutes. If the oxidation of cuprous sulphide is exclusively controlled by chemical reaction at the interphase, then according to Hill¹⁴, Abrahm¹⁶ the equation (24) is valid, which indicates that for a reaction to be controlled by an inter-facial chemical reaction, the plot $[1 - (1-f)^{1/3}]$ versus time should be linear. Figure 28 shows that plot $[1 - (1-f)^{1/3}]$ versus time is approximately linear during this period.

The activation energy was calculated from the plot (30) between $\log K$ and $1/T$. The apparent activation energy in the transition period is found to have a larger value i.e., 29.7 K.cal- g-mole⁻¹.

The linearity of plot $[1 - (1-f)^{1/3}]$ versus t together with higher activation energies suggest that reaction

is chemically controlled, but according to Hill¹⁴, same characteristics are also displayed when the reaction is heat and mass transfer controlled. This, then, gives rise to conflicting situation to decide the true nature of controlling mechanism. The previous workers¹⁻⁵ had a misconception that the chemical reaction at the interface is rate controlling as they had not taken into consideration the effect of the exothermic nature of the reactions (20 and 21).

Assuming that oxidation of cuprous sulphide is chemically controlled, then rate must increase continuously at higher temperatures caused by the generation of exothermic heat at the reaction front but instead, rate slows down after the few minutes from the start as indicated by Fig. 24. Secondly as the temperature rises, chemical rate constant K_c also increase and should, therefore, result in rapid variation in the velocity of reaction interphase but it is evident from Figure 28 that reaction front velocity does not substantially deviate from linearity i.e. $dv/dt = \text{constant}$. and velocity of moving interface is uniformly accelerated. So the possibility of chemical reaction as rate controlling is absolutely ruled out. Now the reaction is either diffusion controlled or heat and mass transfer controlled.

If the reaction is diffusion controlled, Gander's⁵⁴ equation should be valid .

$$\left[1 - (1-f)^{1/3} \right]^2 = kt \quad (5-1)$$

i.e. plot $\left[1 - (1-f)^{1/3} \right]^2$ versus time should be linear.

Fig. 27 is such plot which clearly shows non-linearity during this period. Secondly higher activation energies obtained in this period also refute the idea that it is diffusion controlled. Complete analysis, however, will differentiate two rate controlling mechanisms operative in the transition period i.e. , diffusion and mass transfer as the first and heat transfer as the second . Theoretical rates on diffusion and mass transfer and heat transfer were determined according to the equations (25) and (32) respectively and compared with those experimental rates at 2.5 mts, 5 minute, 10 minute and 15 minute. The results of the calculations are summarised in Tables 18, and graphically represented in Fig. 31.

Figure 31 shows that theoretical rates are never greater than mean experimental rates at any instant. Theoretical rates based on heat transfer are slower in the first 6 minutes showing thereby , that heat transfer is the rate controlling in this period but after 6 minutes the condition is reversed and diffusion and mass transfer is the rate controlling thus it is concluded that reaction is controlled by heat and mass transfer in the transition period. This can be explained as follows : In the beginning higher temperature at the reaction interphase increases the diffusivities of O_2 and SO_2 through reactant solid and product solid phase respectively with the

result that diffusion and mass transfer steps are faster but later on diffusion steps become the rate controlling as the CuO layer is build sufficiently thick whereas the heat transfer across the product layer is not markedly affected as indicated by Figure 31.

5.2.2 Analysis of Isothermal Period

Low value of the activation energy i.e., 10.37 K.cal. g-mole⁻¹ (Fig. 30) together with linear nature of the plot⁵⁴ $[1-(1-f)^{1/3}]^2$ versus t during this period can be taken as positive indication for the reaction to be diffusion controlled. According to Rao and Abrahm¹⁶, the equation 26 is still valid in this region where $[R_M]_T$ is the total mass transfer resistance offered to the diffusion of the reactant gas from the bulk gas phase to the reaction front. Equation (25) is then the modified expression according to which the plot

$$\frac{[P_{O_2}]_G}{\eta} \quad \text{Vs} \quad \left(\frac{1}{r^{*'}} - 1 \right) \quad \text{should be linear and its}$$

slope and intercept should yield the value of D_{eff} and α_1 respectively. This plot is as shown in Fig. 32 which is a straight line. The calculated values of D_{eff} and α are in fair agreement with those obtained from experimental data (Table 20) which confirms that reaction is diffusion controlled in the isothermal period.

5.2.3 Effect of Porosity

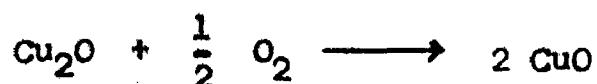
From Figure 34, it is observed that increasing the porosity about 10% led to the increase in the rate of cuprous sulphide oxidation about 18%. This is attributed to the increase in the pore volume per unit weight of the pellet which, in turn, facilitates higher diffusion and mass transfer rates of oxygen to the $\text{Cu}_2\text{S} / \text{CuO}$ interphase through solid product and product SO_2 liberated at reaction interphase out of the solid product phase.

5.2.4 Effect of Pellet Diameter

Fig. 35 shows that by decreasing the pellet diameter from 1.552 cm to 1 cm increases the rate of oxidation of cuprous sulphide. This may be attributed to increase in the surface area per unit volume exposed for reaction.

5.2.5 Effect of SO_2/O_2 Ratio

An interesting result plotted in Figure 33 has come up in the present investigation. It is shown that reaction is strongly governed by partial pressure of SO_2 in the product gases during isothermal period. Apparently the reaction,



should not be influenced by the partial pressures of SO_2 , since the reaction in this period is diffusion controlled, it is

surprising if SO_2 could have any effect because it has already been established that at 850°C there is no weight loss observed confirming that no sulphates are present. The same effect has also been reported in case of oxidation of zinc, by Hauffe and Engell³⁹ where the parabolic rate constant was found to vary with the oxygen partial pressure by the relation

$$K = a \ln p_{\text{O}_2} + b \quad (5-2)$$

This equation was derived considering development of an electrical potential at the solid-gas interphase. The same can be explained in terms of this model³⁹. Here adsorbed SO_3 produces a potential at the CuO surface, thereby increasing the rate of diffusion of Cu^+ ions through CuO .

CHAPTER VI

CONCLUSIONS

C O N C L U S I O N S

The following conclusions have been drawn from the present investigation -

1. In the temperature range of 750 - 950°C, copper sulphide only exists as Cu_2S i.e. cuprous sulphide and the final oxidation product is CuO i.e., cupric oxide. No sulphates are found to be present in this temperature range.
2. Increasing the air flow rate beyond 0.5 litres per minute does not increase the oxidation rate of cuprous sulphide which is thus the critical flow rate for the present case.
3. The rate of oxidation is very fast in the beginning and slows down after 20 minutes when sufficiently thick layer of CuO is formed.
4. The oxidation of copper sulphide proceeds in a topo-chemical manner (shown in Fig. 36) and the heat liberated at the reaction_{front} results in the higher sample temperature than its surroundings, in the beginning. These temperature differences level off after 20 minutes. Heat and mass transfer effects are pronounced in this transition period and do govern kinetics to great extent.
5. The activation energies were found to be 10.37 ± 2 and 29.7 ± 2 K.cal per g.mole for isothermal and non-isothermal period respectively.
6. Heat transfer across the solid product layer is the rate controlling factor during first 6 minutes later on followed

by diffusion and mass transfer of both reactant and product gases as rate controlling factor. In other words the reaction is heat and mass transfer controlled during non-isothermal period and not chemical reaction controlled as suggested earlier¹⁻⁵.

7. Diffusion of Oxygen from bulk gas phase to the reaction front is, solely, the rate controlling step in the isothermal period. D_{eff} and α values calculated in this period are in fair agreement with those obtained from experimental data. This supports the above conclusion.

8. Rate of oxidation of copper sulphide is increased by about 18% by increasing the porosity by about 10%.

9. Rate of oxidation of copper sulphide increases with decrease in pellet diameter.

10. Increase in the partial pressure of SO_2 in the atmosphere accelerate the oxidation of Cu_2O to CuO , has been explained in terms of a model³⁹ where adsorbed SO_3 produces a potential at the CuO surface, thereby, increasing the rate of migration of Cu^+ through CuO .

SUGGESTIONS FOR FURTHER WORK

It is suggested that following investigations should be carried out to obtain better understanding of the oxidation or roasting kinetics of cuprous sulphide.

1. Effect of foreign constituents on the oxidation kinetics of cuprous sulphide should be studied.
2. The kinetics of fluidised bed roasting of Cu_2S should be investigated in detail.
3. To minimise errors due to leakage of SO_2 if any, electro-metric method⁵¹ should be adopted to study oxidation kinetics or else, An absorption cell should be designed using platinum and calomel electrodes. Increase in acidity following the absorption of SO_2 can be recorded by a sensitive pH meter. The pH changes can be calibrated against amount of SO_2 evolution. This process, of course, is trouble free, more accurate and thorough continuous.
4. An electronic model (similar to as proposed by Anderson³⁵) can be proposed by measuring the changes in conductivity that follow with increasing partial pressures of oxygen.

B I B L I O G R A P H Y

1. E.A. Perreti . Disc. Faraday Soc., 1948, Vol.4, pp.174-9.
2. T.A. Henderson. Bull. Inst.Min.Met., 1958, Vol.620 pp.497-520
3. C.L. McCabe and J.A. Morgan . Trans. AIME, 1956, Vol.206, p. 800 A.
4. R.I. Rajouk et.al. J. opp. chem. (London), 1962, Vol. 12, p. 190-96
5. M.E. Wadsworth et.al., Trans. AIME, 1960, Vol. 218, p519
6. C.W. Dannat & H.J.T.Ellingham, Disc.Faraday Soc., Vol.4. pp. 126-139 .
7. Butt. Copper The Science and Technology of the metal, its alloys and compounds , Reinhold publishing Corp. N.Y. 1954 pp. 78, 80, 111, 138 .
8. O. Kubaschewski and E.LL.Evans, Metallurgical Thermochemistry Pergamon Press, London, 1955, pp. 214-356 .
9. W.H. Dennis, Flash Smelting, Extractive Metallurgy, Sir Issac Pitman & Sons Ltd., London.
10. T.Tsurumoto, Oxygen Smelting of Cu, Min & Met.Inst of Japan June 1953.
11. Howard & Warner, WORCRA PROCESS, Advances in Extractive Metallurgy Inst. of Mining and Metallurgy.
12. T.Tsurumoto, Cu Smelting in Converter, J. Metals, Nov. 1961, Vol. 13, p. 820 .
13. R.G. Ward, An Introduction to the Physical Chemistry of Iron and Steel making', Edward Arnold Ltd., 1962, p.1.

14. A.W.D. Hills, Heat & Mass Transfer in Process Metallurgy
Inst. of Min. & Met., 1967, London, pp. 39-77
15. N.J. Themelis & J.C. Yanopoulos, Trans. TMS-AIME, 1966,
Vol. 236. pp 414-420.
16. Rao and K.P. Abrahm, Met. Trans. , 1971, Vol.2 pp 2463-2470
17. Paul R.Rmman and Thomas A. Loose. Met Trans., 1971,
Vol. 2, pp. 889-893.
18. E.M. Kurian and R.V. Tamranker, Trans. IIM, 1970,
Vol. 23, No.4, pp. 59-64.
19. T.D.Roy and K.P. Abrahm, Paper presented in 24th
Annual Tech. Meeting of IIM held at Roorkee in Dec. 1970.
20. N.P. Diev., Y.V. Karyakin and Toshkarev. J.app.chem(USSR)
1938, Vol. 11. p.112.
- 20.a Diev. et.al. J. app. chem.(USSR) , 1938, Vol. 11 p 112
21. J.R. Lewis, J.H. Hemilton, J.C. Nixon & C.L. Graverson,
Metals Technology June, 1948.
22. E.A. Ashcroft. Trans. Electrochem. Soc., 1933, Vol.23
23. C.L. McCabe and J.A. Morgan, J.Metals, 1956, Vol.8 p 800A
24. P.G. Thomhill and L.M.Pidgeon. A Microscopic study of
Sulphide roasting, AIME, annual meeting, N.Y., Feb. 1956.
25. I.D. Shah and S.E. Khallafalla, Met.Transactions,
Sept. 1971, Vol. 2, p.2637.
26. F.H. Smyth and H.S. Roberts. J.Am.Chem.Soc., 1920, Vol.42
pp 2582, 2607.
27. V. Reuter & X. Schroder, U. Allgem.Chem., 1953, Vol.277,
pp. 146.

28. P.H. Smyth, Hastings & Roberts, J.Am.Chem.Soc., 1920,
Vol. 42, p. 2582.
29. F.Becker, Physikalisch-chemische Tabellen 3, Ergaanzungband,
1935, 3 Teil, Springer.
30. W.E. Gainer, F.S. Stone, & P.F. Tiley . Proc.Roy.Soc.,
1952, Vol. A 211, p 472.
31. B.Trappnell . Chemisorption, Academic press, N.Y. Inc., 1955.
32. M.E. Wadsworth et.al., Trans. AIME, 1960, V-218, p.519.
33. E.H.Roseboom, Econ.Geol.& Bull.Soc.Econ.Geol., 1966,
Vol.61, pp 641-72.
34. H.Rau, J. Physics-chem.solids, 1967, Vol. 28. pp 903-16.
35. J.S. Anderson, Physical Chemistry of Process Metallurgy,
Discs of Faraday Soc. 1948, Vol.4, pp 163-73.
36. Buerger, J.Chem.Physics, 1939, Vol.7 pp 1067.
37. W.K.Lu, Trans. AIME, 1963, Vol. 227, page 203
38. W.K.Lu, Bitasianes, G., Trans. AIME, 1966, Vol.236,p531.
39. K.Hauffe & H.J. Engell, Z.Electrochem., 1952, Vol.56, p.366
40. P.N.Rowe, K.T.Claxton & J.B.Lewis, Trans.Inst of Chem.Engrs
1965, Vol. 43 pp. 14-31.
41. N.Wakao and J.M. Smith, Chem. Enngg. Soc., 1967, Vol.17,p.825.
42. Chemical Engrs Hand Book, 4th edition, J.H.Perry ed., McGrah
Hill Book Co., N.Y., 1963.
43. Ranz and Marshall, Chem.Enngg. Progress, 1952, Vol.48,
pp 141-46.

44. Stanley M. Walas, Internal porosity and pore size. Heterogeneous Catalysis, Reaction Kinetics for Chem. Engrs., 1959. McGraw Hill Book Co Inc. N.Y. London. pp. 233.
45. J. Szekely & J.W. Evans, Met. Trans. Vol.2, June 1971, p. 1691-1710.
46. K. Nateson, W.O. Philbrook, Trans. AIME, 1969, V.245, pp. 2243.
47. J. Newton, Extractive Metallurgy, John Wiley & Sons Inc., N.Y., 1959 p. 286.
48. S.K. Malhotra, Study of Roasting Kinetics of ZnS, M.E. Thesis, 1972.
49. Gulbransen, E.A., Trans. Electrochem. Soc., 1942, Vol.81, pp 327, 82, 375.
50. O. Kubaschewski and Schneider, J.Inst. of Metals, 1949 Vol. 75 p 403.
51. Campbell & Thomas, Trans. Electro Chem. Soc. 1936, Vol.76, p 303.
52. International Critical Tables of Numerical data Vol.5. Thermal Conductivity of solids, 1929, McGraw Hill Book Co. Inc. N.Y. & London, p.213.
53. Harold E. McGannon, MSTIS Table, 12-II, p. 250
54. W. Jander, I.Z. Anorg.chem., 1927, Vol.163.

APPENDICES

TABLES I to XVII and XXI

TABLE - 1

% Oxidation versus time plot at 750°C.

Weight of the pellet = 4.25 gm. Load = 1 T,

Dia = 1.552 cm

Normality = 0.0512 N. I₂ soln.

Theoretical SO₂ = 1.71 gm.

me s.	Vol. of N/10 Na ₂ S ₂ O ₃ z (v) cc.	Correspond- ing Vol. of Iodine $\frac{z}{10N}$ cc	Vol. of Iodine react- ed with SO ₂ $(V - \frac{z}{10N})$	SO ₂ in gm. .03203N $(V - \frac{z}{10N})$	%age oxidation
	19(100)	37.10	62.9	0.103	6.00
	21.5(50)	42.00	18.0	0.01300	6.9
	10.5(50)	20.50	29.5	0.04850	9.7
	18.0(50)	35.20	14.8	0.02450	11.2
	11.5(50)	22.50	27.5	0.04510	14.4
	22.5(50)	44.00	6.0	0.00985	15.00

TABLE - 2

PERCENTAGE OXIDATION Versus t at 800°C

= 4.4485

Normality = 0.1 N , h = 1.965 cm.

= 1.552 cm

Theoretical SO₂ = 1.8 gm.

Time s.	Decinormal iodine sol- z(v) cc	Correspond- ing vol. of iodine $\frac{z}{10N}$ cc	I ₂ reacted with SO ₂ $(V - \frac{z}{10N})$ cc	SO ₂ gms. .03203N $(V - \frac{z}{10N})$	Cumulative SO ₂ gms.	%age oxida- tion
	6(50)	6	44	0.1408	0.1408	7.8
	6(50)	6	44	0.1408	0.2816	15.8
	22(50)	22	28.0	0.0896	0.3712	20.7
	11.5(50)	11.5	38.5	0.1232	0.4944	27.6
	24(50)	24	26.0	0.0832	0.5776	32.2
	37(50)	37	13.0	0.04160	0.6192	34.7
	17(50)	17	23.0	0.1056	0.7248	40.5
0	29(50)	29	21.0	0.0672	0.7920	44.2
	29.5(50)	29.5	20.5	0.0652	0.8576	47.8

TABLE - 3

PERCENTAGE OXIDATION Versus Time at 850°C

Weight of the pellet = 4.1 gm , D = 1.5525 cm ,

Normality of iodine solution = 0.0976 N.

Time min.	Vol. of $\text{Na}_2\text{S}_2\text{O}_3$ $z(v)$	Corres. vol. of I_2 $z/10 N$	Vol. of I_2 reacted with SO_2 $V = \frac{z}{10N}$	Cumulative total	SO_2 in gms .03203N $(V = \frac{z}{10N})$	%age oxidation
	40 (100)	41.0	59.0	9.0	0.198	12.3
	35.5 (50)	36.40	13.60	72.6	0.240	14.4
	6.5 (50)	6.65	43.35	115.95	0.376	23.3
	38.5 (50)	39.50	10.50	125.45	0.409	25.4
	43 (100)	44.00	56.00	181.45	0.582	36.2
)	16.5 (50)	16.90	33.10	214.55	0.685	42.5
)	24 (50)	24.60	25.40	239.95	0.764	47.4
)	25.5 (50)	26.16	23.84	263.79	0.838	52.0
)	43.5 (50)	44.60	5.40	269.19	0.854	53.0

TABLE - 4

PERCENTAGE OXIDATION VERSUS T at 900°C

W = 2.7375 gm Dia. = 1.552 Cm, Theoretical SO₂ = 1.1002 gm

Time mts.	N/10 Na ₂ S ₂ O ₃ z (v)	Correspond- ing vol. of N/10 I ₂ solution z/10N cc.	Vol. reacted by SO ₂ cc ($v = \frac{z}{10N}$) cc	Cumula- tive total	SO ₂ mgms .03203N ($v = \frac{z}{10N}$) gm.	%age oxida- tion
12	37.5	37.5	62.5	62.5	0.2	18.2
40	66.0 (100)	66	34.0	96.5	0.3088	28.1
60	27.5 (50)	27.5	22.5	118.5	0.3792	35.3
80	41.0 (50)	41.0	9.0	127.5	0.4080	37.2
100	33.0 (50)	33.0	17.0	144.5	0.4624	42.0
200	23.0 (50)	23.0	27.0	171.5	0.5488	49.8
280	35.0 (50)	35.0	15.0	186.5	0.5968	54.3
320	40.0 (50)	40.0	10.0	196.5	0.6288	57.0

TABLE - 5

PERCENTAGE OXIDATION VERSUS t at 950°

W = 2.508 gm , D = 1.552 Cm. Theoretical SO₂ = 1.006 gm.

Time mts.	N/10 Na ₂ S ₂ O ₃ z (v)	Corresponding 10 iodine Solution $\frac{z}{10 N}$ cc	Vol. of iodine reacted with SO ₂ $(v - \frac{z}{10N})$ cc	SO ₂ mgms .03203N $(v - \frac{z}{10N})$ cc	Cumulative SO ₂ mgms	%age oxidation
12	17.5 (100)	17.5	82.5	264	264.00	26.20
40	48.5 (100)	48.5	51.5	164.8	428.8	42.50
60	42.0 (50)	42.0	8.0	25.6	454.4	45.0
80	38.5 (50)	38.5	11.5	36.8	491.2	48.75
100	41.5 (50)	41.5	8.5	27.2	518.4	51.50
200	24.0 (50)	24.0	26	83.2	601.6	59.75
280	38.5 (50)	38.5	11.5	36.8	638.4	63.50
320	48.0 (50)	48.0	2.0	6.4	644.8	64.00

TABLE - 6

$1 - (1-f)^{1/3}$ and $[1 - (1-f)^{1/3}]^2$ Vs t at 750°C

Time	f	$(1-f)^{1/3}$	$1-(1-f)^{1/3}$	$[1 - (1-f)^{1/3}]^2$
1	2	3	4	5
20	0.06	0.98	0.020	0.00040
40	0.0693	0.976	0.024	0.000576
80	0.0975	0.967	0.033	0.001089
120	0.1121	0.960	0.040	0.001600
180	0.144	0.95	0.050	0.002500
300	0.150	0.9475	0.0525	0.002750

TABLE - 7

$1 - (1-f)^{1/3}$ and $[1 - (1-f)^{1/3}]^2$ Vs time (minute) at 800°C

Time (min)	f	$1 - (1-f)^{1/3}$	$[1 - (1-f)^{1/3}]^2$
10	0.078	0.0251	0.000625
20	0.158	0.0553	0.003025
40	0.207	0.0754	0.005625
80	0.276	0.1012	0.010201
120	0.322	0.1225	0.01500625
140	0.347	0.1325	0.01755625
200	0.405	0.1692	0.02862864
240	0.442	0.1775	0.03150625
320	0.478	0.1952	0.03710304

TABLE - VIII

$1 - (1-f)^{1/3}$ & $[1 - (1-f)^{1/3}]^2$ Vs time (minutes) at 850°C

Time mts.	f	$(1-f)^{1/3}$	$1 - (1-f)^{1/3}$	$[1 - (1-f)^{1/3}]^2$
5	0.123	0.9528	0.0472	0.002225
10	0.144	0.949	0.0510	0.002601
20	0.233	0.91536	0.08464	0.007164
30	0.254	0.90698	0.09302	0.00862
90	0.362	0.86099	0.13901	0.0193
150	0.425	0.83638	0.16362	0.02675
210	0.474	0.80724	0.19276	0.03718
270	0.520	0.78308	0.21692	0.04651
330	0.530	0.77752	0.2225	0.04825

TABLE - 9

$1 - (1-f)^{1/3}$ and $[1 - (1-f)^{1/3}]^2$ Vs t plots at 900°C

Time mts.	f	$1 - (1-f)^{1/3}$	$[1 - (1-f)^{1/3}]^2$
12	0.182	0.06418	0.0041
40	0.281	0.10420	0.01084
60	0.353	0.13415	0.0179
80	0.372	0.14418	0.0207
100	0.420	0.16516	0.02718
200	0.498	0.20512	0.0421
280	0.543	0.22910	0.0522
320	0.570	0.24723	0.0610

TABLE - 10

$1 - (1-f)^{1/3}$ and $[1 - (1-f)^{1/3}]^2$ Vs time plots at 950° C

Time mts.	f	$1 - (1-f)^{1/3}$	$[1 - (1-f)^{1/3}]^2$
12	0.262	0.09512	0.009
40	0.425	0.16614	0.0225
60	0.450	0.18159	0.03342
80	0.4875	0.19511	0.038102
100	0.515	0.21312	0.04240
200	0.5975	0.26042	0.0677
280	0.6350	0.28521	0.0812
320	0.640	0.28812	0.0830

TABLE - 11

$$[1 - (1-f)^{1/3}] = kt \text{ for non isothermal Period } k = Ae^{-Q/RT}$$

$$[1 - (1-f)^{1/3}]^2 = kt \text{ for isothermal period } \ln k = \ln A - \frac{Q}{R} \left(\frac{1}{T}\right)$$

Temperature T°K	$\frac{1}{T} \times 10^4$	Non-isothermal		Steps Result	Isothermal		Results
		$1 - (1-f)^{1/3}$	log k		$[1 - (1-f)^{1/3}]^2$	log k	
1020	9.78	5	0.69897		14	1.14613	
1073	9.32	13	1.11394	Slope = .65 x 10 ⁴	38	1.57978	Slope = $\frac{5}{22} \times 10^4$
1123	8.90	31	1.49136	Q=29.7	52	1.71600	Q=10.37
1173	8.52	-	-	K.cal	60	1.77815	K.Cal
1223	8.17	43	1.63347	g mole ⁻¹	83	1.91908	g mole ⁻¹

TABLE - 12

W = 2.3158 gm , D = 1 cm , Porosity = 49.1 ± .5 %
 h = 1 cm.

Time mts.	N/10 $\text{Na}_2\text{S}_2\text{O}_3$ z (v)	Vol. of .1 N I_2 z/10N cc	I_2 consumed by SO_2 $(v - \frac{z}{10N})$ cc	Cumula- tive	Amt. of SO_2 in gms. .03203N $(v - \frac{z}{10N})$	Fractional oxidation
20	26.5 (50)	26.5	23.5	23.5	0.0752	0.802
40	27.0 (50)	27.0	23.0	46.5	0.1488	0.160
60	32.5 (50)	32.5	17.5	64.0	0.2048	0.22
80	41.0 (50)	41.0	9.0	73.0	0.2236	0.25
120	30.0 (50)	30.0	20.0	93.0	0.3076	0.32
180	32.5 (50)	32.5	17.5	110.5	0.3536	0.38
240	35.0 (50)	35.0	15.0	125.5	0.4016	0.43
300	41.5 (50)	41.5	8.5	134.0	0.4288	0.46
320	47.0 (50)	47.0	3.0	137.0	0.4384	0.47

TABLE - 13

W = 1.96 gm , h = 1.04 cm , D = 1 cm , Porosity = 52.45 ± 0.5%

Time Mts.	z(v)	Correspon- ding Vol. of I ₂ z/10N	Vol. of I ₂ reacted by SO ₂ ($v - \frac{z}{10N}$) cc	Cumula- tive.	Amt. of SO ₂ gm 0.00203N ($v - \frac{z}{10N}$)	Fractional oxidation
20	23	23	27.0	27.0	0.0868	0.11
40	33	33	17.0	44.0	0.142	0.18
60	35	35	15.0	59.0	0.189	0.24
80	40	40	10.0	69.0	0.220	0.28
120	35	35	15.0	84.0	0.268	0.34
180	35.5	35.5	14.5	98.5	0.315	0.40
240	37.5	37.5	12.5	111.0	0.355	0.45
300	37.5	37.5	12.5	123.5	0.394	0.50
320	45.5	45.5	4.5	128.0	0.410	0.52

TABLE - 14

w = 2.123 gm , h = 1.04 cm, D = 1.0 cm , Porosity = 55.17 ± 0.5%

Theoretical SO₂ = 0.845 gm.

Time mts.	z(v)	$(v - \frac{z}{10N})$	Total	$.03203N$ $(v - \frac{z}{10N})$	%age oxidation
20	16(50)	34.0	34.0	0.1098	13.0
40	31(50)	19.0	53.0	0.1690	20.0
60	30(50)	20.0	73.0	0.2239	26.5
80	39(50)	11.0	84.0	0.2691	31.0
120	31(50)	19.0	113.0	0.3633	43.0
240	41.5(50)	8.5	121.5	0.3887	46.0
300	34.5(50)	15.5	137.0	0.4394	52.0
320	46(50)	4.0	141.0	0.4520	53.5

TABLE - 15

w = 1.797 gm , h = 0.966 cm, D = 1.0 cm, Porosity = 59.13±0.5%

Theoretical SO₂ = 0.7233 gm

Time mts	z (v)	$(v - \frac{z}{10 N})$	Total	$0.3203N$ $(v - \frac{z}{10N})$	%age oxidation
20	14.0 (50)	36.0	36.0	0.1147	16
40	29.5(50)	20.5	56.5	0.1808	25
60	41.0 (50)	9.0	65.5	0.2097	29
120	35.5(50)	14.5	90.0	0.2893	40
180	39.0(50)	11.0	101.0	0.3327	46
240	36.0(50)	14.0	115.0	0.3689	51
300	43(50)	7.0	122.0	0.3906	54
320	48(50)	2.0	124.0	0.398	55

TABLE - 16

w = 1.952 gm D = 1 cm , h = 0.875 cm , Porosity = 52 ± 0.5%
 Air flow rate = 1 ℓ per minute , Theoretical SO₂ = 0.785gm

Time mts	z(v) cc	z/10N cc	$(v - \frac{z}{10N})$	Total	.03203N $(v - \frac{z}{10N})$	f
60	41.5(100)	41.5	59.5	59.5	0.1960	0.25
120	28.5(50)	28.5	21.5	81	0.2590	0.33
180	31.5(50)	31.5	19.5	100.5	0.3220	0.41
240	37.5(50)	37.5	12.5	113	0.3610	0.46
300	43(50)	43	7	120	0.4844	0.49
320	45(50)	45	5	125	0.4000	0.51

TABLE - 17

w = 2.345 gm , h = 1.08 gm , Air flow rate = 1.5 ℓ mt^{-1} , D = 1, cm
 Porosity = 52 ± 0.5 % , Theoretical SO_2 = 0.943 gm.

Time mts.	z(v)	z/10N	$v = \frac{z}{10N}$	Total	.03203N $(v = \frac{z}{10N})$	f
60	20.5(100)	20.5	79.5	79.5	0.2544	0.27
120	26.5(50)	26.5	23.5	103.0	0.33	0.35
180	29.5(50)	29.5	20.5	123.5	0.396	0.42
240	35 (50)	35.0	15.0	138.5	0.443	0.47
300	41 (50)	41.0	9.0	147.5	0.4715	0.50
320	38.5 (50)	38.5	11.5	159.0	0.51	0.54

TABLE - 21

Plot of Parabolic rate constant k Vs % SO_2 in Atm.
at 850°C

Time mts.	Amount of SO_2 gm.	Oxygen flow rate. g mt^{-1}	Oxygen		SO_2/O_2 in the Atmos- phere.	(mg/cm^2) min^{-1}
			Reacted.	Unreacted		
20	0.376	0.135	0.188	0.2512	0.149	6.35
30	0.409	0.135	0.205	3.745	0.109	4.6
90	0.582	0.135	0.291	11.859	0.049	2.19
150	0.685	0.135	0.342	19.808	0.0346	1.45
210	0.764	0.135	0.385	27.968	0.0274	1.23
270	0.838	0.135	0.419	36.031	0.0231	1.05

UNIVERSITY OF ROORKEE
ROORKEE

REPORT OF THE EXAMINERS FOR AWARD OF M.E. DEGREE.

1. Name of the Candidate; SURENDRA DEWAN
2. Department; METALLURGICAL ENGINEERING
3. specialised subject; Extractive Metallurgy
4. Title of dissertation; KINETICS STUDIES OF OXIDATION OF COPPER SULPHIDE.
5. The Viva-Voce examination was held on 26.10.1972. at ROORKEE.

Examiner's Report;

(Note:- The examiner is requested to give here a concise report not exceeding 100 words).

Roasting is an important step in non-ferrous metallurgy and Kinetic studies on oxidation of Copper Sulphide are therefore very useful.

Experimental techniques used are quite reliable and accurate and experimental observation are very useful to understand the oxidation rate controlling step.

presentation and thesis defence is satisfactor

the dissertation is approved;

sd/- S.prakash
Signature of Internal Examiner

sd/- S.K. saraf.
Signature of external Examiner

dated 26.10.1972

UNIVERSITY OF ROORKEE
ROORKEE

NO.EX/

/PF/SD

dated december ,1972.

Copy forwarded for information to:-

1. Prof. & Head of Met. Engg. Deptt.